



**Dipartimento di Scienze Ambientali**

**Dottorato di Ricerca in Genetica e Biologia Cellulare XXIII ciclo**

**Understanding temperature-related physiological processes  
through proteomics in vegetal and animal systems**

**Applicazioni della proteomica alla comprensione di processi  
fisiologici influenzati dalla temperatura in sistemi vegetali e  
animali**

**Docente guida: Prof. Lello Zolla**

**Coordinatore: Prof. Luigi Prantera**

**Dottoranda: Maria Giulia Egidi**

## INDICE

Two-dimensional electrophoresis coupled to mass spectrometry: tips and pitfalls	3
<b>PART I- The influence of temperature on plant development in a vernalization-requiring winter wheat: a proteomic investigation</b>	6
Aim of the study	6
Background	9
Material and Methods	14
Results	22
Discussion	46
<b>PART II- Proteomic analysis of a drought-resistant spring wheat cultivar in response to prolonged cold stress</b>	63
Aim of the study	63
Background	65
Cold stress in wheat	67
Material and Methods	71
Results	78
Discussion	95
<b>PART III- Platelet storage temperature and new perspectives through proteomics</b>	102
Background	103
New proteomic applications to study platelet storage	108
Proteomic analysis of plasma derived from platelet buffy coats during storage at room temperature. An application of ProteoMiner™ technology.	112
Aim of the study	112
Materials and Methods	113
Results	118
Discussion	132
<b>Supporting Information</b>	141



## **Two-dimensional electrophoresis coupled to mass spectrometry: tips and pitfalls**

Despite alternative technologies that have emerged, 2-dimensional (2-D) electrophoresis is currently the only technique that can be routinely applied for parallel quantitative expression profiling of large sets of complex protein mixtures. 2-D electrophoresis is a powerful and widely used method for the analysis of complex protein mixtures extracted from cells, tissues, or other biological samples. This technique separates proteins according to two independent properties in two discrete steps. The first-dimension step, isoelectric focusing (IEF), separates proteins according to their isoelectric points (pI); the second-dimension step, sodium dodecyl sulfate-polyacrylamide gel electrophoresis (SDS-PAGE), separates proteins according to their molecular weights ( $M_r$ , relative molecular mass). Each spot on the resulting two-dimensional gel potentially corresponds to a single protein species in the sample. Thousands of different proteins can thus be separated, and information such as the protein pI, the apparent molecular weight, and the amount of each protein can be obtained. Two-dimensional electrophoresis was first introduced by O'Farrell (1975). In the original technique, the first dimension separation was performed in carrier-ampholyte-containing polyacrylamide gels cast in narrow tubes. 2D-E delivers a map of intact proteins that reflects changes in protein expression level, isoforms, or post-translational modifications. 2-DE shows as main advantages the simplicity, reproducibility, a wide size range (10 kDa to 500 kDa) and the fact that both moderately hydrophobic and very acidic-basic proteins can be isolated and visualized. A large and growing application of 2-D electrophoresis is within the field of proteomics. The analysis involves the systematic separation, identification, and quantitation of many proteins simultaneously from a single sample. Two-dimensional electrophoresis is used in this field due to its unparalleled ability to separate thousands of proteins simultaneously. The technique is also unique in its ability to detect post- and co-translational modifications, which cannot be predicted from the genome sequence.

Historically, two-dimensional PAGE has been the primary method of separation and comparison for complex protein mixtures. This method has been critical in developing our



understanding of the complexity and variety of proteins contained in cells and bodily fluids. Although impressive improvements in two-dimensional PAGE technologies have occurred in recent years, limitations are apparent when dealing with low abundance and membrane proteins, which escape from detection and may limit the broad mapping of proteins in samples. Moreover, two-dimensional PAGE is laborintensive, requires relatively large sample quantities, is poorly reproducible, has a limited dynamic range for protein detection, and has difficulties in detecting proteins with extremes in molecular mass and isoelectric point (Rabilloud, 2002). To address these limitations several types of mass spectrometry, in conjunction with various separation and analysis methods, are increasingly being adopted for proteomic measurements (Yates, 2000).

Protein identification can be done only after tryptic digestion of spots cut out from 2DE maps, and subsequent mass spectrometry analysis. This can be performed either by PMF (peptide mass finger printing) or by MS/MS analysis, although nowadays, to enhance proteome resolution it is often necessary to use multiple techniques that provide complementary results. A PMF database search is usually employed following MALDI TOF mass analysis. The premise of peptide mass finger printing is that every unique protein will have a unique set of peptides and hence unique peptide masses. This technique does well with 2DE gel spots where the protein purity is high. PMF protein identification can run into difficulties with complex mixtures of proteins. Low level identification also becomes difficult due to common place contamination by keratin, and is not suitable for those organisms with little genomic information (Hughes and Dunn, 1996; Gilmour et al., 2000). Moreover, since Peptide Mass Fingerprinting is performed by matching their constituent fragment masses (peptide masses) to the theoretical peptide masses generated from a protein or DNA database, it can only be used for species where the genome is known. Unfortunately, genetic and genomic information for crops and vegetables is still limited despite the complement of genome of Arabidopsis, rice and Poplar is rapidly advancing. Regarding the MALDI/TOF analysis, a limitation is that the measured signal intensity is not linear with the quantity of introduced sample, and

therefore the method is not applicable for determining concentrations of peptides/proteins in a mixture. Strengths of MALDI-TOF, instead, are its high sensitivity, broad mass range, relative tolerance to salts/buffers and suitability for the analysis of relatively complex mixtures. HPLC and  $\mu$ LC coupled to ESI-MS/MS presently dominate the field of protein identification by tandem mass spectrometry and database searching. ESI-MS/MS offers definitive information about protein structure; in some cases amino acid sequence and specific chemical modifications can be unequivocally deduced from the pattern of product ions generated. It is indicated for screening and structural characterization of complex mixtures of peptides, giving more reliable results for protein identification. MS/MS methods can be employed to identify unknown proteins and posttranslational modifications. Additionally, since the technique uses soft ionization, it is possible to observe labile species, e.g., nitrosothiols, protein multimers and even biologically native non-covalent interactions which would be destroyed and therefore undetected in a MALDI-TOF MS experiment, such as sites of non-covalent association with small molecules or other proteins. Limitations of ESI-MS/MS are the need for relatively high purity protein samples and a poor tolerance for electrolytes and detergents.

## References

- O'Farrell, P. H. High resolution two-dimensional electrophoresis of proteins. *J. Biol. Chem.* 250, 4007–4021 (1975).
- Hughes MA, Dunn MA. The molecular biology of plant acclimation to low temperature. *J Exp Biol* 1996;47:291–305.
- Gilmour SJ, Sebolt AM, Salazar MP, Everard JD, Thomashow MF. Overexpression of the Arabidopsis CBF3 transcriptional activator mimics multiple biochemical changes associated with cold acclimation. *Plant Physiol* 2000;124:1854–65.
- Rabilloud, T. (2002) Two-dimensional gel electrophoresis in proteomics: old, old fashioned, but it still climbs up the mountains. *Proteomics* 2, 3–10.
- Yates, J. R., III (2000) Mass spectrometry. From genomics to proteomics. *Trends Genet.* 16, 5–8

## **PART I**

### **The influence of temperature on plant development in a vernalization-requiring winter wheat: a proteomic investigation**

#### **Aim of the study**

The first objective of my PhD was the study of the influence of prolonged cold treatment on the expression of cold-induced proteins in a vernalized common wheat (*Triticum aestivum* L.), to identify proteomic changes in vernalization-treated plants when the key steps in controlling the flowering time occur. Non-proteomic studies on protein changes in plants upon prolonged cold exposure have been already performed, leading to the undisclosure of new protein isoforms, modulation of pre-existing products and accumulation of frost resistance-related proteins (Karimzadeh et al., 2005; Jahanbakhsh et al., 2007). In contrast, proteomics has been used so far to study the mechanisms of plant responses to short-term cold treatments, in order to focus on major protein modulations which are likely to be involved in defence processes against adverse conditions (Goulas et al., 2006; Hashimoto et al., 2007; Lee et al., 2007; Cui et al., 2005). Although vernalization is the same as cold treatment except for the length of the low temperature exposure, it is physiologically different in that the cold treatment usually does not affect flowering time significantly whereas vernalization does it dramatically.

We choose for this study a winter-habit wheat cultivar (named Cheyenne) with a long vernalization requirement and excellent cold tolerance (Mahfoozi *et al.* 2001). Seedlings were grown at optimal environmental conditions for 14 days, then transferred into conditioned chambers kept at 4 °C and 20 °C, respectively, both for a period of 63 days. Leaf proteome of cold acclimated and vernalized winter wheat were compared with the control non acclimated ones grown at control temperature of 20 °C. Total protein was extracted from the leaves of cold treated or control plants, then separated by 2-dimensional electrophoresis. The identities of differentially expressed proteins were determined by tandem mass spectrometry. Cold tolerance and vernalization requirement

were respectively determined by LT<sub>50</sub> and final leaf number (FLN) measurements. Leaf proteomes were examined and cross-compared through classical two-dimensional electrophoresis maps, followed by LC-ESI-MS/MS analysis.

The data demonstrated a differential expression of several proteins involved in different cellular functions. Identifying proteins that up/down regulated during cold acclimation or in response to vernalization does provide information about the mechanisms involved in cold tolerance and their effect on regulating vernalization in temperate cereals.

## References

- Jahanbakhsh S, Karimzadeh G, Rastgar F. 2007. Low temperature induced accumulation of, and SDS-PAGE changes in soluble proteins in the leaves of spring and winter wheat genotypes. *The journal of Agricultural Science* 16, 73-83.
- Karimzadeh G, Darvishzadeh R, Jalali-Javaran M, Dehghani H. 2005. Cold-induced accumulation of protein in the leaves of spring and winter barley cultivars. *Acta Biologica Hungarica* 56, 83-96.
- Goulas E, Schubert M, Kieselbach T, Kleczkowski LA, Gardeström P, Schröder W, Hurry V. The chloroplast lumen and stromal proteomes of *Arabidopsis thaliana* show differential sensitivity to short- and long-term exposure to low temperature. *Plant J* 2006;47:720-34.
- Hashimoto M, Komatsu S. Proteomic analysis of rice seedlings during cold stress. *Proteomics* 2007;7:1293-302.
- Lee DG, Ahsan N, Lee SH, Kang KY, Lee JJ, Lee BH. An approach to identify cold-induced low-abundant proteins in rice leaf. *C R Biol* 2007;330:215-25.
- Cui S, Huang F, Wang J, Ma X, Cheng Y, Liu J. A proteomic analysis of cold stress responses in rice seedlings. *Proteomics* 2005;5:3162-72.
- Mahfoozi S, Limin AE, Fowler DB. Developmental regulation of low-temperature tolerance in winter wheat. *Ann Bot-London* 2001;87:751-7.

## Background

*Triticum aestivum* L., commonly termed bread wheat, is among the most resistant crops able to grow under severe and diverse environmental conditions. This successful fitness is achieved through strict control of the flowering process, in other words getting the flowering time right is crucial to the plant's survival.

Vernalization is defined as a period of exposure to low, non-freezing temperatures, which certain plants require in order to be able to flower in spring (Streck et al., 2003).

This term refers to the acceleration of flowering that occurs in many plant species after a prolonged exposure of their imbibed seeds or young seedlings to extended periods of cold. This is not all-or-none, but a slow, quantitative process in which increasing periods of cold cause progressively earlier flowering until a saturation point is reached. Plants that are vernalized as seeds or young seedlings do not flower immediately upon being raised to higher temperatures, but often weeks later. There is, therefore, a delay between the perception of cold and the switch from vegetative to reproductive growth. The perception of and response to cold is localized in the meristematic cells of embryos, growing points, and buds. The changes induced in meristems by vernalization are conserved through many generations of cell division even at temperatures much higher than those required for the cold induction of flowering. In some species, this "memory" of vernalization can be maintained for up to 330 d. Vernalization is required in each generation for winter annuals and biennials and each year for perennials. Thus, meiosis appears to reset the requirement for vernalization. There is tremendous natural variation between *Arabidopsis* ecotypes in the extent to which their time to flowering is shortened by vernalization.

Many plant species have developed this adaptive strategy, among them fall-planted cereals such as winter wheat (*Triticum aestivum* L.), which survives the cold season in the vegetative stage, entering the more sensitive reproductive phase when both long day photoperiod and mild climate occur. In contrast, spring cereals do not have a vernalization requirement, normally developing rapidly into their reproductive phase when grown under long day photoperiod (Fowler et al., 1996a; Mahfoozi et al., 2006). The molecular basis of

vernalization has been recently elucidated in *Arabidopsis* (Sung and Amasino, 2004; Michaels and Amasino, 1999; Mylne et al., 2006) and wheat (Laurie et al., 2004; Trevaskis et al., 2007).

Through genetic mapping it has been established that winter wheat possesses recessive *vrn-A1*, *vrn-B1*, and *vrn-D1* loci, which are induced upon vernalization, whereas spring wheat carries at least one dominant *VRN1* allele. This characteristic determines absolute independence from (*Vrn-A1*) or partial requirement of (*Vrn-B1* and *Vrn-D1*) vernalization to flower. The three *VRN1* loci encode proteins related to the *Arabidopsis* meristem identity *APETALA1*-like (*AP1*) MADS-box factors (Danyluk et al., 2003; Trevaskis et al., 2003; Yan et al., 2003). *VRN1* induces flowering competency during the vernalization process and also presides over inflorescence meristem development during the second stage towards flowering (Preston and Kellogg, 2008). Another important vernalization factor is *VRN2*, which acts as a floral repressor in non-vernalized plants grown under long day conditions (Yan et al., 2004). A recent study aimed at characterizing *VRN2* gene from *Triticum aestivum* (*TaVRN2*) demonstrated that its regulation is also exerted by salt, heat shock, dehydration, wounding and abscissic acid, suggesting its pleiotropic effect in phenological development and plant responsiveness to the environment (Diallo et al., 2010). Finally, *VRN3* is the homologue of the flowering integrator flowering locus *T* (*FT*) gene in *Arabidopsis*; it is induced in leaves under long day conditions and promotes early flowering when overexpressed in winter wheat (Yan et al., 2006). Allelic differences for the three homeologous *FT* loci on the group 7 chromosomes determine variations in flowering times (Yan et al., 2006; Bonnini et al., 2008). On the other hand, the recent molecular genetic analyses of *Arabidopsis* winter annuals revealed that the epigenetic regulatory mechanism of vernalization tends to suppress a strong floral repressor located in a specific genomic locus, termed *FLC* (flowering locus C), through a series of modifications in the chromatin structure. The result is the triggering of a flowering cascade process (Sung and Amasino, 2004). A recent paper (Oliver et al., 2009) has shown that the induction of *VRN1* in barley is epigenetic, and involves histone modifications of the same

type as occur in *FLC* in *Arabidopsis*. However, these change in opposite directions to those in *FLC*. In *VRN1* there is a decrease in trimethylation of histone H3 lysine 27 (H3K27me3), the mark of a transcriptionally inactive gene, and an increase in trimethylation of histone H3 lysine 4 (H3K4me3), a mark of an active gene.

The requirement for vernalization is linked to a plant capacity to cold acclimate and develop freezing tolerance. A study on crop plants has revealed that low temperature (LT) tolerance usually depends on a complex network of inducible genes, which are fully expressed during the vegetative stage; in contrast, this control appears to be switched off during reproductive stage when the plant has limited ability to adapt to cold (Fowler et al., 1996b). Genes involved in development, such as those involved in the photoperiod and vernalization processes, determine the duration of expression of LT-tolerance genes (Fowler et al., 1996a; Mahfoozi et al., 2000). It makes sense that these two processes should be linked to avoid plants in regions that have cold winters making the transition from the vegetative to the reproductive phase too early. It has been postulated that developmental genes are mainly responsible for the duration of expression of LT-induced structural genes; in contrast, the rate of acquisition of LT tolerance is determined at the genetic level by differences in cold-hardiness potential (Fowler et al., 1996a; Mahfoozi et al., 2001). Fowler and co-workers, through studies on wheat (*T. aestivum* L.) and rye (*Secale cereale* L.) cultivars, reported a very close association between the point of vernalization saturation and a decline in cold tolerance (Limin and Fowler, 2006). Vernalization-requiring plants go through a process of reducing their final leaf number (FLN) up to the point of vernalization saturation (Fowler *et al.* 1996a). After this point, cold tolerance is gradually reduced, as it has been observed in many studies on over wintering cereals (Fowler *et al.* 1996a, b; Trevaskis et al., 2007).

## References

- Streck N.A, Weiss A, Baenziger PS. A Generalized Vernalization Response Function for Winter Wheat. *Agron J* 2003;95:155-9.



- Fowler DB, Limin AE, Wang S-Y, Ward RW Relationship between low-temperature tolerance and vernalization response in wheat and rye. *Can J Plant Sci* 1996a;76:37-42.
- Mahfoozi S, Limin AE, Ahakpaz F, Fowler DB. Phenological development and expression of freezing resistance in spring and winter wheat under field conditions in north-west Iran. *Field Crop Res* 2006;97:182-7.
- Sung S, Amasino RM. Vernalization in *Arabidopsis thaliana* is mediated by the PHD finger protein VIN3. *Nature* 2004;427:159-64.
- Michaels SD, Amasino RM. FLOWERING LOCUS C encodes a novel MADS domain protein that acts as a repressor of flowering. *Plant Cell* 1999;11:949-56.
- Mylne JS, Barrett L, Tessadori F, Mesnage S, Johnson L, Bernatavichute YV, Jacobsen SE, Fransz P, Dean C. LHP1, the *Arabidopsis* homologue of ETEROCHROMATIN PROTEIN1, is required for epigenetic silencing of FLC. *P Natl Acad Sci USA* 2006;103:5012-7.
- Laurie DA, Griffiths S, Dunford RP, Christodoulou V, Taylor SA, Cockram J, Beales J, Turner A. Comparative genetic approaches to the identification of flowering time genes in temperate cereals. *Field Crop Res* 2004;90:87-99.
- Trevaskis B, Hemming MN, Dennis ES, Peacock WJ. The molecular basis of vernalization-induced flowering in cereals. *Trends Plant Sci* 2007;12:352-7.
- Danyluk J, Kane NA, Breton G, Limin AE, Fowler DB, Sarhan F. TaVRT-1, a putative transcription factor associated with vegetative to reproductive transition in cereals. *Plant Physiol* 2003;132:1849-60.
- Trevaskis B, Bagnall DJ, Ellis MH, Peacock WJ, Dennis ES. MADS box genes control vernalization-induced flowering in cereals. *P Natl Acad Sci USA* 2003;100:13099-104.
- Yan L, Loukoianov A, Tranquilli G, Helguera M, Fahima T, Dubcovsky J. Positional cloning of wheat vernalization gene VRN1. *P Natl Acad Sci USA* 2003;100:6263-8.
- Preston JC, Kellogg EA. Discrete developmental roles for temperate cereal grass VERNALIZATION1/FRUITFULL-like genes in flowering competency and the transition to flowering. *Plant Physiol* 2008;146:265-76.
- Yan L, Loukoianov A, Blechl A, Tranquilli G, Ramakrishna W, SanMiguel P, Bennetzen JL, Echenique V, Dubcovsky J. The wheat VRN2 gene is a flowering repressor down-regulated by vernalization. *Science* 2004;303:1640-4.
- Diallo A, Kane N, Agharbaoui Z, Badawi M, Sarhan F. Heterologous expression of wheat VERNALIZATION 2 (TaVRN2) gene in *Arabidopsis* delays flowering and enhances freezing tolerance. *PLoS ONE* 2010;5:e8690.
- Yan L, Fu D, Li C, Blechl A, Tranquilli G, Bonafede M, Sanchez A, Valarik M, Yasuda S, Dubcovsky J. The wheat and barley vernalization gene VRN3 is an orthologue of FT. *P Natl Acad Sci USA* 2006;103:19581-6.
- Bonnin I, Rousset M, Madur D, Sourdille P, Dupuits C, Brunel D, Goldringer I. FT genome A and D polymorphisms are associated with the variation of earliness components in hexaploid wheat. *Theor Appl Genet* 2008;116:383-94.

- Oliver SN, Finnegan EJ, Dennis ES, Peacock WJ, Trevaskis B. Vernalization-induced flowering in cereals is associated with changes in histone methylation at the VERNALIZATION1 gene. *P Natl Acad Sci USA* 2009;106:8386-91.
- Fowler DB, Chauvin LP, Limin AE, Sarhan F. The regulatory role of vernalization in the expression of low-temperature-induced genes in wheat and rye. *Theor Appl Genet* 1996b;93:554-59.
- Mahfoozi S, Limin AE, Hayes PM, Hucl P, Fowler DB. Influence of photoperiod response on the expression of cold hardiness in wheat and barley. *Can J Plant Sci* 2000;80:721-4.
- Mahfoozi S, Limin AE, Fowler DB. 2001. Developmental regulation of low-temperature tolerance in winter wheat. *Annals of Botany* 87, 751–757.
- Limin A, Fowler DB. Low-temperature tolerance and genetic potential in wheat (*Triticum aestivum* L.): response to photoperiod, vernalization, and plant development. *Planta* 2006;224:360-6.

## Material and Methods

**Determination of cold tolerance and phenological development stage.** For  $LT_{50}$  determination, actively germinating seeds were transferred to plastic trays (40 x 25 x 15 cm) filled with mixture of soil, loamy sand and soft mold leaves (2:1:1) and returned to germinating conditions. Germinated seeds were then grown at 20 °C under 12 h day lengths at a light intensity of  $350 \mu\text{mol m}^{-2} \text{s}^{-1}$  for 14 d before being exposed to 4 °C for cold acclimation. The procedure outlined by Limin and Fowler (1988) was used to determine the  $LT_{50}$  of Cheyenne cultivar at the 0 d (14 d establishment with no exposure to cold), 63 d acclimation and vernalization treatment at 4 °C and 63 d at 20 °C (no exposure to cold). At the end of each treatment plant crowns were covered in moist sand in aluminum weighing cans and placed in a programmable freezer that was held at -3 °C for 12 h. After 12 h, they were cooled at a rate of 2 °C/h down to -17 °C, then cooled at 8 °C/h. Five crowns were removed at 4 °C intervals for each of eight test temperatures in each replication. Samples were then thawed overnight at 4 °C. Thawed crowns were planted into flats containing soil, sand and soft mold leaves (2:1:1) that was kept moist. The flats were placed in a growth room maintained at 20 °C with a 16 h day/8 h night. Plant recovery was rated (alive vs. dead) after 3 weeks and a  $LT_{50}$  was calculated for each treatment. At the end of each cold-acclimation period (0, 21, 42, and 63 days), pots containing two plants were moved to 20 °C until flag leaf emergence and leaf numbered on the main shoot. The control non-vernalized seedlings were maintained continuously at 20 °C with the same light intensity and length. Two methods were used to determine the stage of phenological development: (i) dissection of the plant crown to reveal the shoot apex development, and (ii) the FLN procedure (Fowler et al., 1996b; Mahfoozi et al., 2001). Plants for FLN measurements were grown in 15 cm pots filled with mixture of field soil, loamy sand and soft mold leaves (2:1:1) (2 plants/pot). Plants were uniformly watered and fertilized with sustained-release fertilizer and a nutrient-complete water-soluble solution. Measurements of FLN were made in a three-replicate completely randomized design (CRD) with a 1 (cultivar) x 4 (vernalization period) factorial arrangement. Analysis

of variance (ANOVA) was conducted by Multi-Factorial Balanced model in Minitab Statistical software. Duncan's Multiple Range Test at 5 % probability level was used for mean comparisons. Finally, shoot apices of plants were dissected, recorded and photographed at each sampling date to determine when the double ridge (DR) occurred.

**Proline content.** Proline content was estimated at intervals of 0, 21 and 42 days following the method described by Bates et al. (1973). 0.5 g (fresh weight) of spring wheat leaves were homogenized with 3% sulphosalicylic acid and centrifuged. The supernatant was treated with acetic acid and acid-ninhydrin and boiled for 1 h. The mixture was eluted in benzene and the absorbance was read at 520 nm using a Cary 4 Varian spectrophotometer.

**Soluble sugar extraction.** Total water soluble carbohydrate determination was based on the phenol sulphuric acid method of Dubois *et al.* (1956). Data were measured at 485 nm by a Cary 4 Varian spectrophotometer.

**Protein Extraction.** 1 g of wheat leaves (2-4 leaves above the crown on main stem samples) was finely ground in liquid nitrogen and the protein extraction was performed according to Damerval *et al.* (1986) with some modifications. Four biological replicates (different plants grown side by side in the same growth chamber) were used. The resulting powder was suspended (1 g/10 ml) in chilled (- 20 °C) 10% TCA in acetone containing 0.007% DTT and 1% plant protease inhibitor cocktail (P9599; Bio-Rad, Hercules, CA, USA). The mixture was incubated at - 20 °C for at least 1 h then centrifuged at 35000 g for 15 min. The pellet was washed three times (10 ml) with chilled (- 20 °C) acetone containing 0.007% DTT centrifuging at 12000 g at 4 °C for 15 min. The supernatant was removed and the pellet was lyophilized for 1 h. If dried powder was not to be solubilised immediately, it was stored at - 80 °C until use.

**Protein solubilisation and two-dimensional electrophoresis.** The wheat leaf proteins in the dried powder were solubilised in 9 M urea, 4% CHAPS, 1% DTT, 1% pH 3-10 ampholytes (Bio-lyte; Bio-Rad, Hercules, CA, USA), 35 mM Tris base via incubation at 37 °C for 1 h with continuous stirring. The mixture was centrifuged at 12000 g at room temperature for 15 min and a small aliquote was used to determine protein content by Bradford assay (Bradford, 1976). IEF was performed using Biorad Multiphore II and Dry Strip Kit (Bio-Rad-Protean-IEF-Cell-System). Seventeen centimeter IPG strips (Bio-Rad, Hercules, CA, USA) pH 4-7 were passively rehydrated overnight with 750 µg of protein in 300 µl of solubilisation solution containing 1% carrier ampholyte (Bio-lyte 4-7; Bio-Rad, Hercules, CA, USA). The total product time × voltage applied was 80 000 V h for each strip at 20 °C. Strips were subsequently reduced (1 % DTT, 15 min) and alkylated (2.5% IAA, 15 min) during the equilibration step (30 min in 50 mM Tris-HCl pH 8.8, 6 M urea, 30% glycerol v/v, 1% SDS, bromophenol blue). Equilibrated strips were then placed on SDS-polyacrylamide gels, 16 cm × 20 cm, 13% acrylamide, and sealed with 0.5% agarose. SDS-PAGE was performed using the Protean II xi Cell, large gel format (Bio-Rad) at constant current (40 mA per gel) at 7 °C until the bromophenol blue tracking dye was approximately 2–3 mm from the bottom of the gel. Protein spots were stained by Blue Silver (Candiano et al., 2004). To ensure protein pattern reproducibility, four replicates were done.

**Image Analysis.** Two dimension gel images were digitised using a flatbed scanner (model ImageScanner-II, GE Healthcare, Uppsala, Sweden) with a resolution of 300 dpi and 16-bit greyscale pixel depth. Image analysis was carried out with Progenesis SameSpots software vers. 2.0 (Nonlinear Dynamics), which allows spot detection, background subtraction, and protein spot OD intensity quantification (spot quantity definition). The gel image showing the highest number of spots and the best protein pattern was chosen as a reference template, and spots in a standard gel were then matched across all gels. Spot quantity values were normalised in each gel dividing the

raw quantity of each spot by the total quantity of all the spots included in the standard gel. For each protein spot, the average spot quantity value and its variance coefficient in each group was determined. One-way analysis of variance (ANOVA) was carried out at  $p < 0.05$  in order to assess for absolute protein changes among the different treatments; only 1.5-fold or higher quantitative variations were taken into consideration. The false discovery rate (FDR) was estimated by calculating q-values with a threshold of 0.05. The least significant difference (LSD) test was used to determine significant differences among group means.

**Functional annotation.** Gene Ontology (GO) lists were downloaded from the TAIR website (<http://www.arabidopsis.org/tools/bulk/go/index.jsp>): each protein was classified with respect to its cellular component, biological process, and molecular function using GO annotation. When no GO annotation was available, proteins were annotated manually based on literature searches and closely related homologues.

**In-Gel Digestion and Protein identification by MS/MS.** Protein spots were carefully cut out from Blue Silver stained gels and subjected to in-gel trypsin digestion according to Shevchenko *et al.* (1996) with minor modifications. Peptide mixtures were separated using a nanoflow-HPLC system (Ultimate; Switchos; Famos; LC Packings, Amsterdam, The Netherlands). A sample volume of 10  $\mu\text{L}$  was loaded by the autosampler onto a homemade 2 cm fused silica precolumn (75  $\mu\text{m}$  I.D.; 375  $\mu\text{m}$  O.D.; Reprosil C18-AQ, 3  $\mu\text{m}$ , Dr. Maisch GmbH, Ammerbuch-Entringen, Germany) at a flow rate of 2  $\mu\text{L}/\text{min}$ . Sequential elution of peptides was accomplished using a flow rate of 200 nL/min and a linear gradient from Solution A (2% acetonitrile; 0.1% formic acid) to 50% of Solution B (98% acetonitrile; 0.1% formic acid) in 40 minutes over the precolumn in-line with a homemade 10-15 cm resolving column (75  $\mu\text{m}$  I.D.; 375  $\mu\text{m}$  O.D.; Reprosil C18-AQ, 3  $\mu\text{m}$ , Dr. Maisch GmbH, Ammerbuch-Entringen, Germany). Peptides were eluted directly into a High Capacity ion Trap (model HCTplus, Bruker-Daltonik, Germany). Capillary voltage

was 1.5-2 kV and a dry gas flow rate of 10 L/min was used with a temperature of 230 °C. The scan range used was from 300 to 1800 m/z. Protein identification was achieved by searching the National Center for Biotechnology Information non-redundant database (NCBI nr, version 20081128, [www.ncbi.nlm.nih.gov](http://www.ncbi.nlm.nih.gov)) using the Mascot program (in-house version 2.2, Matrix Science, London, UK). The following parameters were adopted for database searches: complete carbamidomethylation of cysteines and partial oxidation of methionines, peptide Mass Tolerance  $\pm 1.2$  Da, Fragment Mass Tolerance  $\pm 0.9$  Da, missed cleavages 2. For positive identification, the score of the result of  $(-10 \times \log(P))$  had to be over the significance threshold level ( $P < 0.05$ ). Even though high MASCOT scores are obtained with values greater than 60, when proteins were identified with only one peptide a combination of automated database search and manual interpretation of peptide fragmentation spectra was used to validate protein assignments. In this manual verification, the mass error, the presence of fragment ion series, and the expected prevalence of C-terminus containing ions (Y-type) in the high mass range, were all taken into account. Moreover, replicate measurements have confirmed the identity of these protein hits.

**RNA extraction, cDNA synthesis and PCR.** Semi-quantitative RT-PCR was carried out following extraction of total leaf RNA by applying RNXplus (Fermentas) from the pulverized plant leaves, followed by phenol/chloroform/extraction, isopropanol precipitation and ethanol wash. The extracted RNA was reverse transcribed using the Roche cDNA synthesis kit, as per manufacturer's instructions. The synthesised cDNA was used in the subsequent PCR by applying specific primers designed for *tubulin* as an internal control housekeeping gene and three other genes whose expression was subjected to change in response to cold stress (*wcor18*, protein spots No. 32, 96; *wrab17*, protein spots No. 39, 44, 90; *rbcS*, protein spots No. 6, 62, 178). The primer pairs used for amplification are listed in Table 1. PCR conditions were identical except for the annealing temperature which was adjusted for each gene as required. Specifically, 60 °C and 35

cycles were used for *tubulin*, *rbcS* and *Wrab17* genes, while a two step annealing procedure was used for *Wcor18* amplification so that a primary gradient amplification for 16 cycles starting from 52 °C and terminating at 60 °C was used to enhance amplification of *Wcor18* followed by 30 cycles of annealing at 60 °C. Apart from annealing, all other conditions of PCR were the same so that initial denaturation was at 94 °C for 4 min followed by denaturation at 94 °C 1 min, annealing 1 min according to the above description, 72 °C extension for 1 min and final extension for 5 min.



Gene	Forward 5'-3'	Reverse 5'-3'
<i>tubulin</i>	TGATGCTTTCAACACCTTCTTCAG	GGGGCGTAGGAGGAAAGCA
<i>Wcor18</i>	TACACGCTGGAGGGGCAGGGC	CCGGGCTGCTTCCAGTCGTTGAC
<i>Wrab17</i>	GGCTGTCACGAAGGCTGCCTC	CCTGCTGGAAGACGTTTTCCTTGG
<i>rbcS</i>	GAGGGCATCAAGAAGTTCGAGACC	TCAGGGTACTCCTTCTTGACCTCC

**Table 1.** Primer sequences used for RT-PCR assays.

## References

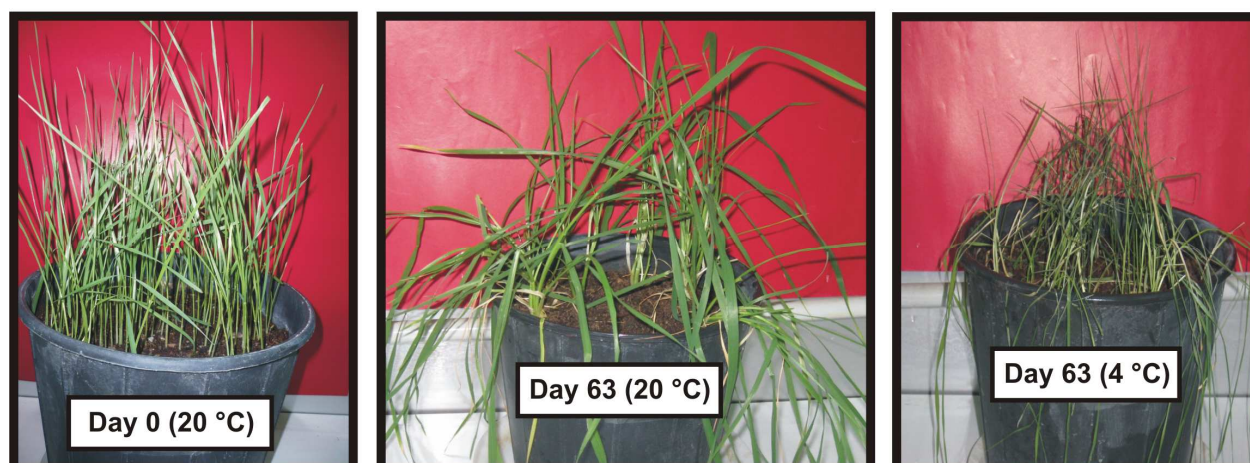
- Bates LS. Rapid determination of free proline for water stress studies. *Plant Soil* 1973;39:205-207.
- Bradford MM. A Rapid and Sensitive Method for the Quantitation of Microgram Quantities of Protein Utilizing the Principle of Protein-Dye Binding. *Anal Biochem* 1976;72:248-54.
- Candiano G, Bruschi M, Musante L, Santucci L, Ghiggeri GM, Carnemolla B, Orecchia P, Zardi L, Righetti PG. Blue silver: a very sensitive colloidal Coomassie G-250 staining for proteome analysis. *Electrophoresis* 2004;25:1327-33.
- Damerval C, De Vienne D, Zivy M, Thiellement H. Technical improvements in two-dimensional electrophoresis increase the level of genetic variation detected in wheat-seedling proteins. *Electrophoresis* 1986;7:52-4.
- Dubois MK, Gils JK, Hanniton PA, Robes L, Smith F. Colorimetric Method for Determination of Sugars and Related Substances. *Anal Chem* 1956;28:350-356.
- Fowler DB, Chauvin LP, Limin AE, Sarhan F. The regulatory role of vernalization in the expression of low-temperature-induced genes in wheat and rye. *Theor Appl Genet* 1996b;93:554-59.
- Limin AE, Fowler DB. Cold hardiness expression in interspecific hybrids and amphiploids of the Triticeae. *Genome* 1988;30:261-5.
- Mahfoozi S, Limin AE, Fowler DB. Developmental regulation of low-temperature tolerance in winter wheat. *Ann Bot-London* 2001;87:751-7.
- Shevchenko A, Wilm M, Vorm O, Mann M. Mass spectrometric sequencing of proteins silver-stained polyacrylamide gels. *Anal Biochem* 1996;68:850-8.

## RESULTS

### Phenological development and low-temperature tolerance

For our study, plants of the winter wheat variety Cheyenne were grown at room temperature (RT) for 14 days under a 12 h photoperiod (experimental day 0), then half were transferred to 4 °C low-temperature growth chamber over 63 days of cold-acclimation. The remaining plants were left to grow at room temperature for the same period. Growth morphology of 14-d establishment plants (0-day cold treatment) was not much different from 63-d cold acclimated plants, as 0-d and 63-d were in 2 and 4 leaves growth stage, respectively. On the contrary, plants grown in continuous 20 °C conditions produced about 24 leaves (Figure 1). To exactly establish phenological development stages of wheat plants used in this study, both FLN (final leaf number) measurements and shoot apex dissection were performed. Analysis of variance for the FLN (Table 2) showed that differences of FLN due to the days of vernalization were highly significant ( $p < 0.001$ ). When grown at continuous 20 °C compared to a 21, 42 and 63-d pretreatment at 4 °C, Cheyenne wheat (CNN) showed a reduced FLN from 24 to 12.5 (Table 3), indicating that it is a winter habit genotype with a vernalization requirement (Mahfoozi et al., 2001). Moreover, FLN became constant (12.5) between 42 and 63 days of vernalization (vernalization fulfillment), indicating that a long vernalization requirement period in this winter cultivar causes a delay in its transition from the vegetative to the reproductive phase. On the other hand, double ridge (DR) formation, when leaf and spikelet initials are both apparent on the shoot apex, is considered to be another clear indication that transition to the reproductive phase occurred (McMaster, 1997). Interestingly, double ridge formation was not observed for 0-d and 42-d cold treated CNN plants (Figure 2, panels A-B), whereas beginning of shoot apex elongation was visible in 63-d cold treated plants (Figure 2C). Thus, vernalization fulfillment did not coincide with the physical manifestation of DR formation which is generally considered an unquestionable sign of floral initiation (Hay and Ellis, 1998). These observations showed conclusively that 63-d represented the time-point

after vernalization saturation where flowering processes were undoubtedly in progress and for this reason was chosen for proteomic analysis. On the other hand, the  $LT_{50}$  (lethal temperature at which 50% of the plants are killed) value of CNN at 63-d cold acclimation treatment was  $-9.0 \pm 0.8$  (mean  $\pm$  SE;  $n = 3$ ) °C indicating the ability of plants to cold acclimate after vernalization saturation, while the  $LT_{50}$  of CNN at 0-d (14 d RT) and 63-d warm (no exposure to cold) was  $-2.0 \pm 0.0$  (mean  $\pm$  SE;  $n = 3$ ) °C. Interestingly, plants grown at continuous 20 °C conditions maintained in the vegetative stage for a long time and produced more leaves, while plants vernalized at 4 °C for 63 days and then moved to 20 °C (devernalization) emerged its flag leaf shortly after moving to the warm long-day condition (20 °C, 16h day-length) indicating the highly progressed phenological development toward flowering stage (data not shown).



**Figure 1.** Response of Cheyenne winter wheat cultivar to prolonged cold stress

Source	df	SS	MS	F
Days of vernalization	3	10.146	3.3819	24.90***
Error	12	1.630	0.1358	
Total	15	11.776		

df, degrees of freedom; SS, sum of squares; MS, mean square; F, variance ratio. \*\*\*  $p < 0.001$

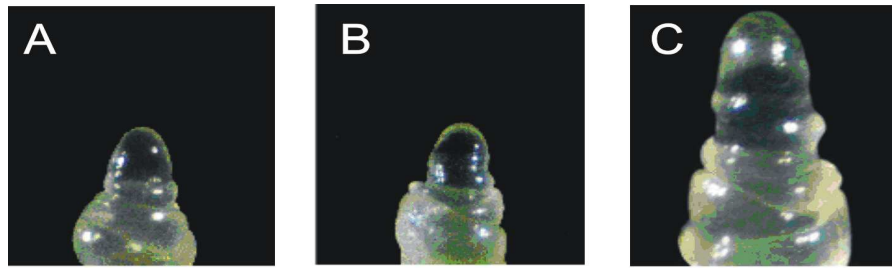
**Table 2.** Summary of the ANOVA one-way analysis on the basis of completely randomized design (CRD) for final leaf number (FLN) in Cheyenne cultivar.

	Days of vernalization	FLN
	0	24.00 <sup>a</sup> $\pm$ 0.41
	21	15.50 <sup>b</sup> $\pm$ 0.29
	42	12.50 <sup>c</sup> $\pm$ 0.29
	63	12.25 <sup>c</sup> $\pm$ 0.00
CV %		1.6
MS		1.134***

Means with the same symbol letters are not significantly different ( $p > 0.05$ ) from each other according to Duncan's multiple range test.

CV, coefficient of variation; MS, mean square. \*\*\*  $p < 0.001$

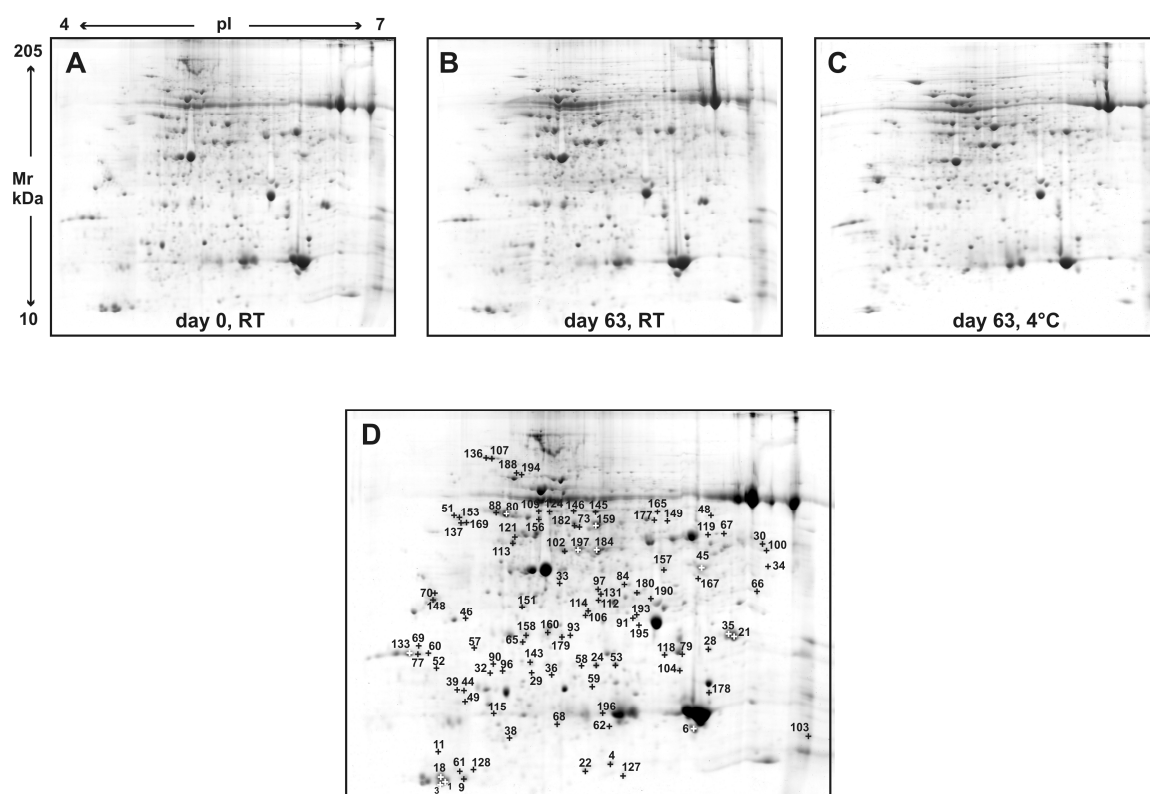
**Table 3.** Mean comparison for final leaf number (FLN) in Cheyenne cultivar.



**Figure 2.** Phenological development stage of Cheyenne (CNN) winter wheat cultivar grown at 4 °C as estimated from shoot apex developmental morphology. A, Shoot apex elongation and single ridge stage of 14-d establishment CNN (0-d cold treatment); B, Shoot apex elongation and single ridge stage of 42-d cold acclimated CNN plants; C, Double ridge stage of 63-d cold acclimated CNN plants.

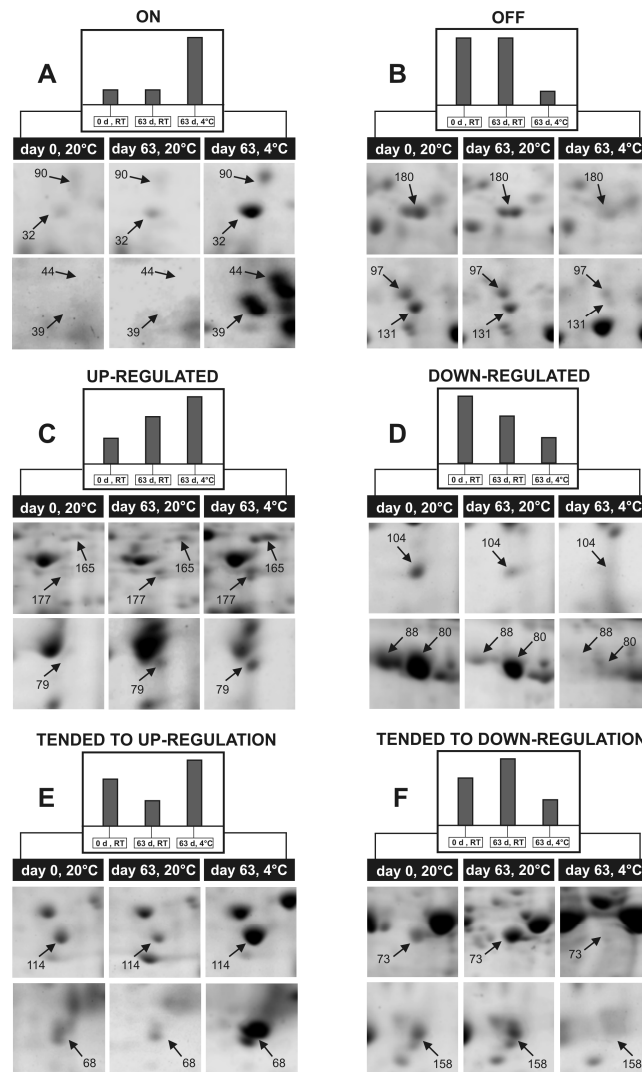
### **Proteome changes in wheat leaves upon exposure to low temperatures**

Figure 3 shows three representative 2DE maps obtained from day 0 (14 d, RT), 63 days at room temperature and 63 days at 4 °C. Each stage of leaf treatment was analyzed in four biological and technical replicates. Approximately 1000 spots could be detected on each gel (Figure 3A-C). Among these spots, 732 could be reliably matched on all the gels and these were included in the statistical analysis. A one-way ANOVA analysis identified 101 spots with significantly different expression levels ( $p < 0.05$ , absolute variation of at least 1.5-fold). These protein spots (indicated with numbers in the reference map showed in Figure 3D) were excised from the gels and digested by trypsin. Peptide mixtures were then analyzed by LC-ESI-MS/MS for protein identification.



**Figure 3.** Representative 2-DE gels of leaf tissues from day 0 (A), 63 days at room temperature (B) and 63 days at 4°C (C). Linear IPGs pH 4-7, 17 cm length. Panel D shows the reference map derived from computerized image analysis performed by using Progenesis SameSpots software. Numbers indicate the differentially expressed proteins.

Table 4 lists the successfully identified proteins, together with the protein spot number, the identification parameters, and the indication of their GO (gene ontology) annotation (cellular component, biological process, and molecular function). An additional table listing peptide sequences of identified proteins is provided in the final section of the thesis “Supporting Information”. Figure 4 displays details of specific gel regions in order to appreciate quantitative changes caused by development and/or vernalization treatment.



**Figure 4.** Close-up views of some 2D-gel regions showing examples of the observed variation patterns in protein spot intensity. A: on; B: off; C: up-regulated; D: down-regulated; E: tended to up-regulation; F: tended to down-regulation. Numbers of spots indicated by the arrows refer to the master map shown in Fig. 3D.



Protein name	Spot No. <sup>a</sup>	Mr, kDa theor/ exper <sup>b</sup>	pI theor/ exper <sup>b</sup>	NCBI GI No.	Homologue At <sup>c</sup>	No. of peptides	Mascot Score	1-ANOVA <sup>d</sup>	Fold of variation (63 d 20 °C/63 d 4°C) <sup>e</sup>	GO process	GO comp	GO funct
OFF												
Oxygen-evolving enhancer protein 2 [Triticum aestivum]	35	27.4/28.1	8.8/6.3	gi 131394	At1g06680	10	752	5.9x10 <sup>-8</sup>	- 0.0082/- 0.8698	photosynthesis	chloroplast	oxygen evolving activity
ATPase, beta subunit [Hordeum vulgare]	57	53.9/24.8	5.1/4.8	gi 11583	AtCg00480	3	162	4.2x10 <sup>-4</sup>	- 0.0121/- 0.7479	electron transport coupled to ATP synthesis		hydrogen ion transmembrane transporter activity
Oxygen-evolving enhancer protein 1 [Triticum aestivum]	61	35.0/13.0	8.7/4.7	gi 131388	At5g66570	1	104	2.0x10 <sup>-3</sup>	+ 0.0254/- 0.7133	photosystem II assembly		oxygen evolving activity
Acyl carrier protein 1, chloroplast precursor [Hordeum vulgare]	69	16.2/25.0	5.7/4.4	gi 113165	At4g25050	2	98	5.0x10 <sup>-3</sup>	- 0.0251/- 0.7159	fatty acid biosynthetic process		acyl carrier activity
Os08g0478200 ATP synthase D chain, mitochondrial [Oryza sativa (japonica cultivar-group)]	118	19.7/24.0	5.2/5.9	gi 115476908	At3g52300	3	150	1.4x10 <sup>-6</sup>	+ 0.0037/- 0.4668	electron transport coupled to ATP synthesis	mitochondrion	hydrogen ion transporting ATPase/ synthase activity
Os08g0382400 cyclophilin-type peptidylprolyl cis- trans isomerase [Oryza sativa (japonica cultivar-group)]	169	46.8/56.4	4.8/4.7	gi 115476198	At3g01480	7	367	3.1x10 <sup>-2</sup>	+ 0.0043/- 0.3779	photosynthesis	chloroplast	peptidyl-prolyl cis-trans isomerase activity
2-Cys peroxiredoxin BAS1, chloroplastic [Triticum aestivum]	179	23.4/27.0	5.7/5.3	gi 2829687	At5g06290	3	166	5.9x10 <sup>-5</sup>	+ 0.0041/- 0.3271	response to cold		peroxiredoxin activity
Os02g0634500 [Oryza sativa (japonica cultivar-group)]	180	32.1/35.5	6.7/5.8	gi 115447465	At5g23140	2	112	9.2x10 <sup>-6</sup>	+ 0.0167/- 0.3100	proteolysis		clp protease
ferredoxin-NADP(H) oxidoreductase [Triticum aestivum]	197	40.5/47.2	6.9/5.4	gi 20302473	At5g66190	2	175	3.0x10 <sup>-3</sup>	- 0.0661/- 0.2971	electron transport coupled to ATP synthesis		electron transporter
Os03g0278900 ATP synthase B/B' CF(0) [Oryza sativa (japonica cultivar-group)]	115	22.8/18.1	5.8/4.9	gi 115452259	At4g32260	4	208	9.0x10 <sup>-3</sup>	+ 0.1894/- 0.2838			hydrolase activity

Phosphoribulokinase, chloroplast precursor [Triticum aestivum]	121	45.5/53.1	5.7/5.0	gi 125580	At1g32060	16	855	2.0x10 <sup>-2</sup>	- 0.0479/ - 0.5437	carbon utilization by fixation of carbon dioxide	chloroplast	phosphoribulokinase activity
Sedoheptulose-1,7-bisphosphatase, chloroplast precursor [Triticum aestivum]		42.5/53.1	6.0/5.0	gi 1173347	At3g55800	11	588	2.0x10 <sup>-2</sup>				sedoheptulose-bisphosphatase activity
hypothetical protein OsJ_031021 [Oryza sativa (japonica cultivar-group)]	128	20.1/13.2	9.0/4.8	gi 125575528	At4g01150	3	107	8.0x10 <sup>-3</sup>	+ 0.0868/- 0.3849	metabolic processes	chloroplast	serine carboxypeptidase activity
OSJNBa0041A02.10 [Oryza sativa (japonica cultivar-group)]	131	38.0/35.1	8.8/5.6	gi 38344143	At4g09010	3	172	3.4x10 <sup>-6</sup>	+ 0.0277/- 0.4213	response to oxidative stress	cytoplasm	peroxidase activity
FtsH-like protein Ptf precursor [Nicotiana tabacum]	143	74.5/23.5	6.0/5.1	gi 4325041	At2g30950	4	216	1.0x10 <sup>-3</sup>	+ 0.0805/- 0.3547	protein catabolic process	thylakoid membrane	ATPase activity
RuBisCO small chain, chloroplast precursor [Hordeum vulgare]	178	19.7/20.6	9.0/6.2	gi 3914588	At1g67090	5	221	1.6x10 <sup>-2</sup>	+ 0.0473/- 0.3312	carbon utilization by fixation of carbon dioxide	chloroplast	ribulose-bisphosphate carboxylase activity
mitochondrial ATP synthase precursor [Triticum aestivum]	190	27.1/34.6	7.7/5.9	gi 47607439	At2g21870	10	604	2.0x10 <sup>-3</sup>	+ 0.1062/- 0.2113	electron transport coupled to ATP synthesis	mitochondrion	unknown
Os07g0469100 thylakoid membrane phosphoprotein 14 kDa [Oryza sativa (japonica cultivar-group)]	9	15.8/12.5	9.4/4.7	gi 115472001	At1g52220	2	106	7.0x10 <sup>-9</sup>	+ 0.0574/- 1.2379	unknown	chloroplast	unknown
Os03g0843400, 30S ribosomal protein S6, chloroplast precursor [Oryza sativa (japonica cultivar-group)]	36	23.3/22.2	7.8/5.2	gi 115456525	At1g64510	1	70	4.4x10 <sup>-5</sup>	+ 0.0460/- 0.8308	translation, ribosome biogenesis	ribosome	structural constituent of ribosome
Os10g0502000, thylakoid lumenal 17.4 kDa protein [Oryza sativa (japonica cultivar-group)]	38	25.0/15.5	7.5/5.0	gi 115482792	At1g12250	2	137	7.4x10 <sup>-5</sup>	+ 0.0329/- 0.8191	unknown	chloroplast	unknown
Translationally-controlled tumor protein homolog (TCTP) [Triticum aestivum]	46	18.9/30.4	4.5/4.7	gi 75246527	At3g16640	3	175	2.0x10 <sup>-3</sup>	+ 0.1370/- 0.7138	regulation of cell growth	cytoplasm	calcium binding and microtubule stabilization
RuBisCO small subunit [Triticum aestivum]	62	19.7/17.0	9.1/5.6	gi 11990893	At1g67090	6	253	5.3x10 <sup>-5</sup>	+ 0.1056/- 0.5908	carbon utilization by fixation of carbon dioxide	chloroplast	ribulose-bisphosphate carboxylase activity
Os04g0459500 glyceraldehyde-3-phosphate dehydrogenase [Oryza sativa (japonica cultivar-group)]	97	43.0/35.9	7.6/5.5	gi 115458768	At1g12900	4	239	1.3x10 <sup>-4</sup>	+ 0.1190/- 0.4405			glyceraldehyde-3-phosphate dehydrogenase activity

fructose-bisphosphate aldolase [Zea mays]	102	42.0/47.1	7.6/5.3	gi 195634659	At2g21330	10	577	1.0x10 <sup>-3</sup>	- 0.1030/- 0.5283	carbon utilization by fixation of carbon dioxide	chloroplast	fructose-bisphosphate aldolase activity
putative oxygen-evolving complex precursor [Triticum aestivum]	103	21.1/16.3	9.7/6.8	gi 134290407	At1g14150	6	280	2.4x10 <sup>-4</sup>	+ 0.1038/- 0.4061	photosynthesis		oxygen evolving activity
ATP synthase CF1 beta subunit [Triticum aestivum]	109	53.9/60.0	5.1/5.2	gi 14017579	AtCg00480	9	536	5.0x10 <sup>-3</sup>	- 0.0090/- 0.5002	electron transport coupled to ATP synthesis		hydrogen ion transmembrane transporter activity
ON												
Os06g0608700 Fructose-1,6-bisphosphate aldolase [Oryza sativa (japonica cultivar-group)]	30	38.0/50.1	7.6/6.6	gi 115468886	At4g26530	5	311	8.3x10 <sup>-5</sup>	+ 0.1532/+ 0.9084	carbon utilization by fixation of carbon dioxide	chloroplast	fructose-bisphosphate aldolase activity
cold regulated protein (wcor18) [Triticum aestivum]	32	17.8/22.4	4.8/4.8	gi 26017213	At5g01300	4	304	3.3x10 <sup>-4</sup>	+ 0.0965/+ 0.9121	unknown	unknown	phosphatidylethanol amine binding
	96	17.8/22.6	4.8/5.0			4	238	4.0x10 <sup>-3</sup>	+ 0.0417/+ 0.5122			
cold-responsive LEA/RAB-related COR protein (wrab17) [Triticum aestivum]	39	17.1/20.7	4.8/4.7	gi 7716956	At3g15670	6	376	1.0x10 <sup>-3</sup>	- 0.0009/+ 0.8454	developmental processes	nucleus	unknown
	44	17.1/20.6	4.8/4.7			2	98	8.0x10 <sup>-5</sup>	+ 0.1086/+ 0.8314			
group3 late embryogenesis abundant protein (wrab17) [Triticum aestivum]	90	18.3/23.2	5.0/4.8	gi 157073742	At3g15670	9	629	4.1x10 <sup>-2</sup>	+ 0.1105/+ 0.6649	developmental processes	nucleus	unknown
cytosolic NADP <sup>+</sup> -isocitrate dehydrogenase [Populus tremula]	48	47.2/58.2	6.1/6.2	gi 75267781	At1g65930	7	388	6.1x10 <sup>-5</sup>	+ 0.1067/+ 0.7592	metabolic processes	cytoplasm	isocitrate dehydrogenase (NADP <sup>+</sup> ) activity
cytosolic malate dehydrogenase [Triticum aestivum]	119	24.5/54.1	6.6/6.2	gi 37928995	At5g43330	4	230	8.0x10 <sup>-3</sup>	- 0.1211/ + 0.3856	glycolysis	plasma membrane	malate dehydrogenase activity
Os12g0244100 molecular chaperone DnaK [Oryza sativa (japonica cultivar-group)]	136	74.3/91.0	5.1/4.8	gi 115487998	At5g28540	17	1118	1.7x10 <sup>-6</sup>	- 0.0470/+ 0.3849	protein folding	chloroplast plasma membrane	ATP binding
RuBisCO activase A, chloroplastic [Hordeum vulgare]	146	51.4/60.1	8.0/5.4	gi 12643756	At2g39730	14	928	6.0x10 <sup>-5</sup>	- 0.0663/+ 0.3530	response to cold	chloroplast	RuBisCO activase activity
cp31BHv [Hordeum vulgare subsp. vulgare]	148	30.7/33.9	4.8/4.5	gi 3550483	At4g24770	9	553	6.1x10 <sup>-5</sup>	-0.0523/+ 0.3607	RNA processing	chloroplast envelope	poly(U) binding RNA binding
Plastid glutamine synthetaseGS2b [Triticum aestivum]	156	47.0/57.6	6.0/5.2	gi 71362638	At5g35630	2	107	3.4x10 <sup>-4</sup>	+ 0.0535/+ 0.3982	aging, ammonia assimilation cycle	chloroplast	glutamate-ammonia ligase activity
protein disulfide	194	56.8/77.0	5.0/5.0	gi 13925723	At1g21750	20	1296	5.8x10 <sup>-4</sup>	+ 0.0527/+ 0.3087	developmental	vacuole	protein disulfide

isomerase 1 precursor [Triticum aestivum]										processes		isomerase activity
Os02g0259600, 50S ribosomal protein L21, chloroplast precursor [Oryza sativa (japonica cultivar-group)]	195	23.4/29.2	6.2/5.8	gi 115445399	At1g35680	2	98	1.2x10 <sup>-2</sup>	+ 0.0588/+ 0.3213	response to cold, translation	ribosome	structural constituent of ribosome
putative fructokinase [Oryza sativa Japonica Group]	113	43.8/49.6	6.0/5.0	gi 51535181	At2g31390	6	345	5.6x10 <sup>-4</sup>	+ 0.1855/ + 0.6250	sucrose metabolic process	plasma membrane	kinase activity
Plastid glutamine synthetase GS2c [Triticum aestivum]	153	47.0/57.0	5.7/4.7	gi 71362640	At1g66200	8	488	1.0x10 <sup>-3</sup>	- 0.0518/+ 0.3396	nitrate assimilation	chloroplast	glutamate-ammonia ligase activity
DOWN-REGULATED												
plastocyanin precursor [Hordeum vulgare]	3	15.8/12.2	5.6/4.6	gi 22705	At1g76100	1	77	9.4x10 <sup>-4</sup>	- 0.2445/- 1.8874	electron transport coupled to ATP synthesis	chloroplast	copper ion binding
Oxygen-evolving enhancer protein 2 [Triticum aestivum]	4	27.4/13.5	8.8/5.6	gi 131394	At1g06680	3	255	1.9x10 <sup>-4</sup>	- 0.2411/- 1.7634	photosynthesis	chloroplast	oxygen evolving activity
RuBisCO small subunit [Triticum aestivum]	45	19.7/42.1	9.1/6.2	gi 11990893	At1g67090	10	483	2.0x10 <sup>-3</sup>	- 0.5222/ - 0.7602	carbon utilization by fixation of carbon dioxide	chloroplast	ribulose- biphosphate carboxylase activity
RuBisCO large chain [Avena sativa]	66	53.5/35.5	5.9/6.4	gi 1346964	AtCg00490	4	212	3.6x10 <sup>-4</sup>	- 0.0603/- 0.6772			
Glutamine synthetase chloroplast precursor [Hordeum vulgare]	80	47.4/59.0	5.1/5.0	gi 121340	At5g37600	9	604	1.8x10 <sup>-5</sup>	- 0.1029/ - 0.5976	nitrate assimilation	chloroplast	glutamate-ammonia ligase activity
	88	47.4/59.9	5.1/4.9			11	649	6.9x10 <sup>-4</sup>	- 0.1251/- 0.5850			
oxygen-evolving enhancer protein 1 [Leymus chinensis]	104	34.7/22.8	6.1/6.0	gi 147945622	At5g66570	5	297	1.9x10 <sup>-5</sup>	- 0.1333/- 0.5183	photosystem II assembly and stabilization	chloroplast	oxygen evolving activity
Os08g0162800 Acyl-CoA binding protein [Oryza sativa (japonica cultivar-group)]	127	10.1/12.9	5.2/5.7	gi 115474931	At5g53470	3	134	3.0x10 <sup>-3</sup>	- 0.1407/- 0.4776	lipid transport	plasma membrane	acyl-CoA binding
UP-REGULATED												
S-adenosylmethionine synthetase 1 [Triticum monococcum]	165	43.2/60.0	5.6/5.9	gi 115589744	At4g01850	6	414	5.1x10 <sup>-4</sup>	+ 0.0403/+ 0.3681	S-AdoMet biosynthetic process	cell wall	methionine adenosyltransferase activity
Os01g0104400, ricin B- related lectin domain containing protein [Oryza sativa (japonica cultivar-group)]	67	30.3/54.9	6.3/6.3	gi 115434012	At2g39050	2	83	2.8x10 <sup>-5</sup>	+ 0.2224/+ 0.6793	unknown	unknown	unknown
Patatin-13 precursor [Solanium tuberosum]	79	42.4/24.0	5.5/6.0	gi 122201873	At4g37070	6	360	2.4x10 <sup>-4</sup>	+ 0.3515/ + 0.5694	lipid metabolic process		nutrient reservoir activity

												enzymatic activity
Os02g0634900 proteasome alpha type 2 [Oryza sativa (japonica cultivar-group)]	112	25.8/34.0	5.4/5.5	gi 115447473	At1g16470	9	555	3.1x10 <sup>-5</sup>	+ 0.1606/+ 0.4923	ubiquitin- dependent protein catabolic process	cytosolic ribosome proteasome complex	peptidase activity
RuBisCO small subunit [Triticum aestivum]	167	19.7/38.9	9.06/6.1	gi 11990893	At1g67090	5	224	6.0x10 <sup>-3</sup>	+ 0.2755/+ 0.3671	carbon utilization by fixation of carbon dioxide	chloroplast	ribulose- bisphosphate carboxylase activity
Os08g0532200 Acetyl ornithine aminotransferase family [Oryza sativa (japonica cultivar-group)]	177	50.4/57.2	6.5/5.9	gi 115477483	At3g48730	5	308	8.6x10 <sup>-5</sup>	+ 0.1909/+ 0.3372	porphyrin biosynthetic process		glutamate-1- semialdehyde 2,1- aminomutase activity
TENDED TO DOWN-REGULATION												
RuBisCO small subunit [Triticum aestivum]	6	19.7/16.9	9.1/6.1	gi 11990893	At1g67090	5	221	4.0x10 <sup>-6</sup>	+ 0.1447/ - 1.3347	carbon utilization by fixation of carbon dioxide	chloroplast	ribulose- bisphosphate carboxylase activity
Os07g0469100 thylakoid membrane phosphoprotein 14 kDa, [Oryza sativa (japonica cultivar-group)]	18	15.8/12.7	9.4/4.6	gi 115472001	At1g52220	2	96	1.7x10 <sup>-4</sup>	+ 0.1435/- 1.0091	unknown		unknown
ATP synthase CF1 beta subunit [Triticum aestivum]	33	53.9/37.4	5.1/5.3	gi 14017579	AtCg00480	12	800	1.6x10 <sup>-6</sup>	+ 0.3185/- 0.5652	electron transport coupled to ATP synthesis		hydrogen ion transmembrane transporter activity
VER2 Dirigent-like protein [Triticum aestivum]	34	32.5/42.2	6.7/6.6	gi 16151819	At4g11210	2	94	2.0x10 <sup>-3</sup>	+ 0.4677/- 0.4769	lignan biosynthetic process	endomembrane system	unknown
chloroplast oxygen-evolving enhancer protein 1 [Leymus chinensis]	58	34.7/23.0	6.1/5.4	gi 147945622	At5g66570	4	199	2.7x10 <sup>-7</sup>	+ 0.1688/- 0.5376	photosynthesis	chloroplast	oxygen evolving activity
Cyt b6-f complex iron- sulfur subunit, chloroplastic [Triticum aestivum]	59	24.1/21.3	8.8/5.5	gi 68566191	At4g03280	2	108	4.7x10 <sup>-8</sup>	+ 0.1677/- 0.5334	electron transport coupled to ATP synthesis		electron transporter
RuBisCO activase alpha form precursor [Deschampsia antarctica]	73	51.4/55.5	6.0/5.4	gi 32481061	At2g39730	13	881	7.0x10 <sup>-7</sup>	+ 0.2707/- 0.3358	response to biotic/abiotic stresses		RuBisCO activase activity
Os05g0110300 similar to Putative 3-beta hydroxysteroid dehydrogenase/ isomerase [Oryza sativa(japonica	84	31.4/37.1	9.1/5.7	gi 115461679	At5g02240	3	218	1.1x10 <sup>-4</sup>	+ 0.1398/- 0.4474	response to abscisic acid stimulus	plasma membrane	coenzyme binding

cultivar-group])												
2-Cys peroxiredoxin BAS1, chloroplastic [Triticum aestivum]	158	23.4/27.4	5.7/5.0	gi 2829687	At5g06290	9	479	3.9x10 <sup>-4</sup>	+ 0.1057/- 0.2864	response to cold	chloroplast	peroxiredoxin activity
LHC I [Hordeum vulgare]	160	24.4/28.1	8.1/5.2	gi 544700	At3g54890	5	283	5.7x10 <sup>-5</sup>	+ 0.1150/- 0.2679	photosynthesis		chlorophyll binding
ATP synthase CF1 epsilon subunit [Triticum aestivum]	196	15.3/18.3	5.2/5.6	gi 14017578	AtCg00470	10	554	3.9x10 <sup>-4</sup>	+ 0.1187/- 0.1790	electron transport coupled to cesis		hydrogen ion transmembrane transporter activity
Os01g0649100 malate dehydrogenase [Oryza sativa (japonica cultivar-group)])	100	35.7/47.6	8.7/6.6	gi 115438875	At1g53240	3	194	3.6x10 <sup>-4</sup>	+ 0.4282/- 0.1353	response to cold	mitochondrion	malate dehydrogenase activity
TENDED TO UP-REGULATION												
glycine-rich RNA-binding protein [Triticum aestivum]	68	16.0/17.2	6.3/5.3	gi 114145394	At2g21660	5	304	6.5x10 <sup>-8</sup>	- 0.1245/+ 0.5280	vegetative to reproductive phase transition of meristem	chloroplast	ss/ds DNA binding RNAbinding
putative chaperonin 21 precursor [Oryza sativa Japonica Group]	114	26.4/32.3	7.7/5.5	gi 51090748	At5g20720	5	246	1.4x10 <sup>-7</sup>	- 0.1332/+ 0.3483	response to cold	mitochondrion chloroplast	calmodulin binding
Phosphoglycerate kinase, chloroplast precursor [Triticum aestivum]	124	50.0/60.1	6.6/5.2	gi 129915	At1g56190	3	244	1.1x10 <sup>-2</sup>	- 0.2263/+ 0.2783	carbon utilization by fixation of carbon dioxide	chloroplast	phosphoglycerate kinase activity
RuBisCO activase alpha form precursor [Deschampsia antarctica]	159	51.4/56.1	6.0/5.5	gi 32481061	At2g39730	12	707	6.4x10 <sup>-7</sup>	- 0.1365/+ 0.2435	response to cold		RuBisCO activase activity
	182	51.4/56.2	6.0/5.4			18	1049	2.7x10 <sup>-4</sup>	- 0.1240/+ 0.2087			
fructose 1,6-bisphosphate aldolase precursor [Avena sativa]	184	42.1/47.2	9.0/5.5	gi 8272480	At4g38970	10	576	3.0x10 <sup>-3</sup>	- 0.0747/+ 0.2486	carbon utilization by fixation of carbon dioxide		fructose- bisphosphate aldolase activity
peptide methionine sulfoxide reductase; cPMSR [Gossypium barbadense]	193	28.8/31.7	8.4/5.8	gi 29469000	At4g25130	3	144	1.0x10 <sup>-3</sup>	- 0.1473/+ 0.1622	protein modification and metabolic process		peptide-methionine- (S)-S-oxide reductase activity

<sup>a</sup> Spot number represents the number on the master gel (see Figure 1)

<sup>b</sup> Theoretical Mr/pI was calculated with Mr/pI tool on the ExPASy web site ([http://expasy.org/tools/pi\\_tool.html](http://expasy.org/tools/pi_tool.html))

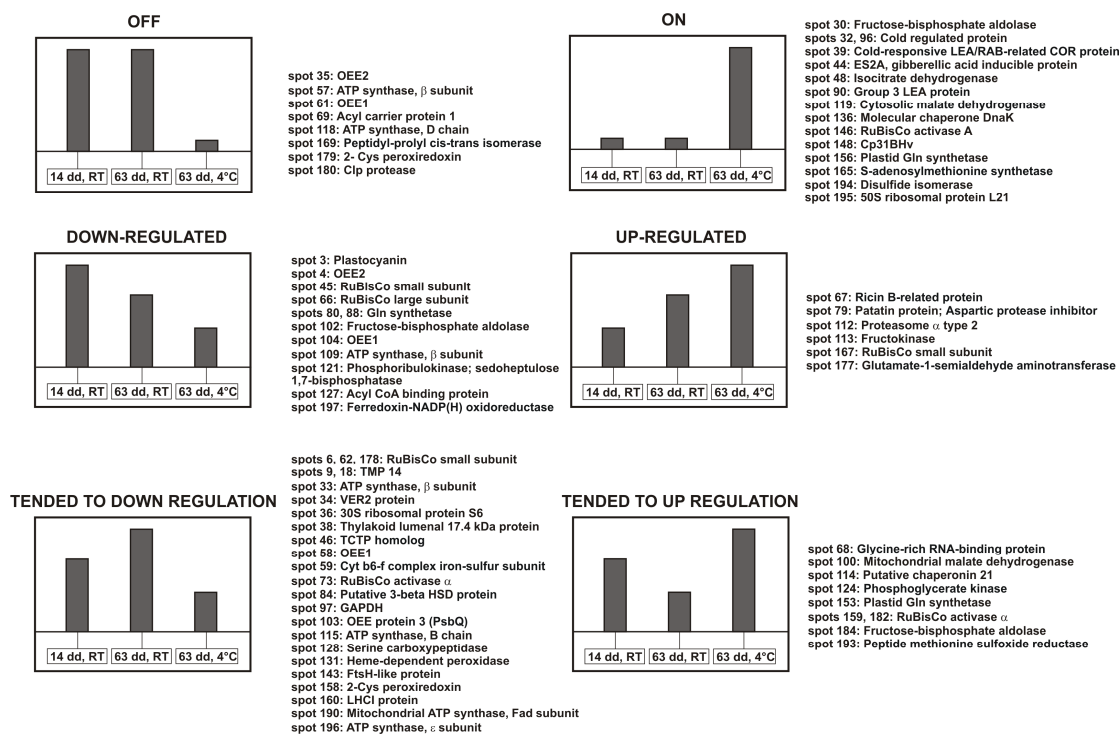
<sup>c</sup> TAIR Accession no. of the closest homologue in *Arabidopsis thaliana*

<sup>d</sup> p-value of one-way ANOVA analysis

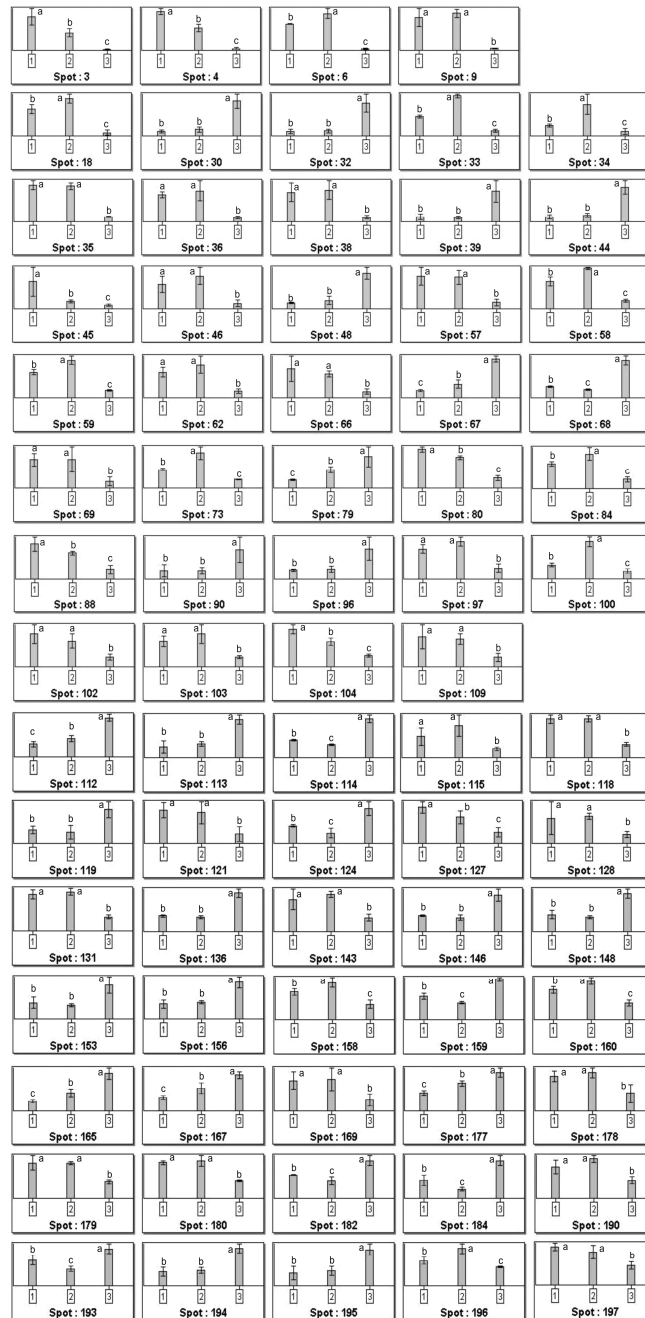
<sup>e</sup> Fold of protein variation is calculated by standardizing the mean of the normalized spot volumes of samples at 63 days 20 °C and at 63 days of cold treatment with the mean of the normalized spot volumes of the sample at day 0.

**Table 4.** List of differentially expressed proteins identified by LC-MS/MS

A schematic representation of main trends observed in spot modulations after quantitative analysis of 2-DE gels by Progenesis SameSpots software is provided in Figure 5, whereas spot quantification results are shown in Figure 6. To provide a classification of the differential proteins into functional categories, we used the automated MapMan annotation dataflow (Thimm et al., 2004). Figure 7 shows a global overview of the metabolic pathways and cellular processes mostly affected by 63-day cold treatment. Most of the proteins were related to metabolism (62.2 %), but also, among others, to the following MapMan based categories (BINs): stress (2.7 %), redox (4 %), RNA (2.7 %), protein (12.2 %), development (6.8 %), not assigned (9.4 %).

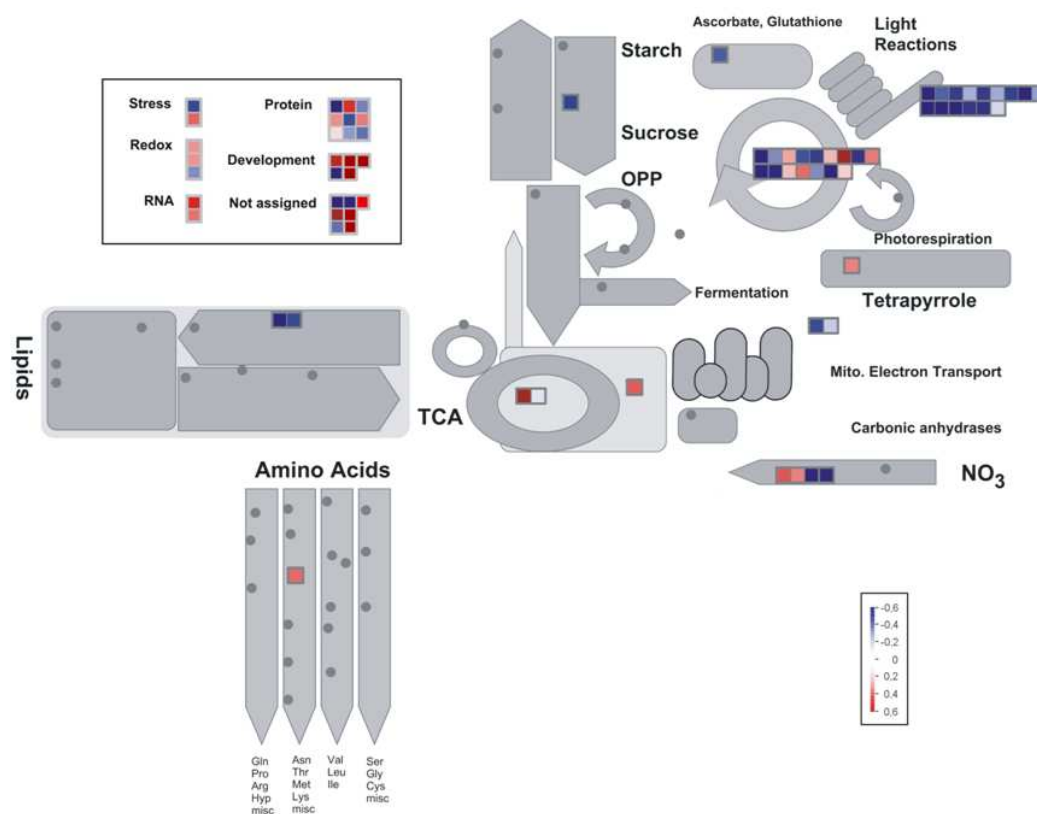


**Figure 5.** Schematic representation of main trends observed in spot modulations after quantitative analysis of 2-DE gels by Progenesis SameSpots software. Proteins identified are listed and grouped into the different categories.



**Figure 6 .** Histograms representing the mean of the spot normalized volumes for each treatment: **1** stands for sample at day 0 (14 days, room temperature), **2** means 63 days at room temperature, **3** is 63 days at 4 °C. Error bars indicate the SD of four replicates. The analysis was performed by Progenesis SameSpots software (Nonlinear Dynamics). The same letters above the bars indicate no statistically significant difference, whereas different letters indicate a statistically significant difference ( $p < 0.05$ ) according to the LSD (least significant difference) test.

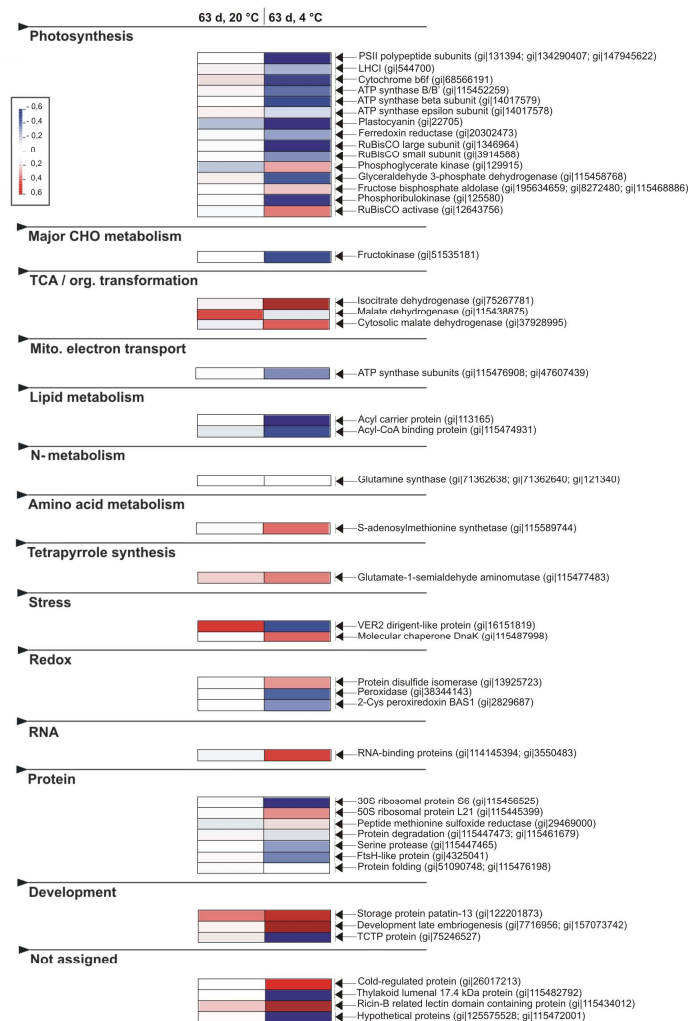




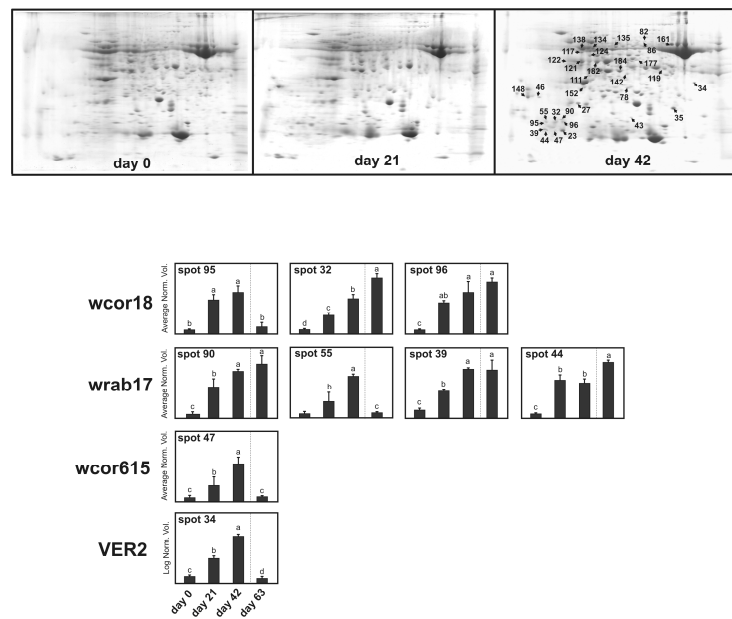
**Figure 7.** Visualization of cellular processes affected by prolonged cold acclimation using the MapMan software (<http://mapman.gabipd.org/>) (Thimm *et al.* 2004). Protein spots significantly up- and down-regulated in 63-day cold acclimated leaves with respect to day 0 are indicated with red and blue squares, respectively. Color scale bars display log normalized volumes. Gray dots are automatically assigned to empty subpathways by the program.

We also loaded quantitative data into the PageMan program (Usadel *et al.*, 2006) in order to have a direct comparison between growth and cold effects on wheat leaves (Figure 8). Although our analysis provided direct evidence for a programmed and precise cellular response raised by Cheyenne after prolonged cold stress, the question whether such modulations are also influenced by short term cold exposures needed to be addressed. For this reason, proteomic investigation was extended to intermediate time points (21 and 42 days). Results are presented in Figure 9, which also displays the expression trends of proteins whose involvement in cold acclimation has been assessed by many previous studies. Table 5 lists those proteins not classically involved in cold acclimation which shown a differential expression at these intermediate points, whereas Table 6 shows peptides of cold-related proteins identified by means of mass spectrometry. Only

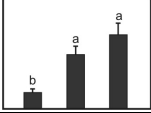
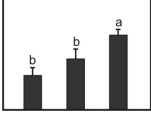
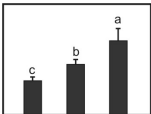
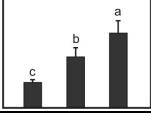
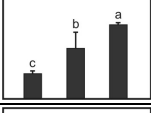
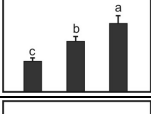
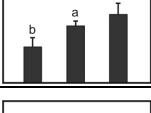
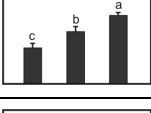
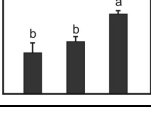
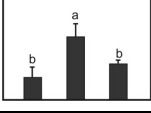
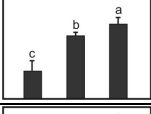
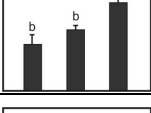
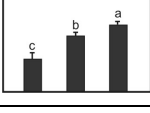
few new proteins were identified, thus confirming that the deepest changes at the protein expression level occurred at 63 days. However, the time-course monitoring of cold-induced expression of *Cor/Lea* gene products yielded interesting information about the development of cold hardiness in the examined winter wheat cultivar (Figure 9). Of particular interest was the maintenance of high expression level of wrab17 and wcor18 proteins even after vernalization fulfillment suggesting a fundamental correlation between their production and cold resistance. Multiple spots of both proteins were detected as a result of either post-translationally modified forms or different gene copies.

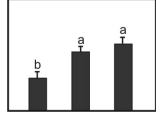
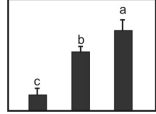
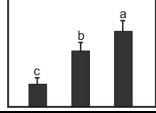
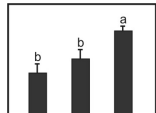
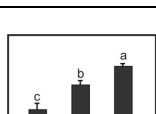

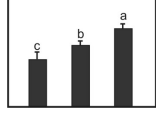
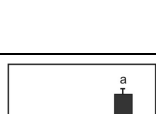
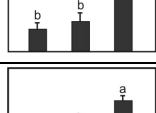
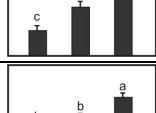
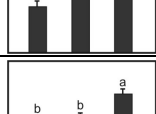


**Figure 8.** Growth and cold-induced changes in proteins, organized at the level of functional categories using the PageMan software (<http://mapman.mpimp-golm.mpg.de/pageman/>) (Usadel *et al.* 2006). For each protein, the difference between the expression level at the given data points (63 d, 20 °C; 63 d, 4 °C) and the control (day 0) was calculated and converted to a false color scale (increasing red and blue indicate an up- and down-regulation, respectively). Values are shown as log normalized volumes. The average change for all proteins in a functional category is presented.



**Figure 9.** 2-DE proteomic profiling of wheat leaves collected from plants grown at room temperature (day 0) or exposed to LT (4 °C) for 21 and 42 days. Lower panel shows quantitative variations (expressed as average normalized volume) of spots identified as typically cold-related proteins. The same letters above the bars indicate no statistically significant difference, whereas different letters indicate a statistically significant difference ( $p < 0.05$ ) according to the LSD (least significant difference) test.

Spot No. <sup>a</sup>	Protein name NCBI GI No.	GO function	1-ANOVA <sub>b</sub>	Average Normal. Volume <sup>c</sup>		
				0-d	21-d	42-d
161	Rubisco large subunit [Hordeum vulgare] gi 11587	ribulose-bisphosphate carboxylase activity	$2.5 \times 10^{-4}$			
117	UTP--glucose-1- phosphate uridylyltransferase [Hordeum vulgare] gi 6136111	nucleotidyltransferase activity	$6.1 \times 10^{-3}$			
182	Rubisco activase alpha form [Deschampsia antarctica] gi 32481061	RuBisCO activase activity	$5.2 \times 10^{-6}$			
124	Phosphoglycerate kinase, chloroplastic [Triticum aestivum] gi 129915	phosphoglycerate kinase activity	$1.3 \times 10^{-3}$			
119	cytosolic malate dehydrogenase [Triticum aestivum] gi 37928995	malate dehydrogenase activity	$5.1 \times 10^{-4}$			
122	glutamine synthetase [Triticum aestivum] gi 71361902	glutamate-ammonia ligase activity	$2.4 \times 10^{-5}$			
111	pyruvate dehydrogenase, putative [Ricinus communis] gi 255543140	pyruvate dehydrogenase (acetyl- transferring) activity	$8.1 \times 10^{-4}$			
142	Os09g0277800 NADH- dependent enoyl-ACP reductase [Oryza sativa Japonica Group] gi 115478314	enoyl-[acyl-carrier- protein] reductase (NADH) activity	$7.2 \times 10^{-4}$			
152	OEE1 [Triticum aestivum] gi 131388	oxygen evolving activity	$2.1 \times 10^{-5}$			
78	beta-1,3-glucanase precursor [Triticum aestivum] gi 4741846	glucan 1,3-beta- glucosidase activity	$2.7 \times 10^{-4}$			
148	cp31BHv [Triticum aestivum] gi 226533870	poly(U) binding RNA binding	$3.7 \times 10^{-5}$			
35	OEE2 [Triticum aestivum] gi 131394	oxygen evolving activity	$5.2 \times 10^{-4}$			
43	adenosine diphosphate glucose pyrophosphatase [Triticum aestivum] gi 21322655	adenosine diphosphate glucose pyrophosphatase activity	$6.2 \times 10^{-6}$			

23	50S ribosomal protein L12-1, chloroplastic [Secale cereale] gi 464517	structural constituent of ribosome	$3.1 \times 10^{-5}$	
82	ferredoxin-nitrite reductase precursor [Triticum aestivum] gi 218963620	ferredoxin-nitrate reductase activity	$7.1 \times 10^{-4}$	
86			$6.5 \times 10^{-4}$	
184	chloroplast fructose-bisphosphate aldolase [Triticum aestivum] gi 223018643	fructose-bisphosphate aldolase activity	$3.4 \times 10^{-5}$	
177	Glutamate-1-semialdehyde 2,1-aminomutase, chloroplastic [Hordeum vulgare] gi 1170029	glutamate-1-semialdehyde 2,1-aminomutase activity	$9.1 \times 10^{-5}$	
121	Phosphoribulokinase, chloroplastic [Triticum aestivum] gi 125580	phosphoribulokinase activity	$6.1 \times 10^{-4}$	
	Sedoheptulose-1,7-bisphosphatase, chloroplastic [Triticum aestivum] gi 1173347	sedoheptulose-bisphosphatase activity		
134	ATP synthase CF1 alpha subunit [Triticum aestivum] gi 14017569	hydrogen ion transporting ATP synthase activity, rotational mechanism	$7.9 \times 10^{-4}$	
138			$5.3 \times 10^{-4}$	
46	Translationally-controlled tumor protein homolog [Triticum aestivum] gi 75246527	calcium binding and microtubule stabilization	$6.9 \times 10^{-5}$	
135	ATPase beta subunit [Arabidopsis thaliana] gi 14017579		$8.8 \times 10^{-4}$	
27	chlorophyll a/b-binding protein WCAB precursor [Triticum aestivum] gi 1657859		$7.7 \times 10^{-4}$	

**Table 5.** Protein spots identified during short-term cold acclimation (0, 21 and 42 days). Spot shown in Fig.5 were not included.

Spot No. <sup>a</sup>	Mr, kDa theor/exper <sup>b</sup>	pI theor/exper <sup>b</sup>	Peptides identified by MS/MS					Mascot Ion Score
			Protein name NCBI GI Number	m/z	charge state	start-end <sup>c</sup>	sequence	
90	18.3/23.2	5.0/4.7	group3 late embryogenesis abundant protein (wrab17) [Triticum aestivum] gi 157073742	580.82	2+	9 - 19	SGEVVDVTQVK	41
				808.93	2+	9 - 24	SGEVVDVTQVKAGEAK	81
				582.32	3+	9 - 25	SGEVVDVTQVKAGEAKK	48
				669.80	2+	26 - 37	MASETGQSIQDR+Oxid (M)	104
				612.96	3+	26 - 42	MASETGQSIQDRAVEAK +Oxid (M)	45
				790.41	2+	38 - 52	AVEAKDQTGSFLGEK	101
				541.27	2+	43 - 52	DQTGSFLGEK	63
				546.96	3+	43 - 58	DQTGSFLGEKSAAVTK	62
				555.30	3+	53 - 69	SAAVTKAASETTEAAKK	49
				957.43	2+	146 - 164	ENVFQQAGGNMMGAATGAK +2Oxid(M)	37
55	18.3/22.9	5.0/4.5		670.80	2+	165 - 177	DAVMNTLGMGGDK +2Oxid (M)	62
				580.81	2+	9 - 19	SGEVVDVTQVK	39
				539.63	3+	9 - 24	SGEVVDVTQVKAGEAK	55
				582.33	3+	9 - 25	SGEVVDVTQVKAGEAKK	30
				661.81	2+	26 - 37	MASETGQSIQDR	76
				527.28	3+	38 - 52	AVEAKDQTGSFLGEK	74
				541.27	2+	43 - 52	DQTGSFLGEK	44
39	17.1/20.7	4.8/4.4	cold-responsive LEA/RAB-related COR protein (wrab17) [Triticum aestivum] gi 7716956	670.80	2+	165 - 177	DAVMNTLGMGGDK +2Oxid (M)	59
				622.64	3+	9 - 26	SGDATKTASETGQTIQDR	53
				521.94	3+	27 - 41	AVEAKDQTGAFLGEK	46
				545.54	4+	27 - 47	AVEAKDQTGAFLGEKSEAVTK	51
				533.26	2+	32 - 41	DQTGAFLGEK	54
				560.96	3+	32 - 47	DQTGAFLGEKSEAVTK	66
				924.95	2+	111 - 127	STEAQHVQDTAAQYTK	98
44	17.1/20.6	4.8/4.5		962.45	2+	135 - 153	ENVFQQAGGNMVGAAATDAK +Oxid (M)	75
				622.64	3+	9 - 26	SGDATKTASETGQTIQDR	89
				653.82	2+	15 - 26	TASETGQTIQDR	81
				521.94	3+	27 - 41	AVEAKDQTGAFLGEK	57
				533.26	2+	32 - 41	DQTGAFLGEK	51
				560.95	3+	32 - 47	DQTGAFLGEKSEAVTK	66
				616.96	3+	111 - 127	STEAQHVQDTAAQYTK	61
47	17.8/20.6	4.9/4.7	cold acclimation protein WCOR615 [Triticum aestivum] gi 1657857	670.80	2+	154 - 166	DAVMNTLGMGGDK +2Oxid (M)	30
				569.30	2+	32 - 41	DQTISFIGEK	56
				584.98	3+	32 - 47	DQTISFIGEKSEAVTK	65
				574.78	2+	67 - 77	AASDTADAAMKMGSDAMGK	70
32	17.8/22.6	4.8/4.7	cold regulated protein (wcor18) [Triticum aestivum] gi 26017213	656.97	3+	156 - 175	ASETGQAITDR	35
							DAVMNTLGMGGDKADVGSAAK +2Oxid (M)	
96	17.8/22.0	4.8/4.8		547.78	2+	23 - 32	QYTLEGQGAK	47
				603.31	2+	23 - 33	QYTLEGQGAKK +Gln->pyro-Glu (N-term Q)	39
95	17.8/21.6	4.8/4.4		457.78	2+	23 - 32	QYTLEGQGAK	53
				603.32	2+	23 - 33	QYTLEGQGAKK +Gln->pyro-Glu (N-term Q)	51
				758.39	2+	50 - 63	SLAVVVQDQVDADER	84
34	32.5/45.0	6.7/6.7	VER2 [Triticum aestivum] gi 16151819	547.78	2+	23 - 32	QYTLEGQGAK	56
				611.82	2+	23 - 33	QYTLEGQGAKK	30
				758.38	2+	50 - 63	SLAVVVQDQVDADER	64
				730.85	2+	252 - 264	FVTNEGTYGPYGR	73
				757.00	2+	287 - 300	ADDTQLIAFGVYTV	50

<sup>a</sup> Spot numbers refer to Figure 4

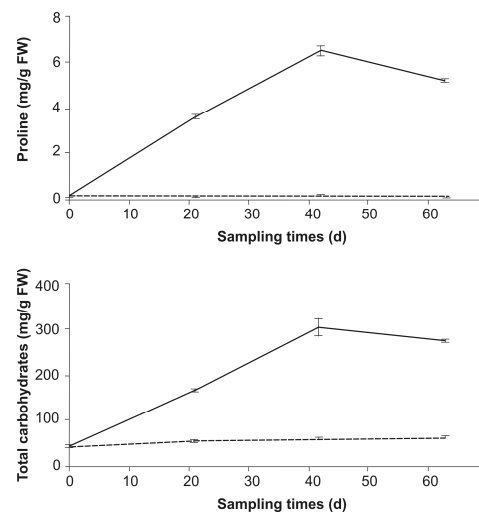
<sup>b</sup> Theoretical Mr/pI was calculated with Mr/pI tool on the ExPASy web site ([http://expasy.org/tools/pi\\_tool.html](http://expasy.org/tools/pi_tool.html))

<sup>c</sup> Start-end positions of identified peptides were calculated against complete amino acid sequence of the protein

**Table 6.** Detailed MS/MS peptide sequence analysis of cold-related proteins which showed modulations in expression after 21 and 42 days of cold treatment

### Biochemical measurements

Since it is well known that cold-acclimation is accompanied by an increase in solutes with cryoprotective effects, such as proline and soluble carbohydrates, we measured the intracellular content of these osmoregulators during the vernalization period. Figure 10 show the time course of proline and sugar accumulation; a similar trend can be seen for both solutes with the majority of the accretion occurring within the first six weeks of exposure to acclimating conditions.

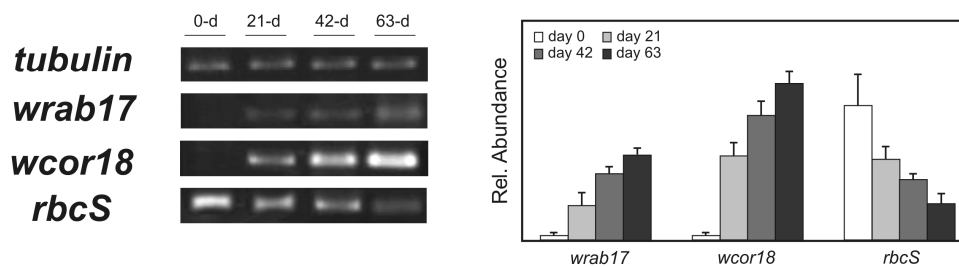


**Figure 10.** Changes in proline (panel A) and soluble sugar (panel B) in leaves of CNN winter wheat at 4 °C (solid line) and 20 °C (dotted line). Bars represent  $t \pm SE$  (n = 3).



### Gene expression at mRNA level

In order to investigate the transcript level of the identified proteins in response to vernalization treatment, reverse transcriptase (RT) PCR assays were conducted (Figure 11). Among all the identified proteins, three gene products were selected to investigate the expression patterns of their mRNA levels after prolonged cold exposure: (i) *LEA* (*wrab17*, spots 39, 44, 90), *wcor18* (spots 32, 96) and RuBisCO small subunit (*rbcS*, spots 6, 62, 178). The first two proteins have long been recognised as typically cold-activated products and their accumulation contribute to promoting the development of freezing tolerance (Thomashow, 1999; Kobayashi et al., 2004). Conversely, little and controversial evidence has been accumulated on the regulation of *rbcS* genes by cold stress (He et al., 2002; Gulick et al, 2005), although its structural involvement in the adjustment of activity of the RuBisCO complexes under cold stress is apparent (Spreitzer, 2003). Interestingly, this protein exhibited diversified expression patterns in 2DE maps. As displayed in Figure 11, transcription profiles of selected genes resulted to be directly correlated with protein expression levels, showing a marked and time-dependent up-regulation of both *wrab17* and *wcor18* and a down-regulation of *rbcS*. Interestingly, plants grown under standard temperature conditions showed an almost constant steady-state level of the transcripts examined (data not shown). The maintenance of high expression level of *Cor/Lea* genes at 63 days confirmed the good ability of CNN cultivar to cold-acclimate even after vernalization fulfilment.



**Figure 11.** Semi-quantitative RT-PCR analysis of the *LEA* (*wrab17*; 300 bp), *wcor18* (260 bp) and *rbcS* (RuBisCO small subunit; 271 bp) expression in control and cold-acclimated CNN leaves. Expression of *tubulin* (720 bp) is shown as an internal control. The densitometric quantification of the mRNA level of the individual genes is expressed as the fold change compared to *tubulin*. Data are presented as the mean  $\pm$  SD from triplicate experiments, and similar results were seen in all replicates.

## References

- Gulick PJ, Drouin S, Yu Z, Danyluk J, Poisson G, Monroy A.F, Sarhan F. Transcriptome comparison of winter and spring wheat responding to low temperature. *Genome* 2005;48:913-23.
- Hay RKM, Ellis RP. The control of flowering in wheat and barley: what recent advances in molecular genetics can reveal. *Ann Bot-London* 1998;82:541-54.
- He C, Wang W, Dongfang Y, Zhang J et al. Transcription regulation of soybean ribulose-
- Kobayashi F, Takumi S, Nakata M, Ohno R, Nakamura T, Nakamura C. Comparative study of the expression profiles of the Cor/Lea gene family in two wheat cultivars with contrasting levels of freezing tolerance. *Physiol Plantarum* 2004;120:585–94.
- Mahfoozi S, Limin AE, Fowler DB. Developmental regulation of low-temperature tolerance in winter wheat. *Ann Bot-London* 2001;87:751-7.
- McMaster GS. Phenology, development, and growth of wheat (*Triticum aestivum* L.) shoot apex: a review. *Adv Agron* 1997;59:63-118.
- Spreitzer RJ. Role of the small subunit in ribulose-1,5-bisphosphate carboxylase/oxygenase. *Arch Biochem Biophys* 2003;414:141-149.
- Thimm O, Blaessing O, Gibon Y, Nagel A, Meyer S, Krüger P, Selbig J, Müller L.A, Rhee S.Y, Stitt M. MAPMAN: a user-driven tool to display genomics data sets onto diagrams of metabolic pathways and other biological processes. *Plant J* 2004;37:914-39.
- Thomashow MF. Plant cold acclimation: freezing tolerance genes and regulatory mechanisms. *Annu Rev Plant Phys* 1999;50:571-99.
- Usadel B, Nagel A, Steinhäuser D, Gibon Y, Bläsing OE, Redestig H, Sreenivasulu N, Krall L, Hannah MA, Poree F, Fernie AR, Stitt M. PageMan: an interactive ontology tool to generate, display, and annotate overview graphs for profiling experiments. *BMC Bioinformatics* 2006;7:535.
- 1,5-bisphosphate carboxylase small subunit gene by external factors. *Chin Sci Bull* 2002;47:38-43.

## DISCUSSION

During vernalization fulfillment, plants react dramatically, modulating their metabolism, shifting to a new equilibrium to guarantee not only overwintering, but also vitality during suboptimal growing conditions. In this context, sugars appear to play a crucial role in preserving both cell structural integrity and maintenance of homeostasis, in concert with several partially characterized proteins, involved in cellular protection. Moreover, membrane lipids, and corresponding proteins devoted to their biosynthesis/proteolysis/conversion, act synergistically to build up this machinery. All biological components undergo major variations in order to attain a new stable equilibrium, so it is of primary importance to explore this situation from a holistic point of view. The main factors potentially responsible for the protein modulations here observed are plant development, cold acclimation/vernalization and flowering processes. Since these are complex and interconnected phenomena, it is almost impossible to quantify their exact contribution to the final proteomic scenario. Nonetheless, the comparison here carried out greatly simplifies the network of these contributions. The most relevant modulations in protein expression are reported below; proteins are grouped according to the major physiological event they preside over.

### LT-induced proteins regulated by vernalization

The characterization of many cold-responsive genes has been carried out in the past decade, leading to their classification into *Dhn* (dehydrins), *Lt* (LT responsive), *Lea* (late embryogenesis abundant), *Rab* [responsive to abscisic acid (ABA)] and *Cor* (cold-regulated). Finally, Thomashow (1999) coined the collective term *Cor/Lea* genes. Although many studies on this functional category have been conducted both at the transcript and protein level, the characterization of *Cor/Lea* products in cereals still remains incomplete. We identified spots 32, 95 and 96 as the products of the cold-regulated gene *wcor18* (gi|26017213). The induction of *wcor18* transcripts following cold-exposure in wheat has been revealed by Kobayashi *et al.* (2004) both in freezing-tolerant and susceptible cultivars. Nonetheless, the *wcor18* expression profile was only assessed during early stages of cold acclimation, thus no correlation has been possible with the vernalization process. For the first time, the present results demonstrated that the protein

expression of *wcor18* was sustained to 63-day cold acclimation. Moreover this protein was resolved into multiple spots on our 2DE gels (as shown in Figure 9) suggesting the occurrence of post-translational modifications. Interestingly, *wcor18* protein belongs to the highly conserved phosphatidylethanolamine binding protein family, members of which are associated with control of flowering time in both dicots and monocots (Chardon and Damerval, 2005). Though further investigations are required, such a property, together with our observations, opens the possibility of an involvement of this protein in promoting the shift from vegetative to reproductive growth and/or floral transition in cereals.

Among typically cold-activated polypeptides, we identified several spots as the *wrab17* protein. Specifically, spots 39 and 44 resulted the products of the gene with accession number gi|7716956, whereas spots 55 and 90 at higher molecular weights were found to be the products of the *wrab* gene isoform with gi|157073742 (see Table 5). The two genes mainly differ for a small N-terminal segment which was successfully discriminated by our MS/MS analyses (residues 9-26; Table 6). On the other hand, the additional heterogeneity was probably due to the presence of post-translational modifications. Accordingly, the maize *rab17* protein was found to be greatly phosphorylated in a serine-cluster region (Goday et al., 1994; Jensen et al., 1998). In principle, *wrab17* is a dehydrin-like protein which was shown to be highly homologous (84% amino acid identity) to ES2A, a barley GA<sub>3</sub> (gibberellic acid)-responsive protein (Tsuda et al., 2000). This could be an interesting feature, especially in the light of recent genome-wide transcriptomic analyses demonstrating an up-regulation of key GA biosynthetic genes during vernalization in wheat (Winfield et al., 2009). However, in spite of the high level of homology, no increase in expression of *wrab17* was revealed after GA<sub>3</sub> treatment (Tsuda et al., 2000). On the other hand, the temporal GA<sub>3</sub>-responsive expression of the *ES2A* transcript has been demonstrated only in a dwarf barley mutant (Speulman and Salamini, 1995). Thus, the role of these novel wheat group-3 *Lea/Rab*-related *Cor* genes in the low temperature tolerance and vernalization process in wheat is far from being completely undisclosed. Nevertheless, our results may add another piece to the puzzle of cereal vernalization understanding. We observed a marked increase in *wrab17* protein expression since 21-day cold treatment and its level remained elevated throughout the whole

period of cold exposure (63 days). On the contrary, wcor615 (spot 47) accumulation reached its peak at day 42 and then sharply decreased to the basal levels detected in control samples.

### **Vernalization-induced flowering**

Flowering is intimately connected to vernalization, in a delicate mechanism involving also photoperiod and gibberellic acid metabolism (Bernier and Périlleux, 2005; Kobayashi and Weigel, 2007). In cereals, the initial steps of this event are subjected both to genetic and environmental control, which are responsible for the FLN produced by the main stem (Hay and Ellis, 1998). The gene regulatory network controlling flowering time represents an example of integration between multiple environmental signals, mediated through a diverse set of regulatory mechanisms, which ultimately affect protein expression and determine the proper timing of the most important event for a plant fitness, transition to the reproductive phase (Gasser and Dean, 2009). Two proteins detected in the present analysis resulted in being particularly interesting in connection with vernalization-induced flowering process: a glycine-rich RNA binding protein (GR-RBP, spot 68) and the VER2 protein (spot 34). The GR-RBP was found to be up-regulated in vernalized samples (4.5-fold the control level). It is known that the cellular level of transcripts for RNA binding proteins is significantly increased under various stress conditions, such as cold, drought or viral infections (Albà and Pagès, 1998; Sachetto-Martins et al., 2000). Interestingly, many RNA binding proteins function as repressor of the flowering locus C (FLC) in Arabidopsis (Quesada et al., 2005). In particular, a recent study elucidated the role of the small glycine-rich RNA binding protein AtGRP7 in promoting floral transition (Streitner et al., 2008). In agreement, Cho *et al.* (2007) demonstrated a dramatic up-regulation of the same protein in vernalization-treated Arabidopsis plants. The GR-RBP detected in our study possesses a high degree of homology with AtGRP7 (approx. 81%), suggesting that this protein could be involved in flowering-time regulation during vernalization response in wheat.

Regarding carbohydrate-binding proteins, a marked up-regulation of a lectin protein (ricin B related protein, spot 67), has been revealed by proteomic analysis. This protein group was previously referred to as the family of “ribosome-inactivating proteins” (RIPs), capable of cleaving

adenine residues from different polynucleotide substrates. Moreover, lectins have been reported to interact with proteins in the cell nucleus (Lannoo et al., 2006). The expression of 67%-84% of lectins is controlled by the jasmonate pathway, which is involved in plant growth, development and resistance to several stresses, especially during flowering and seeding. This is an important feature, since there is evidence of a relationship between vernalization and the signal transduction pathway mediated by jasmonate (Yong et al., 1999).

VER2 is an important lectin protein containing a jacalin-like domain at the C-terminus and has been demonstrated to be induced by both vernalization and jasmonic acid in wheat (Yong et al., 2000, 2003). Our data demonstrated that its synthesis increased up to the vernalization saturation point, followed by a sharp decline at day 63 of cold acclimation. In a recent work, the *ver2* expression pattern was monitored in wheat seedling shoots exposed to low temperatures (Bertini et al., 2009) and the maximum level of the transcript was reached after 28-day cold acclimation. Nonetheless, *ver2* gene was shown to be significantly expressed also in control plants (5-day-old), in contrast with other data reported in literature (Yong et al., 2003) where no signal was detected under normal temperature conditions. Moreover, in agreement with the transcriptional pattern, native VER2 protein was found to be constitutively expressed in control wheat seedlings by western blot analysis, as it appeared to be induced upon vernalization treatments (Bertini et al., 2009). These findings led authors to hypothesize multiple roles for VER2 during the normal plant development, besides those directly linked to cold acclimation. Interestingly, our proteomic analysis revealed for the first time an increase in VER2 expression during plant growth at room temperature (see the expression trend of spot 34 in Figure 9); moreover, its levels at day 0 (14-day-old plants) were already appreciable, in agreement with Bertini and colleagues (Bertini et al., 2009). These results could be combined with the evidence that plant devernization repressed *ver2* expression (Bertini et al., 2009) as to suggest that, even if VER2 does not exert vital functions for seedling development, it could rather take part into those plant molecular mechanisms preparing for flowering and preceding effective switching to the reproductive phase. On the other hand, Xing and co-workers recently demonstrated that VER2 is involved, in a phosphorylation-modulated fashion, in O-GlcNAc signalling during vernalization (Xing et al.,

2009). Basing on these considerations, the down-regulation we observed at the 63<sup>rd</sup> day vernalization treatment may not be so surprising.

### **Major metabolic modifications upon prolonged cold exposure**

#### *Cold acclimation leads to net sugar accumulation*

As previously hinted, sugars are involved in the process of cold acclimation, decreasing the osmotic potential of cell cytoplasm aimed at the compensation of the intracellular loss of water. Sucrose accumulation during plant exposure to low temperature, together with its corresponding effects on winter survival, has been extensively studied (Hurry et al., 1994). In the present study, in accordance with previous reports (Hurry et al., 1995), soluble sugar levels increased dramatically upon cold exposure (see Figure 10), reaching a maximum on the same day as the vernalization saturation point (42<sup>nd</sup> day at 4°C). Besides their known role in energetic cellular processes, sugars, as hormone-like molecules, can act also as primary messengers and regulate signals that control the expression of various genes involved in sugar metabolism. The signalling role of these molecules has been elaborated by many authors, and dubbed the so called “sugar sensing” mechanism, which refers to the interaction between a sugar molecule and a sensor protein that triggers signal transduction cascades and ultimately results in important cellular responses such as modulations of gene expression and enzymatic activities (Gupta and Kaur, 2005). These important effects are exerted during all stages of plant growth, from seed germination to complete development. At the molecular level, two pathways for plant hexose sensing have been suggested, one hexokinase (HXK)-dependent and the other HXK-independent, the former requiring the phosphorylation of sugars while the latter does not (Smeekens, 2000). Relating this to our proteomic results, we observed a variation in expression of a putative fructokinase (spot 113), belonging to the glycolytic pathway. Recently, fructokinase has been proposed as additional sensor that bypasses HXK phosphorylation in the sugar sensing mechanism (Pego and Smeekens, 2000), increasing scientific interest in this enzyme beyond its direct implication in sugar metabolism.

#### *Changes in fatty acid composition during cold hardening*

Alterations in the plasma membrane structure, viscosity and composition are among the most important modifications related to cold acclimation (Uemura et al., 1995). Several factors contribute to structural cell stabilization, among which are accumulation of sucrose, osmolytes and alteration in membrane lipid composition.

The fact that temperature response implies important modifications in the fluidity of cell membranes is now generally accepted (Tasseva et al., 2004). In plants, *de novo* fatty acid biosynthesis takes place in the plastid, where acetate (C2) is elongated by the sequential addition of further C2 units while attached to a soluble acyl-carrier-protein (ACP) (Millar et al., 2000). In the present study, a marked down-regulation of acyl coenzyme A (acyl CoA) binding protein (spot 127) and of chloroplastic ACP1 (acyl carrier protein 1, spot 69), both devoted to the elongation of fatty acid chains, was found in vernalized samples. It has been hypothesized that in chloroplasts, ACP-1 influences the ratio of fatty acids destined to either the prokaryotic (chloroplastic) or eukaryotic (cytosolic) pathways of lipid biosynthesis. In a study conducted in *Arabidopsis*, ACP-1 transgenic overexpression was demonstrated to affect leaf fatty acid composition, causing an increase in linolenic acid (18:3) and a decrease in hexadecatrienoic acid (16:3) (Branen et al., 2001). The authors have hypothesized that an increase in ACP-1 protein expression leads to an increase in the amount of fatty acids sent to the eukaryotic pathway, which produces phospholipids for extrachloroplast membranes. So, in an opposite way, the down-regulation of this protein observed in the present study could cause an increase in the formation of 16:3 chains in the prokaryotic pathway. Furthermore, spot 84, containing a 3 beta-hydroxysteroid dehydrogenase/5-ene-4-ene isomerase (3 beta-HSD protein, responsible for the formation of all classes of steroid hormones), was down-regulated in vernalized samples. In contrast to these findings, spot 79, which has been identified as a patatin-like protein, showed an increase in expression. This protein belongs to a group of potato (*Solanum tuberosum*) storage glycoproteins that show acyl hydrolase activity on membrane lipids (Andrews et al., 1988). Besides functioning as a storage protein, patatins exert lipolytic activity in defence against plant parasites (Strickland et al., 1995) and in plant signal transduction (Holk et al., 2002). Furthermore, it is interesting to note that a subgroup of this family, the most widely represented one, is normally tuber-specific,



but can be induced in leaves by high concentrations of sucrose. Considering what has been said so far, the global behaviour of lipid metabolism from our proteomic point of view seems to be orientated towards fatty acid catabolism rather than anabolic pathways.

#### *Photosynthetic processes during cold acclimation*

Another crucial plant function that may be damaged during cold exposure is photosynthesis; a decrease in temperature, in fact, leads to a concomitant reduction in the irradiance required to saturate photosynthesis (Falk et al., 1992). Since photosynthesis couples temperature-independent photochemical processes with temperature-dependent redox reactions involved in electron transport and carbon assimilation, cold acclimation will exert a unilateral effect, leading to an energy imbalance. In winter wheat, cold acclimation is known to induce an increase in tolerance to photoinhibition (Somersalo and Krause, 1990). This species grows and develops at low temperatures, thus the plant must maintain active photosynthesis during winter (Huner et al., 1998), in contrast to evergreen plants which have evolved by creating other survival strategies, such as cessation of growth during the cold season. This enhancement in plant tolerance appears to be the result of the 'reprogramming' of carbon metabolism. Upon cold exposure, quinone A (QA), which is the first quinone electron acceptor of the PSII reaction centers, will be mostly in the reduced state, since it is normally photochemically reduced under cold conditions, whereas oxidation via redox reactions of the electron transport chain will be affected by low temperatures. Current models concerning sucrose regulation of plant gene expression have revealed an inhibition of photosynthetic genes in the presence of elevated sugar concentrations, a situation which typically occurs during cold acclimation. Although this regulation was contested in other studies conducted on *Arabidopsis* (Strand et al., 1999), rye and wheat (Huner et al., 1993, 1998), our analysis revealed a decrease in expression of the major photosynthesis-related proteins. In particular, we observed a significant down-regulation of the main proteins responsible for electron transfer from H<sub>2</sub>O to NADP<sup>+</sup>: plastocyanin (spot 3), cytochrome b<sub>6</sub>f complex (spot 59), plastidic ATPase [spots 57, 33 and 109 ( $\beta$  subunit), 115 (B chain), 118 (D chain), 196 ( $\epsilon$  subunit)], ferredoxin-NADP(H) oxidoreductase (spot 197).

Although the biochemical significance of the decreased expression for photosynthesis-related gene products in winter wheat warrants further investigations, it is interesting to mention a partial overlapping between our results and a recent transcriptomic study where this tendency to a down-regulation of photosynthetic genes by LT was described (Gulick et al., 2005). OEE1, OEE2 and RuBisCO-containing spots were also found to be down-regulated after prolonged cold exposure. Moreover, these spots were found to be scattered over a wide area of the gel: this is attributable both to protein fragmentation and to post-translational modifications, when we look at their shift in molecular weight and isoelectric point. We suggested that this fact could be due to active recycling of amino acids derived from proteolysis and their subsequent recruitment as substrates in other cellular pathways. This hypothesis has been reinforced by both the increase in expression of proteasome, and by the up-regulation of some TCA cycle enzymes (described below). Interestingly, RuBisCO activase showed an opposite modulation in expression with respect to RuBisCO in all spots examined (146, 159 and 182), being significantly up-regulated in vernalized plants in comparison to those grown at 20 °C for 63 days. The expression trend of RuBisCO activase appears to be related to its role in maintaining the active configuration of RuBisCO.

#### *Carbon fixation*

It is known that the exposure of fully expanded leaves of winter cereals to a short period of low temperature inhibits electron transport capacity and carbon assimilation, whereas low temperature growth exerts the opposite effect. In fact, in contrast to low-temperature stress, cold acclimation of cereals is associated with an increase in light-saturated carbon dioxide (CO<sub>2</sub>) assimilation rates, due to the increased capacity of the Calvin cycle enzymes (Huner et al., 1993, Hurry et al., 1995) and the differential capacity to adjust sucrose-phosphate synthase (SPS) activity (Hurry et al., 1994, Strand et al., 1999). This enhanced photosynthetic capacity seems to reflect an increased flux of fixed carbon (through sucrose) in source tissues, as a consequence of two combined effects: the increased storage of carbohydrate as fructans in the vacuole of leaf mesophyll cells and an enhanced export of product to the crown due to its increased sink activity. In the present analysis, spots 30 and 184, identified as chloroplastic fructose-1,6-bisphosphate aldolase (FBA), were up-regulated in response to cold exposure. Another Calvin cycle enzyme that showed an

increase in expression during cold exposure is phosphoglycerate kinase (PGK, spot 124). In contrast with the previous findings, spot 97, containing chloroplastic glyceraldehyde-3-phosphate dehydrogenase (GAPDH), showed a decrease in expression after prolonged cold treatment. Moreover, spot 121, containing both phosphoribulokinase (PRK) and sedoheptulose-1,7-bisphosphatase, both dedicated to the regeneration of substrates for the renewal of the cycle, decreases in expression in vernalized plants.

Furthermore, it has long been observed that plants exhibit enhanced rates of respiration during growth at low temperature: this physiological behaviour, besides preserving plant vitality under suboptimal growth temperatures, also reflects the availability of high sucrose levels in the plant (Huner et al., 1993). Our study also revealed an increase in expression of the mitochondrial enzymes of the TCA cycle, in particular isocitrate and malate dehydrogenases (spots 48 and 100, respectively).

### **Protein metabolism**

Exposing plants to low temperatures causes them to modulate their amino acid balance, this can be observed in the accumulation of free amino acids involved in the synthesis of stress-related metabolites. The metabolic pathway of proline deserves particular attention, considering its impressive increase in concentration under various abiotic stresses, including cold exposure; its positive effect is exerted mainly through its oxidation to glutamate and 2-oxoglutarate. Physiological measurements of proline concentration in Cheyenne winter wheat confirmed that it does indeed increase significantly during cold exposure, reaching a maximum level at the 42<sup>nd</sup> day, after which a gradual decrease is observed. Again, as we observed for soluble sugar levels, the time of maximum accumulation overlaps with saturation of vernalization. Since the enzymes involved in proline degradation are located in the mitochondrion, this amino acid may also provide carbon to the TCA cycle in plants suffering osmotic stress (such as during prolonged cold exposure). The mitochondrial oxidation of proline produces reducing equivalents available for supporting the generation of ATP, whereas the proline biosynthetic pathway from glutamate involves a high rate of consumption of NADPH and ATP. These facts suggest that proline

biosynthesis may be an important adaptive mechanism to ameliorate an imbalance between light energy absorbed through photochemistry and energy used in intersystem electron transport and carbon metabolism under conditions of stress. Since it is known that transcription of the catabolic genes is principally more sensitive to fluctuations in stress-associated signals than that of the biosynthetic genes (Less and Galili, 2008), probably the main contribution to the increase of free amino acids during cold is protein breakdown.

### *Proteolysis*

In plants, as in all living organisms, regulated proteolysis presides over each major aspect of growth and development (photomorphogenesis, circadian clock, flowering), and is also a key step in hormone-dependent signal transduction. The gene regulatory network controlling flowering time represents an example of integration between multiple environmental signals, mediated through a diverse set of regulatory mechanisms (chromatin regulation, proteolytic pathways, etc), which ultimately affects protein expression and determines the proper timing of the most important event for a plant fitness, transition to the reproductive phase (Gasser and Dean, 2009). Thus, the crucial role of proteolytic enzymes during vernalization appears clear. A plastidial protease (spot 180), belonging to the ATP-dependent chloroplast-localized protease family, was seen to decrease in vernalized plants. A study involving silencing through antisense technology in *Arabidopsis* has previously demonstrated that the loss of chloroplast proteases, particularly ClpP6, was responsible for pleiotropic changes in plant metabolism (Sjögren et al., 2006). Further identification of stromal proteins accumulating in the *Arabidopsis* antisense lines, where expression of this protease was totally repressed, suggests that these proteins are natural ClpP6 substrates, among which we spotted fructose biphosphate aldolase and a putative RNA binding protein. In our analysis, fructose biphosphate aldolase (spots 184 and 30) have shown an up-regulation upon prolonged cold exposure, concurrent with a decrease in the expression of clp protease; these findings seem to be in accordance with previously reported data. In contrast to the decrease in expression of plastidial proteases, the expression of the proteasome complex (spot 112, alpha 2 chain), responsible for the ubiquitin-dependent protein catabolic process of misfolded/targeted proteins, was seen to increase in vernalized plants. The proteasome complex

takes part in many developmental processes, cleaving positive or negative regulators of many genes and thus orientating signaling cascades (Casal et al., 2004). A possible relationship between the increase in expression of proteasome and the presence of protein fragments belonging to photosynthesis-related proteins and RuBisCO (previously described) could also be hypothesized. In fact, proteolysis of the most abundant leaf proteins for energetic purposes could be a realistic possibility during prolonged exposure to sub-optimal conditions. The progressive disappearance of these fragments in function of time corroborates the hypothesis of an active recycling of amino acids for their subsequent recruitment as substrates in other cellular pathways. Since Rubisco is mainly synthesized during leaf expansion and degraded rapidly during leaf senescence, its turnover is closely related to photosynthesis and nitrogen economy in plants, it being the most abundant protein in leaf cells. The majority of Rubisco is thought to be degraded into small nitrogenous molecules (oligopeptides and/or amino acids) within the chloroplasts at the early to middle stage of senescence, being conclusively degraded by vacuolar proteases in the last stage of senescence (Chiba et al., 2003).

#### *Glutamate as a "trading currency"*

Two other important enzymes related to amino acid balance were differentially expressed in vernalized plants: glutamine synthetase (spots 153 and 156) and glutamate-1-semialdehyde aminomutase (GSAM, spot 177), both increasing in expression upon cold exposure. However, the expression pattern of glutamine synthetase is quite controversial, since it also showed an opposite trend, with respect to the previous one, in spots 80 and 88; this result could be tributary to the simultaneous presence of various isoforms, differentially increased/repressed in expression during cold acclimation. GSAM synthesizes 5-aminolevulinate (ALA), which forms the building block for tetrapyrroles in cofactors like heme, chlorophyll, and carotenoids. The first substrate of this pathway comes from glutamate metabolism, a visible sign of the amino acidic catabolic way. Since interconversion of glutamate into glutamine and vice versa is an important switching point for glutamate availability, the up-regulation of these two enzymes appears to be related. Spot 165, found to be up-regulated in vernalized winter wheat, has been identified as S-adenosylmethionine synthase (SAMS1), an enzyme that catalyzes the conversion of ATP and L-methionine into S-

adenosyl-L-methionine (SAM). SAM is second to ATP as the most abundant cofactor in metabolic reactions, acting as a methyl group donor for numerous transmethylation reactions. SAM is cyclically synthesized in the so called "methyl cycle", whose rate is known to increase in response to stress (Boerjan et al., 1994). In plants, adenosylmethionine (AdoMet) is a precursor molecule in the biosynthesis of the phytohormone ethylene and is also involved in the biosynthesis of polyamines. Peptide methionine sulfoxide reductase (spot 193) was found to be greatly up-regulated in vernalized plants with respect to RT-grown seedlings. A transcriptome profiling study aimed at the identification of cold-responsive genes in *Arabidopsis*, revealed 300 cold-responsive genes, among which was the unexpected find of a peptide known as methionine sulfoxide reductase (PMSR) (In et al., 2005). PMSR catalyzes the reduction of protein-bound methionine sulfoxide groups to methionine, preventing the inactivation and potential degradation of proteins oxidized by reactive oxygen species (such as superoxide, hydroxyl radicals and  $H_2O_2$ ). Moreover, Gustavsson and coworkers (Gustavsson et al., 2002) demonstrated that a plastidic PMSR in *Arabidopsis* can efficiently prevent the oxidative inactivation of a chloroplast-localized chaperonin 21, which has been shown to be up-regulated in the present analysis (spot 114).

50S ribosomal protein L21 (spot 195) was also switched on upon vernalization; this protein belongs to the large ribosome subunit, helping to organise and stabilise the tertiary structure of the rRNA. On the contrary, we found an offset in expression of the 30S ribosomal protein S6 (spot 36).

### **Cold acclimation increases the expression of chaperon proteins**

Chaperonins, which are known to be involved in the maintenance of the functional protein configuration, showed a significant up-regulation in vernalized plants (spots 136 and 114, molecular chaperone DnaK and putative chaperonin 21, respectively). An interesting note to mention is that silencing experiments on chaperonin 21 promoted seed abortion in tobacco and tomato fruits (Hanania et al., 2007). Furthermore, subtractive hybridization assays made to isolate differentially regulated genes that participate in the seedlessness machinery, revealed that one of the gene differentially expressed between the seeded and seedless lines, was the chloroplast

chaperonin 21 (ch-Cpn21). Thus, a possible role for this chaperone in reproductive development has been hypothesized. Protein disulfide isomerase (spot 194), which is involved in the formation, cleavage and isomerisation of disulfide bonds in nascent proteins, was also newly expressed in vernalized plants.

### **Down-regulation of redox protein**

Regarding proteins involved in redox balance, a chloroplast-localized protein involved in defence against oxidation showed a marked down-regulation in winter wheat after cold treatment in the present analysis; in particular, spots 158 and 179, both identified as 2-Cys peroxiredoxin BAS1 (a chloroplastic thiol-specific antioxidant protein), decreased in expression in vernalized samples. A recently published proteomic study on the modulation of wheat proteomes in the presence of different nitrogen concentrations (Bahrman et al., 2004) demonstrated an up-regulation of the peroxiredoxin BAS1 in response to high nitrogen availability, and other data from the literature linked the increased expression of this enzyme to plant defence against environmental stressors, such as high levels of alkyl hydroperoxides occurring upon oxidative stress (Costa et al., 1998). Another proteomic study on the response to cold in Arabidopsis (Goulas et al., 2006) at the plastidial level, showed a dramatic modulation of the stroma and lumen subproteomes upon prolonged cold exposure (40 days at 5°C): in particular, two 2-Cys peroxiredoxins (2-Cys Prx A and B) were found to be reduced in abundance, in accordance with our findings.

## References

- Albà MM, Pagès M. Plant proteins that contain the RNA-recognition motif. *Trends Plant Sci* 1998;3:15-21.
- Andrews DL, Beames B, Summers MD, Park WD. 1988. Characterisation of the lipid acyl hydrolase activity of the major potato (*Solanum tuberosum*) tuber protein, patatin, by cloning and abundant expression in a baculovirus vector. *Journal of Biochemistry* 252, 199-206.
- Bahrman N, Le Gouis J, Negroni L, Amilhat L, Leroy P, Lainé A-L, Jaminon O. 2004. Differential protein expression assessed by two-dimensional gel electrophoresis for two wheat varieties grown at four nitrogen levels. *Proteomics* 4, 709–719.
- Bernier G, Périlleux C. A physiological overview of the genetics of flowering time control. *Plant Biotechnol J* 2005;3:3-16.
- Bertini L, Proietti S, Caporale C, Caruso C. Molecular characterization of a wheat protein induced by vernalisation. *Protein J* 2009;28:253-62.
- Boerjan W, Bauw G, Van Montagu M, Inzeb D. 1994. Distinct Phenotypes Generated by Overexpression and Suppression of S-Adenosyl-L-Methionine Synthetase Reveal Developmental Patterns of Gene Silencing in Tobacco. *Plant Cell* 6, 1401-1414.
- Branen JK, Chiou T-J, Engeseth NJ. 2001. Overexpression of Acyl Carrier Protein-1 Alters Fatty Acid Composition of Leaf Tissue in Arabidopsis. *Plant Physiology* 127, 222-229.
- Casal JJ, Fankhauser C, Coupland G, Bla'zquez MA. 2004. Signalling for developmental plasticity. *Trends in Plant Science* 9, 309-314.
- Chardon F, Damerval C. Phylogenomic analysis of the PEBP gene family in Cereals. *J Mol Evol* 2005;61:579-90.
- Chiba A, Ishida H, Nishizawa NK, Makino A, Mae T. 2003. Exclusion of Ribulose-1,5-bisphosphate Carboxylase/oxygenase from Chloroplasts by Specific Bodies in Naturally Senescing Leaves of Wheat. *Plant Cell Physiology* 44, 914–921.
- Cho MR, Lee KH, Hyun Y-B, Lee I, Kim H-J. Proteome analysis of vernalization-treated Arabidopsis thaliana by Matrix-Assisted Laser Desorption/Ionization Time-of-Flight Mass Spectrometry. *B Kor Chem Soc* 2007;28:427-31.
- Costa P, Bahrman N, Frigerio JM, Kermer A, Plomion C. 1998. Water-deficit-responsive proteins in maritime pine. *Plant Molecular Biology* 38, 587–596.
- Falk S, Leverenz JW, Samuelsson G, Oquist G. 1992. Changes in Photosystem II fluorescence in Chlamydomonas reinhardtii exposed to increasing levels of irradiance in relationship to the photosynthetic response to light. *Photosynthesis Research* 31,151-160.
- Feller U, Fischer A. 1994. Nitrogen metabolism in senescing leaves. *Critical Review in Plant Science* 13, 241–273.
- Gasser CS, Dean C. Growth and development: a broad view of fine detail. *Curr Opin Plant Biol* 2009;12:1-3.



- Goday A, Jensen AB, Culianez-Macia FA, Mar Alba M, Figueras M, Serratos J, Torrent M, Pages M. The maize abscisic acid-responsive protein Rab17 is located in the nucleus and interacts with nuclear localization signals. *Plant Cell* 1994;6:351-60.
- Goulas E, Schubert M, Kieselbach T, Kleczkowski LA, Gardeström P, Schröder W, Hurry V. 2006. The chloroplast lumen and stromal proteomes of *Arabidopsis thaliana* show differential sensitivity to short- and long-term exposure to low temperature. *Plant Journal* 47, 720–734.
- Gulick PJ, Drouin S, Yu Z, Danyluk J, Poisson G, Monroy A.F, Sarhan F. Transcriptome comparison of winter and spring wheat responding to low temperature. *Genome* 2005;48:913-23.
- Gupta AK, Kaur N. 2005. Sugar signalling and gene expression in relation to carbohydrate metabolism under abiotic stresses in plants. *Journal of Bioscience* 30, 761–776.
- Gustavsson N, Kokke BPA, Härndahl U, Silow M, Bechtold U, Poghosyan Z, Murphy D, Boelens WC, Sundby C. 2002. A peptide methionine sulfoxide reductase highly expressed in photosynthetic tissue in *Arabidopsis thaliana* can protect the chaperone-like activity of a chloroplast-localized small heat shock protein. *Plant Journal* 29,545–553.
- Hanania U, Velcheva M, Or E, Flaishman M, Sahar N, Perl A . 2007. Silencing of chaperonin 21, that was differentially expressed in inflorescence of seedless and seeded grapes, promoted seed abortion in tobacco and tomato fruits. *Transgenic Research* 16, 515-525.
- Hay RKM, Ellis RP. The control of flowering in wheat and barley: what recent advances in molecular genetics can reveal. *Ann Bot-London* 1998;82:541-54.
- Holk A, Rietz S, Zahn M, Quader H, Scherer GFE. 2002. Molecular identification of cytosolic, patatin-related phospholipases A from *Arabidopsis* with potential functions in plant signal transduction. *Plant Physiology* 130, 90–101.
- Huner NPA, Öquist G, Hurry VM, Krol M, Falk S, Griffith M. 1993. Photosynthesis, photoinhibition and low temperature acclimation in cold tolerant plants. *Photosynthesis Research* 37, 19-39.
- Huner NPA, Öquist G, Sarhan F. 1998. Energy balance and acclimation to light and cold. *Trends in Plant Science* 3, 224-230.
- Hurry VM, Malmberg G, Gardeström P, Öquist G. 1994. Effects of a short-term shift to low temperature and of long-term cold hardening on photosynthesis and ribulose-1,5-bisphosphate carboxylase oxygenase and sucrose-phosphate synthase activity in leaves of winter rye (*Secale cereale* L). *Plant Physiology* 106, 983–990
- Hurry VM, Strand A, Tobiaeson M, Gardeström P, Öquist G. 1995. Cold hardening of spring and winter wheat and rape results in differential effects on growth, carbon metabolism, and carbohydrate content. *Plant Physiology* 109, 697–706.
- In O, Berberich T, Romdhane S, Feierabend J. 2005. Changes in gene expression during dehardening of cold-hardened winter rye (*Secale cereale* L.) leaves and potential role of a peptide methionine sulfoxide reductase in cold-acclimation. *Planta* 220, 941–950.

- Jensen AB, Goday A, Figueras M, Jessop AC, Pagès M. Phosphorylation mediates the nuclear targeting of the maize Rab17 protein. *Plant J* 1998;13:691-97.
- Kobayashi F, Takumi S, Nakata M, Ohno R, Nakamura T, Nakamura C. Comparative study of the expression profiles of the Cor/Lea gene family in two wheat cultivars with contrasting levels of freezing tolerance. *Physiol Plantarum* 2004;120:585–94.
- Kobayashi Y, Weigel D. Move on up, it's time for change-mobile signals controlling photoperiod-dependent flowering. *Gene Dev* 2007;21:2371-84.
- Lannoo N, Peumans WJ, Van Pamel E, Alvarez R, Xiong TC, Hause G, Mazars C, Van Damme EJM. 2006. Localization and in vitro binding studies suggest that the cytoplasmic/nuclear tobacco lectin can interact in situ with high-mannose and complex N-glycans. *FEBS Letters* 580, 6329–6337.
- Less H and Galili G (2008) Principal transcriptional programs regulating plant amino acid metabolism in response to abiotic stresses. *Plant Physiol* 147: 316-330
- Millar AA, Smith MA, Kunst L. 2000. All fatty acids are not equal: discrimination in plant membrane lipids. *Trends in Plant Science* 5, 95-101.
- Pego J, Smeekens SCM. 2000. Plant fructokinases: a sweet family get-together. *Trends in Plant Science* 5, 531–536.
- Quesada V, Dean C, Simpson GG. Regulated RNA processing in the control of Arabidopsis flowering. *Int J Dev Biol* 2005;49:773-80.
- Sachetto-Martins G, Franco LO, de Oliveira DE. Plant glycine-rich proteins: a family or just proteins with a common motif?. *Biochim Biophys Acta* 2000;1492:1-14.
- Sjögren LLE, Stanne TM, Zheng B, Sutinen S, Clarke AK. 2006. Structural and Functional Insights into the Chloroplast ATP-Dependent Clp Protease in Arabidopsis. *Plant Cell* 18, 2635-2649.
- Smeekens S. 2000. Sugar-Induced signal transduction in plants. *Annual Review of Plant Physiology and Plant Molecular Biology* 51, 49-81.
- Somersalo S, Krause GH. 1990. Reversible photoinhibition of unhardened and cold acclimated spinach leaves at chilling temperatures. *Planta* 180, 181-187.
- Speulman E, Salamini F. GA3-regulated cDNA from *Hordeum vulgare* leaves. *Plant Mol Biol* 1995;28:915-26.
- Strand C, Hurry V, Henkes S, Huner N, Gustafsson P, Gardeström P, Stitt M. 1999. Acclimation of Arabidopsis leaves developing at low temperatures. Increasing cytoplasmic volume accompanies increased activities of enzymes in the Calvin cycle and in the sucrose-biosynthesis pathway. *Plant Physiology* 119, 1387–1397.
- Streitner C, Danisman S, Wehrle F, Schöning JC, Alfano JR, Staiger D. The small glycine-rich RNA binding protein AtGRP7 promotes floral transition in Arabidopsis thaliana. *Plant J* 2008;56:239-50.

- Strickland JA, Orr GL, Walsh TA. 1995. Inhibition of *Diabrotica* larval growth by patatin, the lipid acyl hydrolase from potato tubers. *Plant Physiology* 109, 667–674.
- Tasseva G, Davy de Virville J, Cantrel C, Moreau F, Zachowski A. 2004. Changes in the endoplasmic reticulum lipid properties in response to low temperature in *Brassica napus*. *Plant Physiology and Biochemistry* 42, 811-822.
- Thomashow MF. Plant cold acclimation: freezing tolerance genes and regulatory mechanisms. *Annu Rev Plant Phys* 1999;50:571-99.
- Timperio AM, Egidi MG, Zolla L. 2008. Proteomics applied on plant abiotic stresses: Role of heat shock proteins (HSP). *Journal of Proteomics* 71, 391- 411.
- Tsuda K, Tsvetanov S, Takumi S, Mori N, Atanassov A, Nakamura C. New members of a cold-responsive group-3 *Lea/Rab*-related *Cor* gene family from common wheat. *Genes Genet Syst* 2000;75:179-88.
- Uemura M, Raymond AJ, Steponkus PL. 1995. Cold acclimation of *Arabidopsis thaliana*: Effect on plasma membrane lipid composition and freeze-induced lesions. *Plant Physiology* 109, 15–30.
- Winfield MO, Lu C, Wilson ID, Coghill JA, Edwards KJ. Cold- and light-induced changes in the transcriptome of wheat leading to phase transition from vegetative to reproductive growth. *BMC Plant Biol* 2009;9:55-68.
- Xing L, Li J, Xu Y, Xing L, Li J, Xu Y, Xu Z, Chong K. Phosphorylation modification of wheat lectin VER2 is associated with vernalization-induced O-GlcNAc signaling and intracellular motility. *PLoS ONE* 2009;4:e4854.
- Yong WD, Chong K, Liang TB, Xu ZH, Tan KH, Zhu ZQ. 1999. Cloning and characterization of vernalization-related gene (*ver203F*) cDNA 3' end. *Chinese Science Bulletin* 44, 1289-1294.
- Yong WD, Chong K, Xu WZ. Gene control of flowering time in higher plants. *Chinese Sci Bull* 2000;5 :455-66.
- Yong WD, Xu YY, Xu WZ, Wang X, Li N, Wu JS, Liang TB, Chong K, Xu ZH, Tan KH, Zhu ZQ. Vernalization-induced flowering in wheat is mediated by a lectin-like gene VER2. *Planta* 2003;217:261-70.

## **PART II**

### **Proteomic analysis of a drought-resistant spring wheat cultivar in response to prolonged cold stress**

#### **Aim of the study**

This study addresses proteomic approach to delve into a quite challenging issue, that is plant cross-tolerance to different abiotic stresses. In particular, we focused on cold and drought stressors which cause the most fatal economic losses in agriculture due to their wide-spread occurrence. These stressors result in similar plant responses at the cellular and molecular level due to the fact that their impacts trigger similar strains and downstream signal transduction cascades. With the attempt to shed light into those metabolic modulations strictly related to exposure to low temperatures, we choose a drought-resistant spring wheat variety for our proteomic study so to minimize the dehydrative component of cold stress. Thus, we focused the attention on those proteins modulated in expression only upon prolonged cold exposure, coupling these findings to physiological measurements, in order to get a complete view of modulated pathways. We looked for cold-related protein modulations by cross-comparison of leaf proteomes from wheat plants grown for 14 (experimental zero point, control sample) and 42 days at optimal environmental parameters, as well as those subjected to prolonged cold exposure (42 days, 4 °C). In this way it was possible to distinguish them from those proteins normally expressed at the 42-day-growth stage in this particular genotype. This sampling time has been chosen in order to analyze the mechanisms involved in plant response to prolonged abiotic stress, also because cold stress at plant reproductive stage has a more relevant agronomic impact in term of crop yield with respect to the vegetative stage.

Considering the overlap between plant responses to various abiotic stressors and the other components influencing plant performance under adverse conditions - such as developmental stage, plant genotype, environmental factors causing the stress/experimental conditions of stress imposition, type of tissue under analysis and individual variability - it is impossible to unravel and outline the precise mechanism adopted by plants against a particular environmental constraint.

Furthermore, the expression of a cellular product during stress does not imply its mandatory involvement in plant defensive mechanisms, as it can also be an effect of stress-induced damages, or could be simply unrelated to stress-triggered pathways. Finally, experimental findings obtained from a certain crop variety should not be generalized, since similar onsets in expression are known to be induced in desiccation tolerant as well as in less tolerant cultivars. Being aware of these limitations, in this study we tried to fill the gaps existing between the knowledge of the precocious plant response reactions to LT and the delineation of tolerance mechanisms during prolonged cold stress. We chose the drought-resistant spring wheat variety named Kohdasht to provide a starting point in developing a clearer picture, from a proteomic perspective on the molecular mechanisms which help a drought-resistant but cold sensitive variety to acclimate at suboptimal temperatures. The vast majority of the works performed so far have analysed the response of young seedlings to short-term cold stress. On the other hand, our study tried to shed light on the proteomic cold response in an advanced period of plant life, which is the reproductive stage. This allowed us to investigate on those long-term responses in protein expression which may play an important role in the adaptation to stressor events under field conditions.

## **Background**

### *Perception of stress by plants*

Since plants are bound to places, they have to be considerably more adaptable to stressful environments and must acquire greater tolerance to multiple stresses than animals and humans. Examples at the cellular level include temporary modifications in gene expression to survive changing environments, as well as altering cellular structure and function to deal with more permanent adverse conditions. Some abiotic stresses, such as drought, salinity, extreme temperatures, chemical toxicity and oxidative stress are serious threats to agriculture and result in the deterioration of the environment. Thus, elucidating the various mechanisms of plant response to stress and their roles in acquired stress tolerance is of great practical and basic importance (Wang et al., 2004). Unfortunately, genome sequence information alone is insufficient to reveal the facts concerning gene function, developmental/regulatory biology, and the biochemical kinetics of plants to adapt under stresses and consequently to determine the exact responsive mechanism. To investigate these facts, more comprehensive approaches that include quantitative and qualitative analyses of gene expression products are necessary at the transcriptome, proteome, and metabolome levels.

### *The concept of cross-protection*

Usually, an organism is subjected to several stress factors, e.g. lack of water and heat, or a “secondary” stress factor follows a “primary” one (i.e. when the plant lacks water and closes its stomata, internal CO<sub>2</sub> deficiency occurs when the plant is illuminated, and as a further consequence oxidative stress ensues). Combination of several stress factors is the normal case and is referred to as multiple stress. Furthermore, environmental stresses that result in cellular dehydration, such as freezing, salt and water stress, often lead to similar changes in plant gene expression and metabolism (Kaplan et al., 2004; Kreps et al., 2002; Rabbani et al., 2003; Seki et al., 2001), and there exists cross-talk in their signalling pathways (Chinnusamy et al., 2004; Knight and Knight, 2001). There is yet another facet to the question of specificity of stress reactions which is described by the term cross-protection. Previous drought stress or salt stress (osmotic stress) is known to harden plants against temperature stress, and particularly cold stress.

### *Modification induced by stressors at the proteomic level*

Maintaining proteins in their functional conformations and preventing the aggregation of non native proteins are particularly important for cell survival under stress. In fact, as mentioned before, plants are sessile organisms and rely on proteomic plasticity to remodel themselves during periods of developmental change, to endure varying environmental conditions, and to respond to biotic and abiotic stresses. The latter are the primary cause of crop loss worldwide, reducing average yields for most major crop plants by more than 50%. Abiotic stresses usually cause protein dysfunction. Different families of proteins are known to be associated with a plant's response to stresses by being newly synthesized, accumulating or decreasing. Among other things, these proteins are involved in signalling, translation, host-defence mechanisms, carbohydrate metabolism and amino acid metabolism. Now it is a well known fact that proteins mediate these features by playing a role in directing the genome and ultimately physical features (such as in xerophytes) or encountering stressors directly (such as antioxidant enzymes and chaperonins) or indirectly (such as a key enzyme in osmolyte synthesis).

On the other hand, mRNA and protein levels cannot be simply correlated due to inability of total mRNA to translate into protein; protein levels are not directly correlated with the number of transcripts in the cell, and post translational modification is not visible by examination of transcriptome, making proteomics the study of the real players in organisms. Moreover, the proteome is not a static entity, being it affected by multiple modifications such as cell cycle, changes of external conditions, kind of tissue examined, and particular physiological states. For these reasons, proteomics is becoming a powerful tool to analyse biochemical pathways and the complex response of plants to environmental stimuli. In particular, comparative proteomic investigations of plants before and after specific or interactive stresses allow us to obtain information on how defensive mechanisms are adopted from plants. Proteomics also provides an essential link between the transcriptome and metabolome, complementing genomics research. Only by grouping all this information together is it possible to achieve a comprehensive and exhaustive analysis of the strategies induced by the cells as response to stress.

## Cold stress in wheat

Among cereals with agronomic value, both wheat and barley are considered to be relatively cold-tolerant crops. As described in the first part of the thesis, common wheat (*Triticum aestivum* L.) cultivars can be divided into two subclasses on the basis of their different growth habits: spring wheat has a relatively short vegetative period, whereas winter wheat delays transition from vegetative growth to the reproductive stage until it has been exposed to a period of low but non-freezing temperatures, a process called vernalization. The limited level of low temperature (LT) tolerance in spring wheat means that exposure to cold greatly impairs its vitality, even to the point of compromising survival. Cold-induced proteins have been well characterised and categorised as Lea (late embryogenesis abundant), Dhn (dehydrin), Rab (response to abscisic acid), Lt (LT responsive), Cor and many others (Jan et al., 2009). Numerous proteomic studies have been published during recent years dealing with cereal plants undergoing cold stress. To provide a few examples, Yan and colleagues analysed the response of 21 day-old rice seedlings (*Oryza sativa* L. cv. Nipponbare) to 6 or 24 h of exposure to 6 °C, and subsequent recovery, at the proteomic level (Yan et al., 2006). In this study, the Authors managed to identify 85 differentially expressed proteins; further protein classification revealed that the largest functional category of proteins affected by chilling stress was devoted to photosynthesis. In the same year, Yang *et al.* (2006) subjected a cold sensitive rice variety, named Liangyoupeijiu, to 4 °C cold treatment and performed 2D-E on the leaf proteome. MS analysis allowed the identification of many cold-modulated proteins, among which some metabolism-associated proteins were found to be down-regulated, whereas the up-regulated proteins included several stress-resistance polypeptides. One year later, Lee *et al.* (2007) used proteomic techniques to isolate cold-responsive low-abundant proteins in rice leaf tissues. They identified a total of 12 up-regulated protein spots, including several previously unreported proteins (*i.e.*, cysteine proteinase, thioredoxin peroxidase, a RING zinc finger protein-like, drought-inducible LEA, and a fibrillin-like protein). More recently, Hashimoto and Komatsu conducted another study focusing on cold stress-induced changes in protein profiles of leaf blades, leaf sheaths and roots of two-week-old rice seedlings (Hashimoto and Komatsu, 2007). 39 proteins were found to be differentially expressed after a brief (48 h) exposure to LT,



indicating both organ-specific and general plant responses to cold stress. Nevertheless all these works were performed after relatively short periods of cold exposure and a gap still persists in literature about cold-responsiveness of plants during the reproductive stage. Thus, protein changes responding to longer periods of stress may not have been identified so far, even though they may be crucial to adaptation under field conditions. Similarly to cold, drought stress represents a big challenge for plant growth. It affects carbon metabolism and disturbs the relationship between sink and source organs: cellular responses include osmotic adjustment, regulation of water circulation (aquaporins), protection against oxidative stress and, at the protein level, a significant accumulation of heat-shock proteins (HSP) and late embryogenesis abundant (LEA) proteins. Proteomics has been recently coupled to pre-existing molecular techniques to delve into plant responses to drought (Ali and Komatsu, 2005; Caruso et al., 2009; Salekdeh et al., 2002; Hajheidari et al., 2005; Riccardi et al., 1998). Functional categories of modulated proteins demonstrated a broad involvement of pathways presiding the major plant vital functions, among which photosynthesis, lignification, cellular transport and storage. Many proteins are produced by the plant in order to prevent cellular damage (HSP) (Kiyosue et al., 1994), or to maintain the energetic cellular demand upon stress (enzymes belonging to glycolysis and S-adenosyl-methionine synthase pathway) (Umeda et al., 1994; Chang et al., 1996). The analysis of the signaling pathways pointed out an extensive cross talk between drought and cold responses, a conclusion supported by the presence of common physiological components, such as cellular dehydration and accumulation of reactive oxidative species (ROS) (Apel and Hirt, 2004). As mentioned before, plants subjected to a single adverse condition are known to develop increased resistance to other stresses (cross-adaptation/protection). When this observation was tested on plants exposed to drought they were found to have enhanced cold tolerance, and *vice versa*; cold treatment improves drought resistance, making the use of desiccation a convenient strategy to adopt for increasing cold hardiness in plants (Cloutier and Siminovitch, 1982). However, the exact mechanism involved in drought-triggered cold resistance has not been completely clarified at the proteomic level; nonetheless, some physiological studies have recently demonstrated that drought-resistant plants have a greater cold tolerance at intermediate levels of acclimation than the

corresponding drought-sensitive clone (Costa et al., 2009), indicating an enhanced carbon metabolism in the drought-resistant variety, as well as a higher ability in adjusting osmotic potentials.

Starting from these considerations, we used the proteomic approach to examine differences in leaf protein profiles in an Iranian drought-tolerant spring wheat cultivar subjected to prolonged cold stress. In fact, although drought resistance has been demonstrated not to favour crop yield potential (Blum, 1988), it becomes a crucial feature in inhospitable habitats, such as dry regions of the world. In these areas, programmed selection is made for the improvement of crop drought tolerance, through precise strategies of stress-testing. In Iran, drought stress represents a relevant agronomic problem, being 60% of the total wheat area under rainfed cultivation. Furthermore, the majority of such zones lacks a satisfactory and constant amount of rainfalls. Quite recently, the troubleshootings related to dry farming in Iran have found their institutionalization in the Dryland Agricultural Research Institute (DARI), whose major aim is to develop cereal cultivars perfectly fitting in every microenvironment. For the warm-winter areas (Gachsaran, Lorestan, Ilam, and Golestan), the improved cultivars Nicknajat, Gahar, Zagros, Kohdasht, and Seymareh have been released. Their introduction has led to a significant yield increase (from 10 to 30% with respect to the local cultivars), and even more relevant if associated with improved agronomic practices such as weed control and soil fertilization (Mosaad et al., 2005). The spring-habit pure line that we used is Kohdasht, the most drought-tolerant wheat line among the other previously cited (Mahfoozi et al., 2006). The cold sensitivity of Kohdasht variety made the effect of low temperature on metabolism of this plant more revealing, providing molecular information about the role of drought tolerance in adaptation to cold temperatures.

## References

- Ali, G. M., Komatsu, S., Proteomic Analysis of Rice Leaf Sheath during Drought Stress. *J. Proteome Res.* 2006, 5, 396-403.
- Apel, K., Hirt, H., Reactive Oxygen Species: Metabolism, Oxidative Stress, and Signal Transduction. *Annu. Rev. Plant. Biol.* 2004, 55, 373-399.
- Blum, A., Plant breeding for stress environments. CRC Press 1988, Boca Raton, FL.
- Caruso, G., Cavaliere, C., Foglia, P., Gubbiotti, R. et al., Analysis of drought responsive proteins in wheat (*Triticum durum*) by 2D-PAGE and MALDI-TOF mass spectrometry. *Plant Sci.* 2009, 177, 570-576.
- Chang, S., Puryear, J. D., Dias M. A. D. L., Funkhouser, E. A. et al., Gene expression under water deficit in loblolly pine (*Pinus taeda*): isolation and characterization of cDNA clones. *Physiol. Plant.* 1996, 97, 139-148.
- Chinnusamy V, Schumaker K, Zhu JK. Molecular genetic perspectives on cross-talk and specificity in abiotic stress signalling in plants. *J. Exp. Bot.* 2004;55:225-236.
- Cloutier, Y., Siminovitch, D., Correlation between cold- and drought-induced frost hardiness in winter wheat and rye varieties. *Plant Physiol.* 1982, 69, 256-258.
- Cook D, Fowler S, Fiehn O, Thomashow MF. A prominent role for the CBF cold response pathway in configuring the low-temperature metabolome of *Arabidopsis*. *Proc. Natl. Acad. Sci. USA* 2004;101:15243-15248.
- Costa e Silva, F., Shvaleva, A., Broetto, F., Ortuño, M.F. et al., Acclimation to short-term low temperatures in two *Eucalyptus globulus* clones with contrasting drought resistance. *Tree Physiol.* 2009, 29, 77-86.
- Hajheidari, M., Abdollahian-Noghabi, M., Askari, H., Heidari, M. et al., Proteome analysis of sugar beet leaves under drought stress. *Proteomics* 2005, 5, 950-960.
- Hashimoto, M., Komatsu, S., Proteomic analysis of rice seedlings during cold stress. *Proteomics* 2007, 7, 1293-1302.
- Jan, N., Ul-Hussain, M., Andrabi, K. I., Cold resistance in plants: A mystery unresolved. *Electron. J. Biotechnol.* 2009, 12, 1-15.
- Kaplan F, Kopka J, Haskell DW, Zhao W, Schiller KC, Gatzke N, Sung DY, Guy CL. Exploring the temperature-stress metabolome of *Arabidopsis*. *Plant Physiol.* 2004;136:4159-4168.
- Kiyosue, T., Yamaguchi-Shinozaki, K., Shinozaki, K., Cloning of cDNAs for genes that are early-responsive to dehydration stress (ERDs) in *Arabidopsis thaliana* L.: identification of three ERDs as HSP cognate genes. *Plant Mol. Biol.* 1994, 25, 791-798.
- Knight H, Knight MR. Abiotic stress signaling pathways: specificity and cross-talk. *Trends Plant Sci.* 2001;6:262-267.
- Kreps JA, Wu Y, Chang HS, Zhu T, Wang X, Harper JF. Transcriptome changes for *Arabidopsis* in response to salt, osmotic, and cold stress. *Plant Physiol.* 2002;130:2129-41.
- Lee, D. G., Ahsan, N., Lee, S. H., Kang, K. Y. et al., An approach to identify cold-induced low-abundant proteins in rice leaf. *C. R. Biol.* 2007, 330, 215-225.
- Mahfoozi, S., Limin, A. E., Ahakpaz, F., Fowler, D. B., Phenological development and expression of freezing resistance in spring and winter wheat under field conditions in north-west Iran. *Field Crops Res.* 2006, 97, 182-187.
- Mosaad, M., Singh, M., Roustaii, M., Ketata, H., Rajaram, S., in: Buck, H. T., Nisi J. E., Salomón, N. (Eds.), *Wheat Production in Stressed Environments*, Springer Netherlands 2005, 12, pp. 315-320.

- Rabbani MA, Maruyama K, Abe H, Khan MA, Katsura K, Ito Y, Yoshiwara K, Seki M, Shinozaki K, Yamaguchi-Shinozaki K. Monitoring expression profiles of rice genes under cold, drought, and high-salinity stresses and abscissic acid application using cDNA microarray and RNA gel-blot analyses. *Plant Physiol.* 2003;133:1755-67.
- Riccardi, F., Gazeau, P., de Vienne, D., Zivy, M., Protein Changes in Response to Progressive Water Deficit in Maize. Quantitative Variation and Polypeptide Identification. *Plant Physiol.* 1998, 117, 1253-1263.
- Salekdeh, G. H., Siopongco J., Wade, L. J., Ghareyazie, B., Bennett, J., Proteomic analysis of rice leaves during drought stress and recovery. *Proteomics* 2002, 2, 1131-1145.
- Seki M, Narusaka M, Abe H, Kasuga M, Yamaguchi-Shinozaki K, Carninci P, Hayashizaki Y, Shinozaki K. Monitoring the expression pattern of 1300 Arabidopsis genes under drought and cold stresses by using a full-length cDNA microarray. *Plant Cell* 2001; 13: 61-72.
- Umeda, M., Hara, C., Matsubayashi, Y., Li, H. H. et al., Expressed sequence tags from cultured cells of rice (*Oryza sativa* L.) under stressed conditions: analysis of genes engaged in ATP-generating pathways. *Plant Mol. Biol.* 1994, 25, 469-478.
- Wang W, Vinocur B, Shoseyov O, Altman A. Role of plant heat-shock proteins and molecular chaperones in the abiotic stress response. *Trends Plant Sci.* 2004; 9:244-252.
- Yan, S. P., Zhang, Q. Y., Tang, Z. C., Su, W. A., Sun, W. N., Comparative Proteomic Analysis Provides New Insights into Chilling Stress Responses in Rice. *Mol. Cell. Proteomics* 2006, 5, 484-496.
- Yang, P. F., Li, X. J., Liang, Y., Jing, Y. X. et al., Proteomic Analysis of the Response of Liangyoupeijiu (Super High-Yield Hybrid Rice) Seedlings to Cold Stress. *J. Integr. Plant Biol.* 2006, 48, 945-951.

## Materials and Methods

**Plant material, cold treatment and determination of phenological development.** Wheat seedlings (*Triticum aestivum* cv Kohdasht) were grown in a controlled growth chamber at 20 °C for 14 days with 12 h daylight period at 300  $\mu\text{mol m}^{-2} \text{s}^{-1}$  photosynthetic photon flux density (PPFD). Afterwards, plants were transferred to a 4 °C for 42 days (cold treatment) or they were maintained at 20 °C. To determine the stage of phenological development, two methods were used: (i) determination of final leaf number (FLN), and (ii) dissection of the plant crown to reveal the shoot apex development. For FLN determination, three plants were grown in each pot in three replications and were placed in both cold (4 °C) and warm rooms (20 °C) at the same time as the pots for shoot apex analyses. Plants were sampled in 14-day establishment (experimental day 0), 21- and 42-day cold treatments. At each sampling date two pots each with three plants in each replicate were moved into a glasshouse at 20 °C and a 16 h day length (long-day flower induction conditions). Leaves on the main stem of each plant were numbered until the flag leaf emerged. The experimental design for the FLN trial was a 1 (genotype) x 3 (sampling date = 0, 21 and 42-d) factorial. Shoot apices of plants were dissected, recorded and photographed at each sampling date to determine the stage of development. The stage of phenological development was determined from changes in the morphology of the shoot apex and was expressed by decimal code (DC) according to Nátrová and Jokeš (1993). Shoot apices from five plants were dissected and the mean code was calculated.

**Proline content.** Proline content was estimated at intervals of 0, 21 and 42 days following the method described by Bates (1973). 0.5 g (fresh weight) of spring wheat leaves were homogenized with 3% sulphosalicylic acid and centrifuged. The supernatant was treated with acetic acid and acid-ninhydrin and boiled for 1 h. The mixture was eluted in benzene and the absorbance was read at 520 nm using a Cary 4 Varian spectrophotometer.

**Soluble sugar extraction.** Total water soluble carbohydrate determination was based on the phenol sulphuric acid method of Dubois *et al.* (1956). Data were measured at 485 nm by a Cary 4 Varian spectrophotometer.

**Chlorophyll content.** Chlorophyll *a* + *b* content (SPAD readings, dimensionless value) was determined by chlorophyll meter SPAD-502 (Minolta, Tokyo, Japan).

**Protein Extraction.** 1 g of wheat leaves (2-4 leaves above the crown on main stem samples) was finely ground in liquid nitrogen and the protein extraction was performed according to Damerval *et al.* (1986), with some modifications. The resulting powder was suspended (1 g/10 ml) in chilled (-20 °C) 10% TCA in acetone containing 0.007% DTT and 1% plant protease inhibitor cocktail (P9599; Bio-Rad, Hercules, CA, USA). The mixture was incubated at -20 °C for at least 1 h then centrifuged at 35000 g for 15 min. The pellet was washed three times (10 ml) with chilled (-20 °C) acetone containing 0.007% DTT centrifuging at 12000 g at 4 °C for 15 min. The supernatant was removed and the pellet was lyophilized for 1 h. If dried powder was not to be solubilised immediately, it was stored at -80 °C until use.

**Protein solubilisation and two-dimensional electrophoresis.** The wheat leaf proteins in the dried powder were solubilised in 9 M urea, 4% CHAPS, 1% DTT, 1% pH 3-10 ampholytes (Bio-lyte; Bio-Rad, Hercules, CA, USA), 35 mM Tris base via incubation at 37 °C for 1 h with continuous stirring. The mixture was centrifuged at 12000 g at room temperature for 15 min and a small aliquote was used to determine protein content by Bradford assay (Bradford, 1976). IEF was performed using Biorad Multiphore II and Dry Strip Kit (Bio-Rad-Protean-IEF-Cell-System). Seventeen centimeter IPG strips (Bio-Rad, Hercules, CA, USA) pH 4-7 were passively rehydrated overnight with 750 µg of protein in 300 µl of solubilisation solution containing 1% carrier ampholyte (Bio-lyte 4-7; Bio-Rad, Hercules, CA, USA). The total product time x voltage applied was 80 000 V h for each strip at 20 °C. Strips were subsequently reduced (1% DTT, 15 min) and alkylated (2.5% IAA, 15 min) during the equilibration step (30 min in 50 mM Tris-HCl pH 8.8, 6 M urea, 30% glycerol v/v, 1% SDS, bromophenol blue). Equilibrated strips were then placed on SDS-

polyacrylamide gels, 16 cm × 20 cm, 13% acrylamide, and sealed with 0.5% agarose. SDS-PAGE was performed using the Protean II xi Cell, large gel format (Bio-Rad) at constant current (40 mA per gel) at 7 °C until the bromophenol blue tracking dye was approximately 2–3 mm from the bottom of the gel. Protein spots were stained by Blue Silver (Candiano et al., 1996).

**Image Analysis.** Two dimension gel images were digitised using a flatbed scanner (model ImageScanner-II, GE Healthcare, Uppsala, Sweden) with a resolution of 300 dpi and 16-bit greyscale pixel depth. Image analysis was carried out with Progenesis SameSpots software vers. 2.0 (Nonlinear Dynamics), which allows spot detection, background subtraction, and protein spot OD intensity quantification (spot quantity definition). The gel image showing the highest number of spots and the best protein pattern was chosen as a reference template, and spots in a standard gel were then matched across all gels. Spot quantity values were normalised in each gel dividing the raw quantity of each spot by the total quantity of all the spots included in the standard gel. For each protein spot, the average spot quantity value and its variance coefficient in each group was determined. One-way analysis of variance (ANOVA) was carried out at  $p < 0.05$  in order to assess for absolute protein changes among the different treatments; only 1.5-fold or higher quantitative variations were taken into consideration. The false discovery rate (FDR) was estimated by calculating q-values with a threshold of 0.05. The least significant difference (LSD) test was used to determine significant differences among group means.

**Functional annotation.** Gene Ontology (GO) lists were downloaded from the TAIR website (<http://www.arabidopsis.org/tools/bulk/go/index.jsp>): each protein was classified with respect to its cellular component, biological process, and molecular function using GO annotation. When no GO annotation was available, proteins were annotated manually based on literature searches and closely related homologues.

**In-gel digestion.** Protein spots were carefully cut out from Blue Silver stained gels and subjected to in-gel trypsin digestion according to Shevchenko *et al.* (1996) with minor modifications. The gel

pieces were swollen in a digestion buffer containing 50 mM  $\text{NH}_4\text{HCO}_3$  and 12.5 ng/ $\mu\text{L}$  of trypsin (modified porcine trypsin, sequencing grade, Promega, Madison, WI) in an ice bath. After 30 min the supernatant was removed and discarded, 20  $\mu\text{L}$  of 50 mM  $\text{NH}_4\text{HCO}_3$  were added to the gel pieces and digestion allowed to proceed at 37° C overnight. The supernatant containing tryptic peptides was dried by vacuum centrifugation. Prior to mass spectrometric analysis, the peptide mixtures were redissolved in 10  $\mu\text{L}$  of 5% FA (Formic Acid).

**Protein identification by MS/MS.** Peptide mixtures were separated using a nanoflow-HPLC system (Ultimate; Switchos; Famos; LC Packings, Amsterdam, The Netherlands). A sample volume of 10  $\mu\text{L}$  was loaded by the autosampler onto a homemade 2 cm fused silica precolumn (75  $\mu\text{m}$  I.D.; 375  $\mu\text{m}$  O.D.; Reprosil C18-AQ, 3  $\mu\text{m}$ , Dr. Maisch GmbH, Ammerbuch-Entringen, Germany) at a flow rate of 2  $\mu\text{L}/\text{min}$ . Sequential elution of peptides was accomplished using a flow rate of 200 nL/min and a linear gradient from Solution A (2% acetonitrile; 0.1% formic acid) to 50% of Solution B (98% acetonitrile; 0.1% formic acid) in 40 minutes over the precolumn in-line with a homemade 10-15 cm resolving column (75  $\mu\text{m}$  I.D.; 375  $\mu\text{m}$  O.D.; Reprosil C18-AQ, 3  $\mu\text{m}$ , Dr. Maisch GmbH, Ammerbuch-Entringen, Germany). Peptides were eluted directly into a High Capacity ion Trap (model HCTplus, Bruker-Daltonik, Germany). Capillary voltage was 1.5-2 kV and a dry gas flow rate of 10 L/min was used with a temperature of 230 °C. The scan range used was from 300 to 1800 m/z. Protein identification was achieved by searching the National Center for Biotechnology Information non-redundant database (NCBI nr, version 20081128, [www.ncbi.nlm.nih.gov](http://www.ncbi.nlm.nih.gov)) using the Mascot program (in-house version 2.2, Matrix Science, London, UK). The following parameters were adopted for database searches: complete carbamidomethylation of cysteines and partial oxidation of methionines, peptide Mass Tolerance  $\pm 1.2$  Da, Fragment Mass Tolerance  $\pm 0.9$  Da, missed cleavages 2. For positive identification, the score of the result of ( $-10 \times \text{Log}(P)$ ) had to be over the significance threshold level ( $P < 0.05$ ). Even though high MASCOT scores are obtained with values greater than 60, when proteins were identified with only one peptide a combination of automated database search and manual interpretation of peptide fragmentation spectra was used to validate protein assignments. In this manual verification, the mass error, the presence of



fragment ion series, and the expected prevalence of C-terminus containing ions (Y-type) in the high mass range, were all taken into account. Moreover, replicate measurements have confirmed the identity of these protein hits.

**RNA extraction, cDNA synthesis and PCR.** Semi quantitative RT-PCR was carried out following extraction of total leaf RNA by applying RNXplus (Fermentas) from the pulverized plant leaves, followed by phenol/chloroform/extraction, isopropanol precipitation and ethanol wash. The extracted RNA was reverse transcribed using the Roche cDNA synthesis kit, as per manufacturer's instructions. The synthesised cDNA was used in the subsequent PCR by applying specific primers designed for *tubulin* as an internal control housekeeping gene and three other genes whose expression was subjected to change in response to cold stress (*wcor18*, protein spot No. 1; *wrab17*, protein spot No. 22; *rbcS*, protein spots No. 19, 64, 72). The primer pairs used for amplification are listed in Table 1. PCR conditions were identical except for the annealing temperature which was adjusted for each gene as required. Specifically, 60 °C and 35 cycles were used for *tubulin*, *rbcS* and *wrab17* genes, while a two step annealing procedure was used for *wcor18* amplification so that a primary gradient amplification for 16 cycles starting from 52 °C and terminating at 60 °C was used to enhance amplification of *wcor18* followed by 30 cycles of annealing at 60 °C. Apart from annealing, all other conditions of PCR were the same so that initial denaturation was at 94 °C for 4 min followed by denaturation at 94 °C 1 min, annealing 1 min according to the above description, 72 °C extension for 1 min and final extension for 5 min.

Gene	Forward 5'-3'	Reverse 5'-3'
<i>tubulin</i>	TGATGCTTTCAACACCTTCTTCAG	GGGGCGTAGGAGGAAAGCA
<i>Wcor18</i>	TACACGCTGGAGGGGCAGGGC	CCGGGCTGCTTCCAGTCGTTGAC
<i>Wrab17</i>	GGCTGTCACGAAGGCTGCCTC	CCTGCTGGAAGACGTTTTCTTGG
<i>rbcS</i>	GAGGGCATCAAGAAGTTCGAGACC	TCAGGGTACTCCTTCTTGACCTCC

**Table 1.** Primer sequences used for RT-PCR assays.

## References

- Bates, L. S., Rapid determination of free proline for water stress studies. *Plant Soil* 1973, 39, 205-207.
- Bradford, M. M., A rapid and sensitive method for the quantitation of microgram quantities of protein utilizing the principle of protein-dye binding. *Anal. Biochem.* 1976, 72, 248-254.
- Candiano, G., Bruschi, M., Musante, L., Santucci, L. et al., Blue silver: a very sensitive colloidal Coomassie G-250 staining for proteome analysis. *Electrophoresis* 2004, 25, 1327-1333.
- Damerval, C., De Vienne, D., Zivy, M., Thielllement, H., Technical improvements in two-dimensional electrophoresis increase the level of genetic variation detected in wheat-seedling proteins. *Electrophoresis* 1986, 7, 52-54.
- Dubois, M. K., Gils, J. K., Hanniton, P. A., Robes, L., Smith, F., Colorimetric Method for Determination of Sugars and Related Substances. *Anal. Chem.* 1956, 28, 350-356.
- Nátrová, Z., Jokeš, M., A proposal for a decimal scale of the inflorescence development of wheat. *Rostlinná výroba* 1993, 39, 315-328.
- Shevchenko, A., Wilm, M., Vorm, O., Mann, M., Mass spectrometric sequencing of proteins silver-stained polyacrylamide gels. *Anal. Chem.* 1996, 68, 850-858.

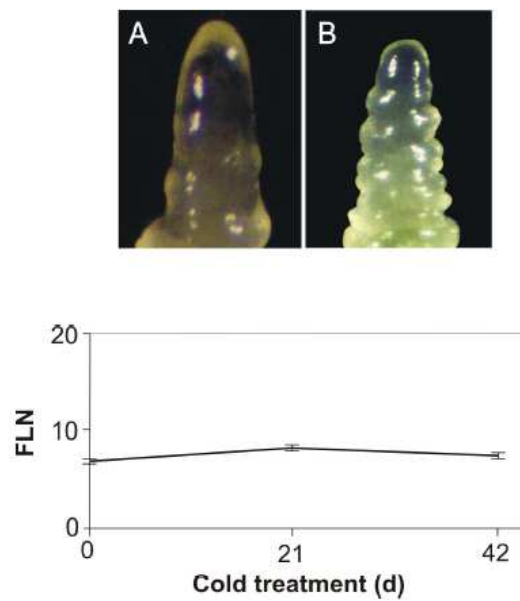
## Results

### Effects of low temperature on phenological development

Figure 1 shows morphological changes induced by cold exposure of Kohdasht seedlings. 42-day cold acclimated wheat plants reduced their growth with respect to non-acclimated plants, particularly at the level of elongation which is strongly impaired. Shoot apex dissection, which is commonly recognized as a good indicator of wheat developmental stage (Hay and Ellis, 1998; McMaster, 1997), was performed and expressed by decimal code (DC) according to Nátrová and Jokeš (1993). In the present study, Kohdasht spring wheat reached the single ridge stage (DC of about 19) within 14 establishment days (0-d cold treatment) (Figure 2A), which was shortly after planting. This early rapid advancement to the beginning of reproductive stage is a characteristic of spring habit cultivars. The phenological development of 42-d cold acclimated plants was found to be relatively similar to the 14-d establishment plants, because low-temperature conditions in cold conditioned chambers did not allow plant developmental progress, thus shoot apex of 42-d cold acclimated plants stopped just at formation of double ridge DR-1 stage (DC = 20) (Figure 2B). Shoot apex elongation and initiation of double ridges are the physical manifestation that the signal for transition to the reproductive stage has occurred, and the results of present study are in agreement with previous observations obtained under field conditions (Mahfoozi et al., 2006). On the other hand, along with dissection of the plant crown to expose the shoot apex, transition from the vegetative to the reproductive phase can also be determined by recording the final leaf number (FLN). As expected, Kohdasht reached its minimum leaf number very shortly after planting (Figure 2, lower panel). Globally, these observations assured that plants with similar developmental stages were compared for proteomic cold acclimation studies. The 42-day plants grown at RT were able to reach the heading stage, thus allowing us to discriminate cold-responsive proteins from ones involved in development.



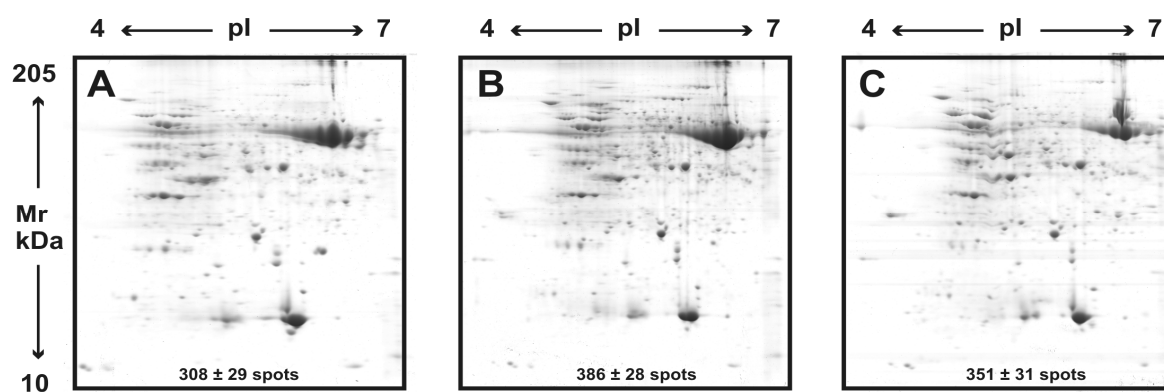
**Figure 1.** Response of Kohdasht wheat cultivar to prolonged cold stress.



**Figure 2.** Phenological development stage of Kohdasht spring wheat cultivar grown at 4 °C as estimated from shoot apex developmental morphology and final leaf number (FLN). Comparative phenological advancement to double ridge formation is illustrated in the upper panel. A, Shoot apex elongation and single ridge stage of 14-d establishment Kohdasht; B, Double ridge stage of 42-d cold acclimated Kohdasht. Lower panel shows changes in FLN. Bars represent  $\pm$  SE ( $n = 3$ ).

### Proteomic analysis of differentially expressed proteins under cold treatment

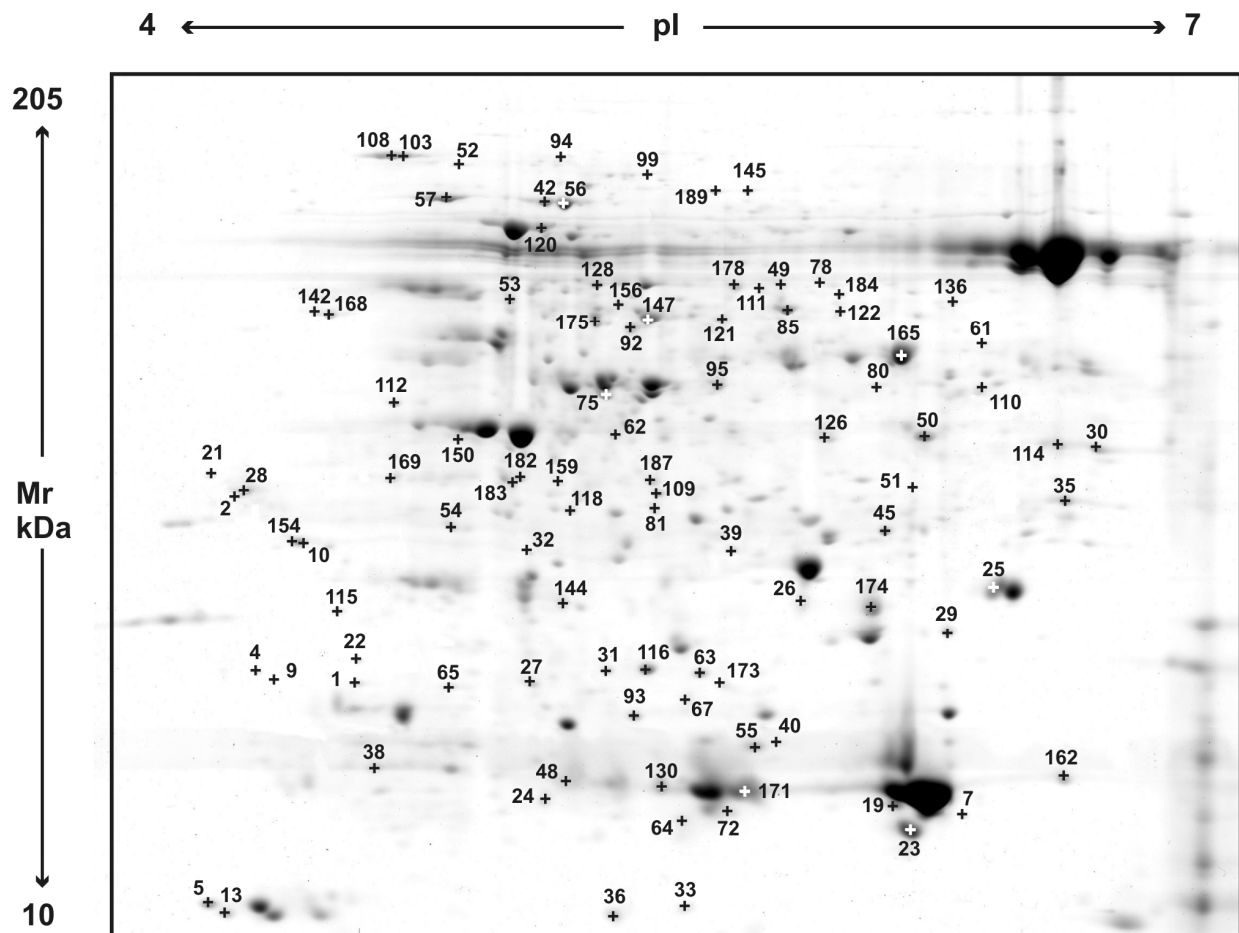
To assess changes related to cold acclimation at the molecular level, we initially conducted a comparative proteomic study by analysing qualitative changes in leaf polypeptide composition between three different experimental stages: (i) at day 0 (plants grown at room temperature (RT) for 14 days), (ii) after 21 or (iii) 42 days of cold acclimation. Small 2DE maps (13 cm, pl 4-7) of leaf soluble protein extracts were performed in three replicates and the results are shown in Figure 3. As can be seen, major accumulation of total proteins, quantified as total spot number, was detected after 21 days of cold treatment (about 30% increase compared with control), then a slight decrease was observed after 42 days (Figure 3B-C).



**Figure 3.** Comparison of Kohdasht spring wheat leaf proteomes by small 2-DE (IPGs 13 cm length, pl 4-7). Maps refer to different stages of leaf development and treatment: A, 14 days at room temperature (zero point); B, after 21 days of cold acclimation at 4 °C; C, after 42 days of cold acclimation at 4 °C. Total spot number was determined and the arithmetic mean  $\pm$  standard deviation (SD) was considered. Values refer to spots matching across all the gel replicates. Total protein sample load: 400  $\mu$ g

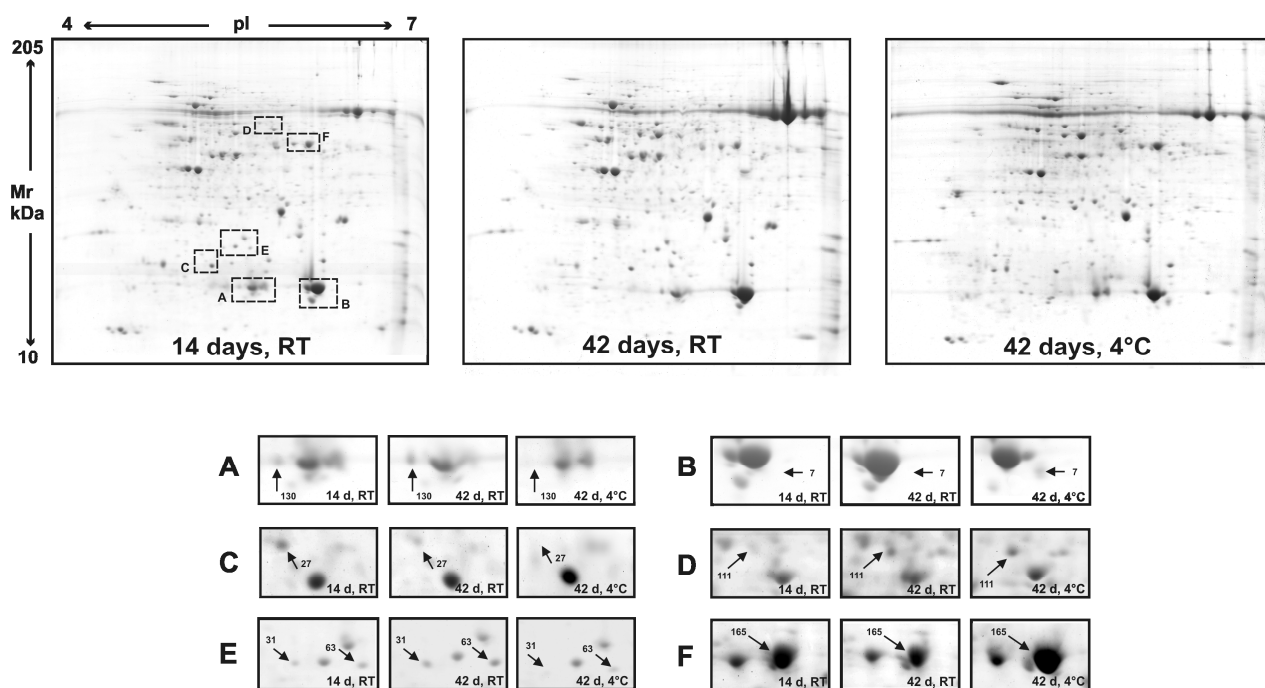
Recent research has shown that transition to the reproductive phase, which is determined by clusters of co-adapted flowering genes, is the critical switch that initiates down-regulation of LT-induced genes (Fowler et al., 1996). Thus, the gradual decrease in the total protein content between 21 and 42 days of cold acclimation confirmed at the protein level that the transition to the reproductive phase occurred during that time, in agreement, on the other hand, with phenological observations. As mentioned before, reproductive development is the most water-sensitive phase in cereals, thus we decided to make an in-depth study on the effects of a long-term cold exposure

(i.e., 42 days at 4 °C) using quantitative differential proteomics. The experimental procedure involved large 2D gel electrophoresis (17 cm, pI 4-7) conducted on total leaf protein extracts from plants grown in controlled environment conditions at 20 °C for 14 (experimental day 0) and 42 days, and from 42 days cold-acclimated plants. Four biological and technical replicates per condition were performed and cross-compared by image software analysis Progenesis SameSpot (NonLinear Dynamics, Newcastle, UK) which generated the final master map shown in Figure 4.



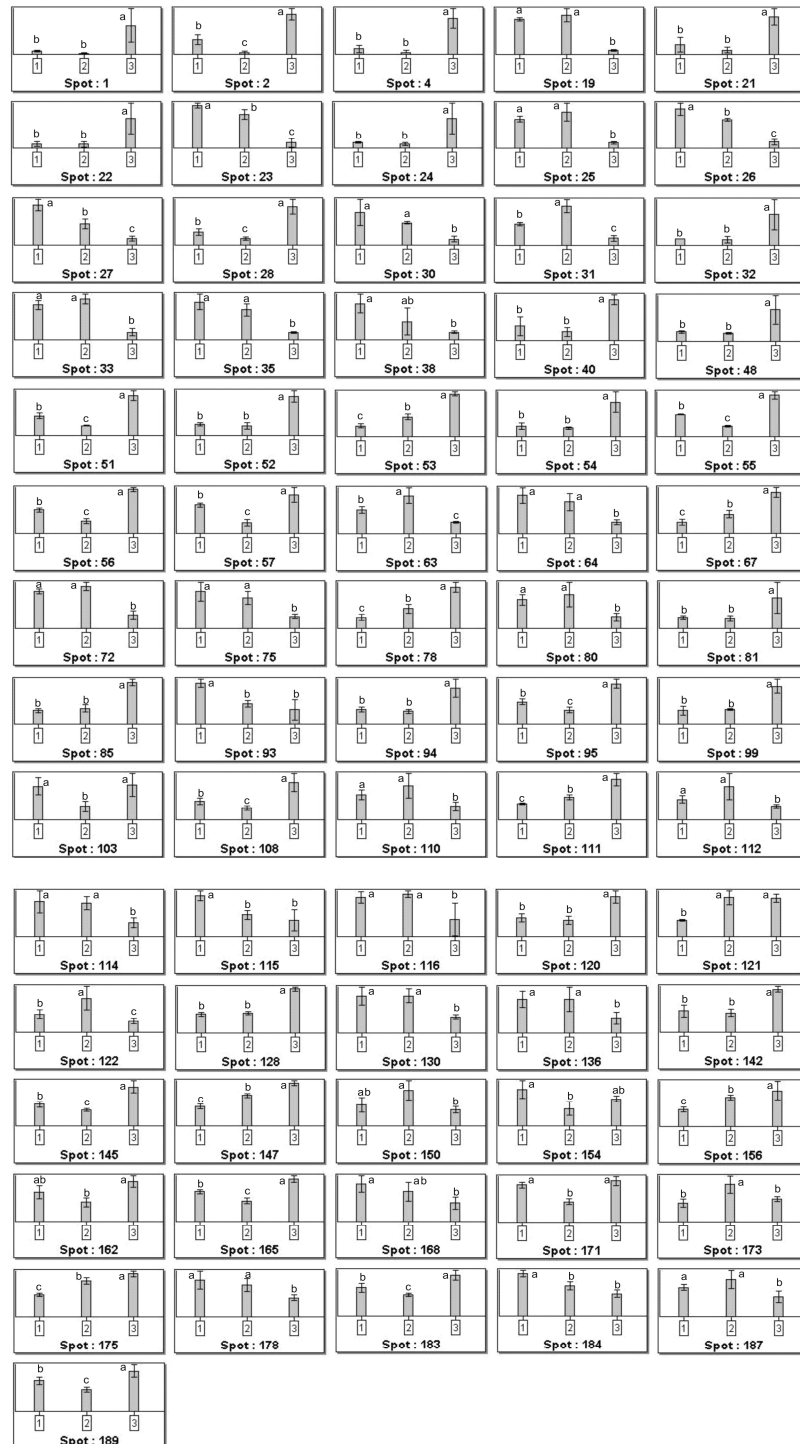
**Figure 4.** Master map obtained comparing 2-DE of leaf tissues from zero point (14 d, RT), 42 days at room temperature and 42 days at 4 °C. Numbers of significantly different spots derive from computerized image analysis of 2-D gels using Progenesis SameSpots software.

We found 598 spots that were common to all the gels, among these were 93 spots with significantly different expression levels (absolute variation of at least 1.5-fold). Figure 5 shows three representative maps for the samples (i) 14-d, RT (zero point, control sample), (ii) 42-d, RT and (iii) 42-d, 4 °C. Some gel regions are zoomed and displayed in order to appreciate quantitative changes (newly induced or totally repressed, up- or down-regulated spots) caused by development and/or cold treatment.



**Figure 5.** Comparison of 2-DE maps of leaf tissues from zero point (14 d, RT), 42 days at room temperature and 42 days at 4 °C. Boxed areas (A-E) in the principal image indicate zoomed regions displayed in the lower panel (examples of spots repressed, induced, and negatively or positively modulated). Numbers of spots indicated by the arrows refer to the master map shown in Figure 3. Linear IPGs pH 4-7, 17 cm length.

Histograms resulting from quantitative analysis obtained by Progenesis SameSpot software (NonLinear Dynamics, Newcastle, UK) are shown in Figure 6.



**Figure 6.** Histograms representing the mean of the spot normalized volumes for each treatment (14 d RT; 42 d RT; 42 d 4 °C).



Differentially expressed spots (indicated with numbers in Figure 4) were excised from the gels, digested by trypsin and peptide mixtures were then analysed by LC-ESI-MS/MS for protein identification. The successfully identified proteins are listed in Table 2, together with the protein spot number, the identification parameters, and the indication of their GO (gene ontology) annotations (cellular component, biological process, and molecular function). An additional table listing peptide sequences of identified proteins is provided in the final section of the thesis "Supporting Information". Taking into account the result of the LSD (least significant difference) test, quantitative data of spots with inter-group statistical significance were loaded into the PageMan software (Usadel et al., 2006) which generated a false-color heat map to directly compare growth and cold effects on wheat leaves (Figure 7). Differentially expressed proteins were automatically included in functional categories (BINs) and spots with similar expression trends were also clustered (Figure 7). Data points which fell within the same BIN were automatically averaged by the software and the average value was used for creating the corresponding colour bar. Four primary clusters were defined: cluster 1 represented proteins slightly down-regulated by development, but strongly enhanced by cold; cluster 2 included proteins with a low or absent modulation by development, but up-regulated by low-temperature; clusters 3 and 4 were characterized by proteins that displayed relatively stable levels of abundance throughout the development, but with a more or less strong down-regulation by cold. This approach helped us to focus on the most interesting spots, which would hopefully provide direct evidence of proteins positively or negatively related to cold-acclimation.

Spot No. <sup>a</sup>	Protein name	Mr, kDa theor/exper <sup>b</sup>	pI theor/exper <sup>b</sup>	NCBI accession No.	Homologue At <sup>c</sup>	No. of peptides	Mascot Score	1-ANOVA <sup>d</sup>	Fold of variation (42 dd 20 °C/42 dd 4°C) <sup>e</sup>	GO comp	GO funct	GO process
22	group3 late embryogenesis abundant protein (wrab17) [Triticum aestivum]	18.3/21.8	5.0/4.5	gi 157073742	At3g15670	4	239	1.0x10 <sup>-2</sup>	- 0.0895/+ 0.8318	nucleus	unknown	embryonic development ending in seed dormancy
48	Glycine-rich RNA-binding protein [Triticum aestivum]	16.0/16.5	6.3/5.1	gi 114145394	At2g21660	3	134	3.0x10 <sup>-3</sup>	- 0.0702/+ 0.4665	chloroplast	ss/ds DNA and RNA binding	response to cold
1	cold regulated protein (wcor18) [Triticum aestivum]	17.7/20.9	4.8/4.5	gi 26017213	At5g01300	7	519	1.0x10 <sup>-3</sup>	- 0.6601/+ 0.8396	-	phosphatidyl-ethanolamine binding	-
116	ribulose-1,5-bisphosphate carboxylase/oxygenase large subunit [Triticum aestivum]	53.4/21.5	6.2/5.3	gi 14017580	AtCg00490	4	321	9.0x10 <sup>-3</sup>	+ 0.0353/- 0.4700	chloroplast	RuBisCO activity	carbon fixation
27		53.4/21.0	6.2/5.0			3	242	4.4x10 <sup>-5</sup>	- 0.2830/- 0.8234			
114		53.4/36.0	6.2/6.5			14	721	2.0x10 <sup>-3</sup>	- 0.0033/- 0.4098			
30		53.4/35.9	6.2/6.6			13	687	1.7x10 <sup>-4</sup>	- 0.1337/- 0.7518			
35		53.4/31.9	6.2/6.5			3	176	9.6x10 <sup>-7</sup>	- 0.1049/- 0.7130			
64	ribulose-1,5-bisphosphate carboxylase/oxygenase small subunit [Triticum aestivum]	19.4/14.5	8.5/5.4	gi 170771	At1g67090	9	394	1.2x10 <sup>-4</sup>	- 0.0897/- 0.5323	chloroplast	RuBisCO activity	carbon fixation
19		19.4/15.1	8.5/6.0			8	369	6.0x10 <sup>-9</sup>	+ 0.0401/- 0.9466			
72		19.4/15.0	8.5/5.6			6	250	1.5x10 <sup>-5</sup>	+ 0.0530/- 0.4663			
55		19.4/18.0	8.5/5.6			4	189	4.4x10 <sup>-9</sup>	- 0.3090/+ 0.2573			
23		19.4/14.1	8.5/6.1			9	420	3.7x10 <sup>-5</sup>	- 0.1046/- 0.9675			
24		19.4/15.7	8.5/5.1			2	73	4.0x10 <sup>-3</sup>	- 0.1859/+ 0.6459			
40		19.4/18.2	8.5/5.7			8	390	1.0x10 <sup>-3</sup>	- 0.2080/+ 0.4983			
171		19.4/15.9	8.5/5.6			8	362	1.5x10 <sup>-5</sup>	- 0.2598/+ 0.0443			
122	Os03g0129300 [Oryza sativa (japonica cultivar-group)] glyceraldehyde-3-phosphate dehydrogenase	47.5/54.8	6.2/5.9	gi 115450493	At1g12900	12	735	5.0x10 <sup>-3</sup>	+ 0.1825/- 0.1924	chloroplast	GAPDH activity	glucose metabolic process
75	Os06g0608700 [Oryza sativa (japonica cultivar-group)] Fructose-bisphosphate aldolase	37.9/41.0	7.5/5.2	gi 115468886	At2g21330	6	369	9.0x10 <sup>-5</sup>	- 0.0757/- 0.4916	chloroplast	FBP aldolase activity	pentose-phosphate shunt
128	Ribulose bisphosphate carboxylase/oxygenase activase, chloroplastic [Oryza sativa Japonica Group]	51.7/58.0	5.4/5.2	gi 109940135	At2g39730	21	1275	1.7x10 <sup>-7</sup>	+ 0.0282/+ 0.3779	chloroplast	ADP binding RuBisCO / oxygenase activase activity	response to cold
121	Rubisco activase alpha form precursor [Deschampsia antarctica]	51.3/ 53.4	5.9/5.5	gi 32481061	At2g39730	18	1022	5.0x10 <sup>-3</sup>	+ 0.3801/+ 0.3807		enzyme regulator activity	
165		51.3/47.0	5.9/ 6.1			10	635	7.6x10 <sup>-6</sup>	- 0.1624/+ 0.1501			
147		51.3/53.4	5.9/5.3			9	491	3.0x10 <sup>-6</sup>	+ 0.1970/+ 0.3454			
175		51.3/ 52.5	5.9/5.2			11	629	2.1x10 <sup>-6</sup>	+ 0.2101/+ 0.2897			
187	putative transketolase 1 [Oryza sativa (japonica cultivar-group)]	69.4/33.0	5.4/5.3	gi 55296168	At2g45290	2	104	1.3x10 <sup>-2</sup>	+ 0.0974/- 0.1858	chloroplast	transketolase activity	-
178		69.4/58.0	5.4/5.6			5	291	2.0x10 <sup>-3</sup>	- 0.0664/- 0.2812			
136	Os01g0654500 NADP-isocitrate dehydrogenase [Oryza sativa (japonica cultivar-group)]	46.3/58.5	6.3/6.2	gi 115438939	At1g54340	11	763	1.2x10 <sup>-2</sup>	- 0.0164/- 0.3814	peroxisome plasma membrane	isocitrate dehydrogenase (NADP+) activity	isocitrate metabolic process

145	Os05g0482700 phosphoglycerate mutase [Oryza sativa (japonica cultivar-group)]	61.0/75.8	5.2/5.6	gi 115464537	At1g09780	5	317	5.8x10 <sup>-5</sup>	- 0.0818/+ 0.2595	cytosol	iPGAM activity	response to cold
189		61.0/75.8	5.2/5.5			9	438	4.5x10 <sup>-4</sup>	- 0.1546/+ 0.1183			
95	fructose 1,6-bisphosphate aldolase precursor [Avena sativa]	42.1/42.2	9.0/5.5	gi 8272480	At4g38970	11	644	1.2x10 <sup>-5</sup>	- 0.1843/+ 0.2537	cytosol	FBP aldolase activity	pentose-phosphate shunt
99	Os02g0774300 [Oryza sativa (japonica cultivar-group)] molecular chaperone DnaK	73.0/ 81.5	5.4/ 5.3	gi 115448989	At5g09590	11	731	2.1x10 <sup>-4</sup>	+ 0.0486/+ 0.4406	plasma membrane chloroplast	ATP binding	protein folding
94	HSP70 [Hordeum vulgare subsp. vulgare]	67.1/90.0	5.7/5.1	gi 476003	At5g28540	14	939	1.1x10 <sup>-4</sup>	- 0.0557/+ 0.3756	vacuole chloroplast	ATP binding	
108	Os12g0244100 [Oryza sativa (japonica cultivar-group)] Heat shock 70 protein	74.2/90.1	5.1/4.7	gi 115487998	At5g28540	21	1357	2.1x10 <sup>-4</sup>	- 0.1109/+ 0.3035			
103		74.2/90.1	5.1/4.7			8	522	5.0x10 <sup>-3</sup>	- 0.4196/+ 0.0165			
4	RuBisCO large subunit-binding protein subunit beta, chloroplastic [Secale cereale] (CPN60, GroEI like)	53.7/21.3	4.8/4.3	gi 2493650	At3g13470	20	1278	4.0x10 <sup>-3</sup>	- 0.7904/+ 0.9204	chloroplast	protein binding ATP binding	
56		53.7/73.2	4.8/5.1			19	1301	3.9x10 <sup>-6</sup>	- 0.2887/+ 0.2743			
57	RuBisCO large subunit-binding protein subunit alpha, chloroplastic (60 kDa chaperonin subunit alpha) [Triticum aestivum]	57.6/73.8	4.8/4.8	gi 134102	At3g13470	29	2006	1.1x10 <sup>-4</sup>	- 0.4410/+ 0.1244			
54	Os09g0438700 [Oryza sativa (japonica cultivar-group)] Chaperonin 10 Kd subunit (cpn10 or GroES)	25.4/29.5	5.9/4.8	gi 115479353	At1g14980	3	173	1.1x10 <sup>-4</sup>	- 0.0631/+ 0.4945	mitochondrion	chaperone binding	
81	Os02g0634900 [Oryza sativa (japonica cultivar-group)] proteasome alpha type 2	25.8/31.1	5.3/5.3	gi 115447473	At1g16470	6	375	2.0x10 <sup>-3</sup>	- 0.0337/+ 0.4164	cytosol	peptidase activity	ubiquitin-dependent protein catabolic process
53	Plastid glutamine synthetase GS2c [Triticum aestivum]	47.0/56.0	5.7/5.0	gi 71362640	At1g66200	11	703	8.3x10 <sup>-7</sup>	+ 0.2502/+ 0.5775	chloroplast	glutamate-ammonia ligase activity	nitrate assimilation
184	unknown [Zea mays] Aspartate aminotransferase family	50.0/56.4	6.5/5.9	gi 195634861	At1g77670	6	320	3.0x10 <sup>-4</sup>	- 0.1497/- 0.2835	-	transaminase activity	aspartate transamidation
52	Protein disulfide-isomerase [Triticum aestivum]	56.7/84.5	4.9/4.8	gi 1709620	At3g54960	25	1443	1.2x10 <sup>-5</sup>	- 0.0615/+ 0.5224	plasma membrane chloroplast	-	-
32	Os09g0279500 [Oryza sativa (japonica cultivar-group)] Plastid-specific 30S ribosomal protein 2	26.5/27.9	6.2/5.0	gi 115478330	At1g64510	3	125	9.5x10 <sup>-4</sup>	- 0.1107+ 0.6204	chloroplast	structural constituent of ribosome	ribosome biogenesis
142	triticain alpha [Triticum aestivum] cysteine proteinase	51.5/53.6	5.0/4.5	gi 111073715	At1g47128	3	205	3.4x10 <sup>-7</sup>	- 0.0331/+ 0.3263	vacuole chloroplast	cysteine-type peptidase activity	response to stress
67	S-adenosylmethionine:2-demethylmenaquinone methyltransferase-like [Oryza sativa Japonica Group]	18.3/20.2	5.3/5.4	gi 18461241	At5g16450	3	159	4.3x10 <sup>-5</sup>	+ 0.1952/+ 0.5272	-	ribonuclease inhibitor activity	regulation of RNA metabolic process
78	S-adenosylmethionine synthetase 1 [Triticum monococcum]	43.2/58.2	5.6/5.8	gi 115589744	At4g01850	6	400	1.4x10 <sup>-4</sup>	+ 0.1591/+ 0.4944	nucleolus cell wall	Methionine adenosyl-	SAM biosynthetic
111		43.2/57.7	5.6/5.7			14	998	4.1x10 <sup>-6</sup>	+ 0.1627/+ 0.4109			

											transferase activity	process
85	Glutamate-1-semialdehyde 2,1-aminomutase, chloroplast precursor [Hordeum vulgare]	49.6/54.8	6.3/5.7	gi 1170029	At5g63570	6	352	1.8x10 <sup>-5</sup>	+ 0.0576/+ 0.4742	chloroplast	GSAM activity	porphyrin biosynthetic process
168	unknown [Zea mays], peptidyl-prolyl cis-trans isomerase (cyclophilin)	46.6/53.4	5.9/4.5	gi 195650293	At3G01480	6	405	1.8x10 <sup>-2</sup>	- 0.1102/+ 0.3188	-	peptidyl-prolyl cis-trans isomerase activity	photosystem II assembly and stabilization
21	Ps16 protein [Triticum aestivum]	31.8/33.3	4.5/4.2	gi 2443390	At4g24770	2	131	5.0x10 <sup>-3</sup>	- 0.2823/+ 0.7283	chloroplast	poly(U) binding RNA binding	RNA binding
2		31.8/31.8	4.5/4.2			3	134	8.2x10 <sup>-4</sup>	- 1.1219/+ 0.4404			
28	Cp31BHv [Hordeum vulgare subsp. vulgare] nucleic acid-binding protein	30.6/32.1	4.7/4.3	gi 3550483	At4g24770	2	114	5.8x10 <sup>-6</sup>	- 0.3249/+ 0.4682			
154		30.6/28.3	4.7/4.4			6	389	1.0x10 <sup>-2</sup>	- 0.3404/- 0.1222			
110	Malate dehydrogenase, mitochondrial precursor [Triticum aestivum]	36.4/42.0	8.8/6.3	gi 126896	At5g09660	3	190	6.0x10 <sup>-3</sup>	+ 0.1275/- 0.2852	mitochondrion	malate dehydrogenase activity	regulation of fatty acid beta-oxidation
162	Nucleoside diphosphate kinase [Lolium perenne]	16.4/16.7	6.3/6.5	gi 9652119	At4g09320	3	239	4.2x10 <sup>-5</sup>	- 0.1875/+ 0.1333	plasma membrane chloroplast vacuole	ATP binding  nucleoside diphosphate kinase activity	response to stress
150	chloroplast lipocalin [Hordeum vulgare] fatty-acid binding protein	36.8/36.0	4.8/4.8	gi 77744909	At3g47860	3	127	1.1x10 <sup>-2</sup>	+ 0.2397/- 0.0938	chloroplast	transporter activity binding	response to oxidative stress
156	Phosphoglycerate kinase chloroplastic [Triticum aestivum]	49.9/55.0	6.5/5.3	gi 129915	At1g56190	7	392	2.0x10 <sup>-3</sup>	+ 0.2336/+ 0.3125	chloroplast	PGK activity	metabolic processes
93	Cytochrome b6-f complex iron-sulfur subunit, chloroplast precursor [Triticum aestivum]	24.1/19.5	8.4/5.3	gi 68566191	At4g03280	2	100	3.0x10 <sup>-3</sup>	- 0.2976/- 0.4923	chloroplast	electron transporter	photosynthetic electron transport in cytochrome b6/f
80	ferredoxin-NADP(H) oxidoreductase [Triticum aestivum]	39.1/42.0	8.3/6.0	gi 20302471	At5g66190	10	631	1.0x10 <sup>-3</sup>	+ 0.0548/- 0.4145	chloroplast	electron transporter	oxidation reduction
38	Os03g0278900 [Oryza sativa (japonica cultivar-group)] ATP synthase B/B' CF(0)	22.7/17.1	5.8/4.6	gi 115452259	At4g32260	3	170	8.0x10 <sup>-3</sup>	- 0.4052/- 0.6705	chloroplast	hydrolase activity	transmembrane ion transport
120	ATP synthase CF1 beta subunit [Triticum aestivum]	53.8/64.9	5.6/5.0	gi 14017579	AtCg00480	23	1417	4.8x10 <sup>-4</sup>	- 0.0683/+ 0.3273	chloroplast	hydrogen ion transmembrane transporter activity	ATP synthesis coupled proton transport
112		53.8/40.0	5.6/4.7			9	590	3.0x10 <sup>-3</sup>	+ 0.1988/- 0.1913			
115		53.8/23.5	5.6/4.5			3	186	1.1x10 <sup>-2</sup>	- 0.2751/- 0.4639			
130	ATP synthase CF1 epsilon subunit [Triticum aestivum]	15.2/16.1	5.2/5.4	gi 14017578	AtCg00470	10	543	4.8x10 <sup>-4</sup>	+ 0.0088/- 0.3594			
25	Oxygen-evolving enhancer protein 2, chloroplast precursor (OEE2) [Triticum aestivum]	27.4/25.3	8.8/6.3	gi 131394	At1g06680	11	713	8.0x10 <sup>-7</sup>	+ 0.0861/- 0.7507	chloroplast	poly(U) binding	photosynthesis, light reaction
26		27.4/24.0	8.8/5.8			5	339	2.5x10 <sup>-5</sup>	- 0.0781/- 0.8498			
33		27.4/11.9	8.8/5.4			4	243	1.6x10 <sup>-5</sup>	+ 0.0721/- 0.6883			
31	chloroplast oxygen-evolving enhancer protein 1(OEE1) [Leymus chinensis]	34.7/21.4	6.0/5.2	gi 147945622	At5g66570	5	297	2.3 x10 <sup>-5</sup>	+ 0.2583/- 0.5096		poly(U) binding oxygen evolving activity	
63		34.7/21.4	6.0/5.5			7	349	4.8x10 <sup>-6</sup>	+ 0.2009/- 0.3232			
173		34.7/21.0	6.0/5.5			6	292	2.8x10 <sup>-4</sup>	+ 0.2987/+ 0.0896			
183	ascorbate peroxidase [Hordeum	27.9/32.8	5.1/5.0		At1g07890	6	328	2.1x10 <sup>-4</sup>	- 0.1188/+ 0.1606	mitochondrion	L-ascorbate	response to

	vulgare]			gi 15808779							peroxidase activity	reactive oxygen species
51	dehydroascorbate reductase [Triticum aestivum]	23.3/32.8	5.2/6.1	gi 28192421	At1g19570	10	622	2.4x10 <sup>-7</sup>	- 0.2757/+ 0.2969	mitochondrion	glutathione dehydrogenase (ascorbate) activity	response to jasmonic acid stimulus

<sup>a</sup> Spot number represents the number on the master gel

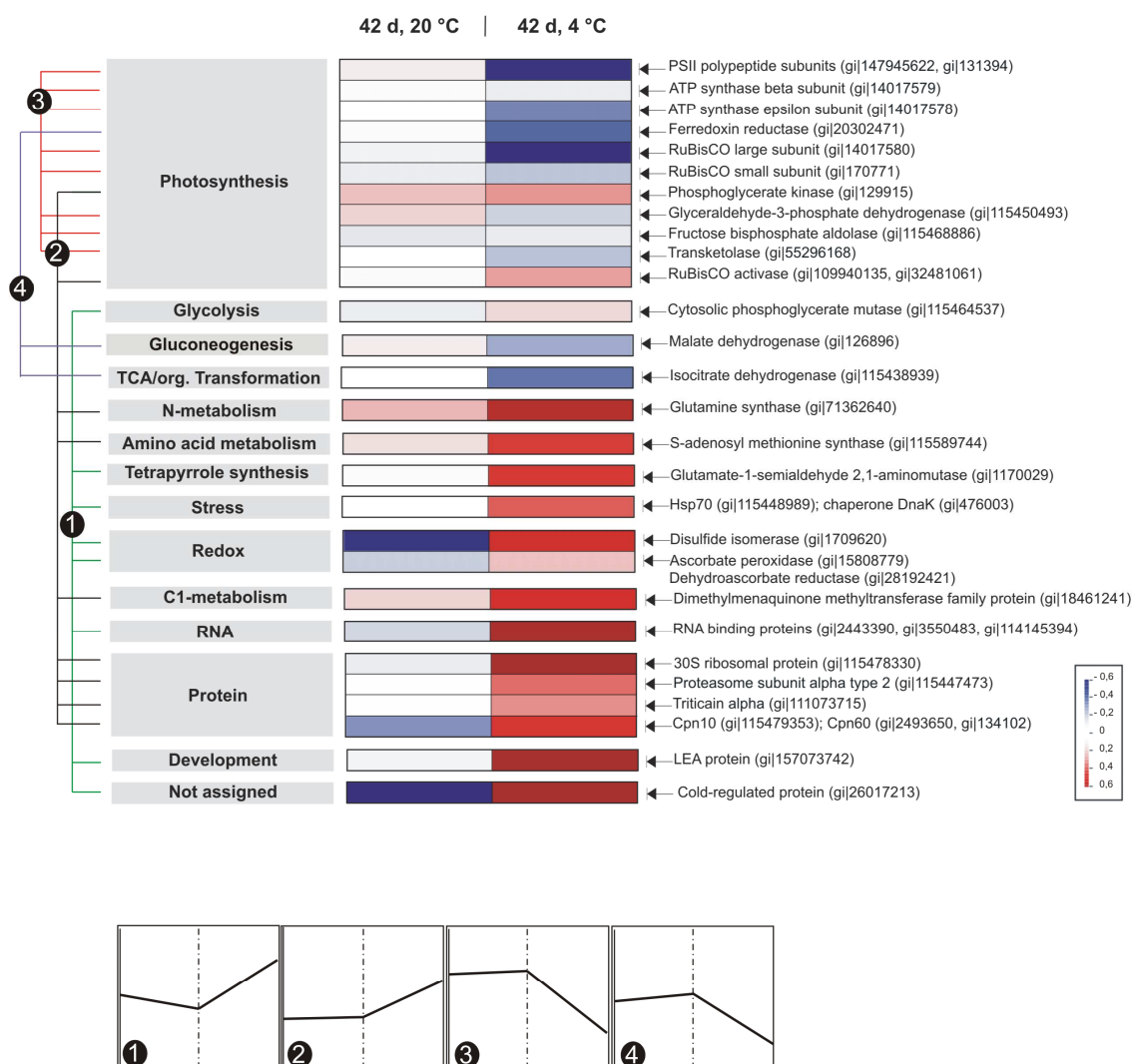
<sup>b</sup> Theoretical Mr/pI was calculated with Mr/pI tool on the Expasy web site ([http://expasy.org/tools/pi\\_tool.html](http://expasy.org/tools/pi_tool.html))

<sup>c</sup> TAIR Accession no. of the closest homologue in *Arabidopsis thaliana*

<sup>d</sup> p-value of one-way ANOVA analysis

<sup>e</sup> Fold of protein variation is calculated by standardizing the mean of the normalized spot volumes of samples at 42 days 20 °C and at 42 days of cold treatment with the mean of the normalized spot volumes of the sample at day 0.

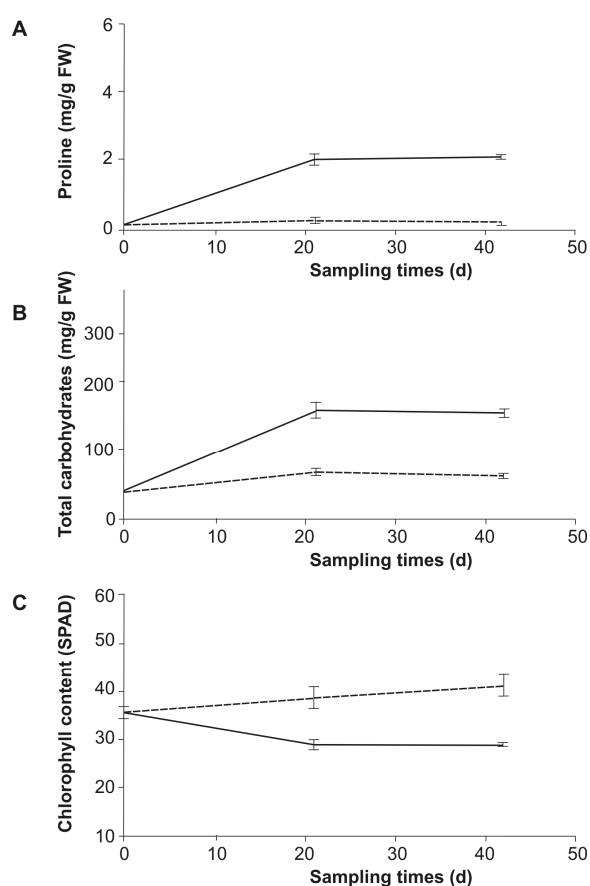
**Table 2.** List of differentially expressed proteins identified by LC-MS/MS.



**Figure 7.** Growth and cold-induced changes in proteins, organized at the level of functional categories using the PageMan software (<http://mapman.mpimp-golm.mpg.de/pageman/>). For each protein, the difference between the expression level at the given data points (42 d, 20 °C; 42 d, 4 °C) and the control (day 0 ) was calculated and converted to a false color scale (increasing red and blue indicate an up- and down-regulation, respectively). Values are shown as log normalized volumes. The average change for all proteins in a functional category is presented. Four primary clusters were defined using Euclidian distance and graphs showing the empirical mean of the expression levels for proteins included in each cluster are presented.

## Biochemical parameters

Since cold-acclimation affects the regulation of both sugar and amino acid metabolism, we firstly measured the intracellular content of proline and soluble carbohydrates during cold-acclimation period (Figure 8A-B). A concomitant increase of both solutes was detected after cold-exposure of wheat leaves with the maximum accumulation value reached after 21 days of treatment. This level was maintained until day 42. Bearing in mind that proteomic analyses showed a substantive down-regulation of the photosynthetic machinery, on-site chlorophyll content measurements were also performed in RT-grown and cold acclimated plants. As shown in Figure 8C, the amount of chlorophyll decreases over time confirming photooxidative stress induced by growing Kohdasht spring wheat at low temperature.

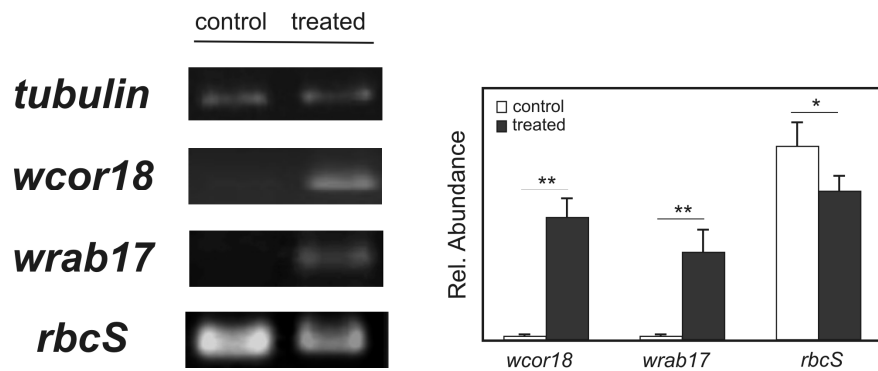


**Figure 8.** Changes in proline (panel A), soluble sugar (panel B) and chlorophyll content (panel C) in leaves of Kohdasht spring wheat at 4 °C (solid line) and 20 °C (dotted line). Bars represent  $\pm$  SE (n = 3).

### **Cold-modulated expression at mRNA level**

Semi-quantitative RT-PCR assays were conducted in order to determine whether some of the changes observed at the protein level could be confirmed as well at the transcription level. The abundance of particular proteins in the cells, in fact, can depend not only on the up (down)-regulation of transcription but also on the further steps in gene expression, such as mRNA stability, its transport from the nucleus to cytoplasm, efficiency of translation, protein stability, and the level of proteolysis. We chose to monitor the expression of *LEA* (*wrab17*), *wcor18* and *rbcS* (RuBisCO small subunit) genes for two main reasons: (i) the first two products have long been recognised, respectively, as typically drought and cold-enhanced proteins (Thomashow, 1999; Tsuda et al., 2000; Kobayashi et al., 2004; Ried and Walker-Simmons, 1993; Figueras et al., 2004), although their expression profiles were so far assessed only during early stages of seedling growth (Kobayashi et al., 2006); (ii) in spite of its key role in plant photosynthesis, being primarily involved in RuBisCO catalytic efficiency and specificity (Spreitzer, 2003), little information is currently available about the regulation of *rbcS* genes by environmental stresses (Hahn and Walbot, 1989; He et al., 2002; Hayano-Kanashiro et al., 2009; Naidu et al., 2003). In agreement with previous reports (Gao et al., 2009), the small subunit of RuBisCO displayed a heterogeneous change pattern in our 2DE maps, although a preferential down-regulation was detected. As displayed in Figure 9, *wrab17* and *wcor18* transcripts markedly increased after 42 days of cold-treatment, whereas *rbcS* showed only a slight decrease. These results clearly suggested that typically cold-related proteins, such as LEA (*wrab17*; protein spot No. 22) and Cor (*wcor18*; spot No. 1) polypeptides, that we identified on 2D-PAGE as *de novo* induced after cold treatment, were up-regulated at the transcription level. Conversely, in the case of RuBisCO small subunit, where a general down-regulation was observed at the protein level (spots No. 19, 64, 72), we detected only a tiny decrease of the corresponding RT-PCR product. Although quantitative reverse PCR would provide a more accurate evaluation of the transcripts, it cannot be ruled out that modulation of protein turnover may also play a role in the changes observed at the protein level.





**Figure 9.** Semi-quantitative RT-PCR analysis of the LEA (*wrab17*; 300 bp), *wcor18* (260 bp) and *rbcS* (RuBisCO small subunit; 271 bp) expression in control and cold-acclimated (42 days, 4 °C) Kohdasht lea ves. Expression of *tubulin* (720 bp) is shown as an internal control. The densitometric quantification of the mRNA level of the individual genes is expressed as the fold change compared to *tubulin*. Data are presented as the mean  $\pm$  SD from triplicate experiments, and similar results were seen in all replicates. Statistical comparisons were made using Student's t-test.

\*  $p < 0.05$ , \*\*  $p < 0.01$ .

## References

- Figueras, M., Pujal, J., Saleh, A., Save, R. et al., Maize Rab17 overexpression in Arabidopsis plants promotes osmotic stress tolerance. *Ann. Appl. Biol.* 2004, 144, 251-257.
- Fowler, D. B., Chauvin, L. P., Limin, A. E., Sarhan, F., The regulatory role of vernalization in the expression of low-temperature-induced genes in wheat and rye. *Theor. Appl. Genet.* 1996, 93, 554-559.
- Gao, F., Zhou, Y., Zhu, W., Li, X. et al., Proteomic analysis of cold stress-responsive proteins in *Thellungiella* rosette leaves. *Planta* 2009, 230, 1033-1046.
- Hahn, M., Walbot, V., Effects of Cold-Treatment on Protein Synthesis and mRNA Levels in Rice Leaves. *Plant Physiol.* 1989, 91, 930-938.
- Hay, R.K.M., Ellis, R.P., The control of flowering in wheat and barley: what recent advances in molecular genetics can reveal. *Ann. Bot.* 1998, 82, 541-554.
- Hayano-Kanashiro, C., Calderón-Vázquez, C., Ibarra-Laclette, E., Herrera-Estrella, L., Simpson, J., Analysis of Gene Expression and Physiological Responses in Three Mexican Maize Landraces under Drought Stress and Recovery Irrigation. *PLoS ONE* 2009, 4: e7531.
- He, C., Wang, W., Dongfang, Y., Zhang, J. et al., Transcription regulation of soybean ribulose-1,5-bisphosphate carboxylase small subunit gene by external factors. *Chin. Sci. Bull.* 2002, 47, 38-43.
- Kobayashi, F., Takumi, S., Egawa, C., Ishibashi, M., Nakamura, C., Expression patterns of low temperature responsive genes in a dominant ABA-less-sensitive mutant of common wheat. *Physiol. Plant.* 2006, 127, 612-623.
- Kobayashi, F., Takumi, S., Nakata, M., Ohno, R. et al., Comparative study of the expression profiles of the Cor/Lea gene family in two wheat cultivars with contrasting levels of freezing tolerance. *Physiol. Plant.* 2004, 120, 585-594.
- Mahfoozi, S., Limin, A. E., Ahakpaz, F., Fowler, D. B., Phenological development and expression of freezing resistance in spring and winter wheat under field conditions in north-west Iran. *Field Crops Res.* 2006, 97, 182-187.
- McMaster, G.S., Phenology, development, and growth of the wheat (*Triticum aestivum* L.) shoot apex: A review. *Adv. Agron.* 1997, 59, 63-118.
- Naidu, S. L., Moose, S. P., Al-Shoaibi, A. K., Raines, C. A. , Long, S. P., Cold Tolerance of C4 photosynthesis in *Miscanthus x giganteus*: Adaptation in Amounts and Sequence of C4 Photosynthetic Enzymes. *Plant Physiol.* 2003, 132, 1688-1697.
- Nátróvá, Z., Jokeš, M., A proposal for a decimal scale of the inflorescence development of wheat. *Rostlinná výroba* 1993, 39, 315-328.
- Ried, J. L., Walker-Simmons, M. K., Group 3 Late Embryogenesis Abundant Proteins in Desiccation-Tolerant Seedlings of Wheat (*Triticum aestivum* L.). *Plant Physiol.* 1993, 102, 125-131.
- Spreitzer, R. J., Role of the small subunit in ribulose-1,5-bisphosphate carboxylase/oxygenase. *Arch. Biochem. Biophys.* 2003, 414, 141-149.
- Thomashow, M. F., Plant cold acclimation: Freezing Tolerance Genes and Regulatory Mechanisms. *Annu. Rev. Plant Physiol. Plant Mol. Biol.* 1999, 50, 571-599.
- Tsuda, K., Tsvetanov, S., Takumi, S., Mori, N. et al., New members of a cold-responsive group-3 Lea/Rab-related Cor gene family from common wheat (*Triticum aestivum* L.). *Genes Genet. Syst.* 2000, 75, 179-188.

- Usadel, B., Nagel, A., Steinhauser, D., Gibon, Y. et al., PageMan: an interactive ontology tool to generate, display and annotate overview graphs for profiling experiments. BMC Bioinformatics 2006, 7, 535.

## Discussion

Proteomic and transcriptional data were combined with morphological and physiological information to provide some insights into the mechanism underneath prolonged cold stress response in a drought-tolerant spring wheat cultivar (*Triticum aestivum* cv Kohdasht). This work complements previous studies focusing on proteomic changes in wheat during short-time cold exposures (14 days) (Yan et al., 2006; Yang et al., 2006; Lee et al., 2007). Identification of differentially expressed spots through MS/MS analysis revealed significant modulations of many enzymes involved in almost all cellular metabolic pathways; the most important features regarding these alterations and their effects on cellular energetic balance are discussed below. First, protein modulations positively or negatively regulated by development and enhanced by cold stress are summarized. Afterwards, a more detailed description of changes in protein expression typically related to LT exposure is provided.

### Wide molecular remodeling during growth at optimal/suboptimal temperatures

Through the observation of differentially regulated proteins both in cold-treated and in 42-day-old plants compared to the 14-day-old control plants, it was possible to delve into protein modulations involved both in phenological development and in responses to LT prolonged exposure. It is interesting to note that the increase/decrease in protein expression occurring during growth at optimal temperatures is always intensified in cold stressed samples.

#### *ROS- and sugar-mediated fragmentation of RuBisCO*

One of the first visible features of two-dimensional gel maps from cold-treated samples is the presence of spots containing protein fragments of ribulose 1,5-bisphosphate carboxylase (RuBisCO) scattered over a wide area of the gel. Furthermore, modulation in expression is different from one spot to another. The synthesis of RuBisCO is known to be impaired by different environmental stressors, especially low temperature. To this regard, Hahn and Walbot (1989) demonstrated that the synthesis of both large and small subunits of RuBisCO drastically decreased in 7-day-cold-treated rice leaves, with a more severe reduction in cold-sensitive cultivars. Moreover, suppression was greater for the small subunit (over 90%) than for the large subunit

(80%), indicating a partial loss of coordination in their synthesis. On the other hand, it is also known that reactive oxygen species deeply increase in concentration upon plant cold exposure, representing the first candidates responsible for RuBisCO fragmentation. In fact, the ROS-triggered cleavage of the large subunit of RuBisCO has been proposed as an alternative non-enzymatic way of fragmentation (Feller et al., 2008). Another factor potentially responsible for RuBisCO proteolysis during cold stress is accumulation of sugars. Physiological measurements of soluble sugar content in Kohdasht wheat leaves confirmed a marked accumulation of carbohydrates during cold exposure (see Figure 8). Apart from their known role in osmotic adjustments during abiotic stresses, soluble sugars are also known to take part in ROS-mediated signalling, influencing both ROS-producing and ROS-scavenging pathways (mitochondrial respiration, photosynthesis and oxidative-pentose-phosphate pathway) (Couée et al., 2006).

#### *Amino acid and prosthetic group metabolism*

The proteomic analysis here performed revealed a differential increase in expression of several enzymes devoted to amino acid and prosthetic group metabolism, both in normally-grown and cold-treated samples. As an example, glutamine synthetase (GS, spot 53) was up-regulated after 42 days of plant growth both at optimal and suboptimal temperatures, although its increase was most dramatic in cold stressed plants. In wheat, GS activity (both GS2 and GS1) has been proven to correlate positively with grain and stem nitrogen content (Habash et al., 2007). The same expression pattern has also been found for S-adenosyl-methionine synthase (SAMS1, spots 78 and 111), which catalyses the conversion of ATP and L-methionine into S-adenosyl-L-methionine (SAM). SAM is second to ATP as the most abundant cofactor in metabolic reactions: it acts as a methyl group donor for numerous transmethylation reactions, being cyclically synthesised in the so called "methyl cycle", whose rate is known to increase in response to osmotic stress (Bohnert et al., 1996). Interestingly, the up-regulation of demethylmenaquinone methyltransferase (DMKT, spot 67), an enzyme involved in the biosynthesis of menaquinone, followed the same pattern. It is worth noting that methyl groups used by DMKT during this reaction derive from S-adenosylmethionine, thereby providing a connection between the up-regulations of SAMS1 and DMKT. Previous transcriptional studies have revealed that the gene encoding demethylmenaquinone

methyltransferase (DMKT) is inducible by low temperatures (Lee et al., 2004). The up-regulation of these enzymes may represent a constitutive feature of the drought-resistant wheat variety.

### **Characterization of proteins exclusively modulated upon cold exposure**

We move on to elucidating in more depth those changes in protein expression that were restricted to long-lasting cold exposure of plants.

#### *Proteins encoded by genes with stress-related cis-regulatory elements*

In the present analysis, we found an up-regulation of a group 3 LEA protein (Wrab 17, spot 22), a cold regulated protein (Wcor18, spot 1) and a glycine-rich RNA-binding protein (GRP2, spot 48) only in wheat leaves subjected to prolonged cold stress. All these proteins share a common feature, which is the presence of cis-regulatory elements in the upstream sequences of their genes. Interestingly, C-repeat/DRE (dehydration responsive elements) motifs were demonstrated to be cold and drought responsive (Haake et al., 2002; Kizis et al., 2002) and were identified in both *cor18* and *rab17* promoter. Rab17 is an ABA-inducible protein and its expression in vegetative tissues was correlated with enhanced osmotic stress tolerance (Figueras et al., 2006). Being Kohdasht a drought-tolerant wheat variety, the monitoring of *rab17* gene expression resulted of extreme interest in order to investigate its eventual constitutive synthesis. Our analysis indicated an onset in expression both at the transcript and protein level only after prolonged cold-treatment, alerting protective cellular and biochemical changes related to cold-associated osmotic adjustments. Accordingly, the increased carbohydrate and proline contents may be viewed as a consequence of the osmotic tolerance. However, the low temperature responsiveness of *wrab17* in spring wheat cultivars was also documented (Tsuda et al., 2000; Kobayashi et al., 2004), although after short-term exposures. Our results demonstrated for the first time that its expression was sustained to 42-day cold acclimation with confirmation at the protein level. Similarly, we observed a marked accumulation of both *wcor18* transcript and the corresponding protein product following 42-day cold stress suggesting a possible role of these genes in long-term adaptation processes. Analogously to *Cor/Lea* gene family, also glycine-rich RNA-binding proteins (GRPs) are known to be drought and cold responsive (Sachetto-Martins et al., 2000). Our findings showed the onset in

expression of GRP2 protein under low temperature growth conditions in Kohdasht variety. Interestingly, the same protein (TaGRP2) was found to specifically accumulate during 14 days of cold exposure in a winter wheat cultivar, whereas its levels remained unchanged in response to drought stress (Christov et al., 2007). This behaviour induced researchers to hypothesize a role of TaGRP2 in plant cold acclimation responses which might not be directly tied to its dehydrative component.

*Impairment of photosynthesis and carbon fixation: possible mechanisms of recovery*

At the level of photosynthetic enzymes, we found a general down-regulation in leaf proteomes from plants kept at 4°C (OEE1, spots 173, 31 and 63; OEE 2, spots 25, 33; ferredoxin NADPH oxidoreductase, spot 80), strongly attributable to cold-induced damages of chloroplasts. Our results also revealed that CO<sub>2</sub> fixation was affected in our variety as we observed a marked down-regulation of the Calvin cycle enzymes upon prolonged cold exposure (GAPDH, spot 122; transketolase, spots 187 and 178; FBP aldolase, spot 75). Furthermore, the expression of two pivotal Krebs cycle enzymes, isocitrate dehydrogenase (spot 136) and malate dehydrogenase (spot 110) decreased notably upon cold exposure. However, it should be considered that the gravity of the observed processes might also be related to the exact physiological stage of this wheat variety. Indeed, it might be possible to explain the deep deterioration of the photosynthetic machinery in the light of the post-flowering leaf senescence. Upon the passage from vegetative growth to the reproductive phase, about 30-40% of the plant's photosynthesis takes place in the spike; consequently, leaf photosynthetic activity is known to sharply decrease after heading (Patterson and Moss, 1979). Despite the generalised cellular distress observed during cold stress, other results of our proteomic analysis seem to indicate that cold-stressed plants attempt to recover from photoinhibition. First, we found that RuBisCO activase expression increased to a great extent in cold-stressed plants. Several groups have reported the up-regulation of RuBisCO activase under abiotic stress (Luo et al., 2002), probably related to both the reactivation of RuBisCO for CO<sub>2</sub> fixation and to its chaperone activity. Second, the up-regulation of glutamate semialdehyde aminomutase (spot 85), involved in the synthesis of tetrapyrroles in cofactors like heme, chlorophyll and carotenoids, appears to be related to the regeneration of damaged

chlorophylls (Thoenen et al., 2007), and particularly to the PSII repair cycle. The first substrate in this pathway comes from glutamate metabolism, a visible sign of an amino acid catabolic pathway. Third, several enzymes dedicated to recycling ascorbate, which is known to be involved in the detoxification of reactive oxygen species, were found to be up-regulated upon prolonged cold exposure (dehydroascorbate reductase, spot 51; ascorbate peroxidase, spot 183). This finding demonstrates that the plant mounts a response to the increase in ROS that occurs following cold injury. Finally, a general up-regulation of chaperonins has been revealed as well (DnaK, spots 103, 99; cpn10, spot 54; Hsp70, spots 94, 108; the enzyme-like chaperonin disulphide isomerase, spot 52), probably attributable to the accumulation of reactive oxygen species which are known to induce their synthesis.

#### *Cold-induced enhancement in proteolysis*

Among proteins involved in protein processing which are highly expressed in cold stressed plants, we could identify the proteasome subunit alpha type 2 (spot 81) and the cysteine proteinase triticain alpha (spot 142). In plants, proteasome-dependent protein degradation is known to control plant development and responses to the environment (Smalle and Vierstra, 2004): in particular, this process is exacerbated in case of oxidative stress to replace misfolded and damaged proteins with newly formed ones, mostly involved in the plant stress response. Regarding cysteine proteinases, their expression at the genetic level has been shown to respond to cold, heat and water deficiency. Studies conducted with cultivars of differing drought-resistance have revealed that the induction of cysteine proteinases is negatively related to their drought-resistance and positively correlated with extracellular ATP-dependent proteolysis (Wićniewski and Zagdańska, 2001). Furthermore, a similar set of experiments carried out on winter wheat confirmed the same correlation between the level of cysteine proteinases and frost tolerance (Grudkowska and Zagdańska, 2004). In our case, levels of cysteine proteinases did not increase in control plants after 42 days of growth at optimal temperature, whereas they showed a sharp enhancement in the expression during cold treatment; this observation is in agreement with both previously mentioned studies, regarding drought tolerance and low frost tolerance, respectively.



## References

- Bohnert H. J., Jensen R. G., Strategies for engineering water-stress tolerance in plants. *Trends Biotechnol.* 1996, 14, 89-97.
- Christov, N. K., Yoneyama, S., Shimamoto, Y., Imai, R., Differential expression of wheat genes during cold acclimation. *Cytol. Genet.* 2007, 41, 142-150.
- Couée, I., Sulmon, C., Gouesbet, G., El Amrani, A., Involvement of soluble sugars in reactive oxygen species balance and responses to oxidative stress in plants. *J. Exp. Bot.* 2006, 57, 449-459.
- Feller, U., Anders, I., Demirevska, K., Degradation of Rubisco and other chloroplast proteins under abiotic stress. *Gen. Appl. Plant Physiol.* 2008, 34, 5-18.
- Figueras, M., Pujal, J., Saleh, A., Save, R. et al., Maize Rab17 overexpression in Arabidopsis plants promotes osmotic stress tolerance. *Ann. Appl. Biol.* 2004, 144, 251-257.
- Grudkowska, M., Zagdańska, B., Multifunctional role of plant cysteine proteinases. *Acta Biochim. Pol.* 2004, 51, 609-624.
- Haake, V., Cook, D., Riechmann, J. L., Pineda, O., et al., Transcription factor CBF4 is a regulator of drought adaptation in Arabidopsis. *Plant Physiol.* 2002, 130, 639-648.
- Habash, D. Z., Bernard, S., Schondelmaier, J., Weyen, J., Quarrie, S. A., The genetics of nitrogen use in hexaploid wheat: N utilisation, development and yield. *Theor. Appl. Genet.* 2007, 114, 403-419.
- Hahn, M., Walbot, V., Effects of Cold-Treatment on Protein Synthesis and mRNA Levels in Rice Leaves. *Plant Physiol.* 1989, 91, 930-938.
- Kizis, D., Pagès, M., Maize DRE-binding proteins DBF1 and DBF2 are involved in rab17 regulation through the drought-responsive element in an ABA-dependent pathway. *Plant J.* 2002, 30, 679-689.
- Kobayashi, F., Takumi, S., Nakata, M., Ohno, R. et al., Comparative study of the expression profiles of the Cor/Lea gene family in two wheat cultivars with contrasting levels of freezing tolerance. *Physiol. Plant.* 2004, 120, 585-594.
- Lee, D. G., Ahsan, N., Lee, S. H., Kang, K. Y. et al., An approach to identify cold-induced low-abundant proteins in rice leaf. *C. R. Biol.* 2007, 330, 215-225.
- Lee, S. C., Kim, J. Y., Kim, S. H., Kim, S. J. et al., Trapping and characterization of cold-responsive genes from T-DNA tagging lines in rice. *Plant Sci.* 2004, 166, 69-79.
- Luo, S., Ishida, H., Makino, M., Mae, T., Fe<sup>2+</sup>-catalyzed sitespecific cleavage of the large subunit of ribulose 1,5-bisphosphate carboxylase close to the active site. *J. Biol. Chem.* 2002, 277, 12383-12387.
- Patterson, T. G., Moss, D. N., Senescence in field grown wheat. *Crop Science* 1979, 19, 635-640.
- Sachetto-Martins, G., Franco, L. O., de Oliveira, D. E., Plant glycine-rich proteins: a family or just proteins with a common motif? *Biochim. Biophys. Acta* 2000, 1492, 1-14.
- Smalle, J., Vierstra, R. D., The ubiquitin 26S proteasome proteolytic pathway. *Annu. Rev. Plant Biol.* 2004, 55, 555-590.
- Thoenen, M., Herrmann, B., Feller, U., Senescence in wheat leaves: is a cysteine endopeptidase involved in the degradation of the large subunit of Rubisco? *Acta Physiol. Plant.* 2007, 29, 339-350.
- Tsuda, K., Tsvetanov, S., Takumi, S., Mori, N. et al., New members of a cold-responsive group-3 Lea/Rab-related Cor gene family from common wheat (*Triticum aestivum* L.). *Genes Genet. Syst.* 2000, 75, 179-188.
- Wićniewski, K., Zagdańska, B., Genotype-dependent proteolytic response of spring wheat to water deficiency. *J. Exp. Bot.* 2001, 52, 1455-1463.

- Yan, S. P., Zhang, Q. Y., Tang, Z. C., Su, W. A., Sun, W. N., Comparative Proteomic Analysis Provides New Insights into Chilling Stress Responses in Rice. *Mol. Cell. Proteomics* 2006, 5, 484-496.
- Yang, P. F., Li, X. J., Liang, Y., Jing, Y. X. et al., Proteomic Analysis of the Response of Liangyoupeijiu (Super High-Yield Hybrid Rice) Seedlings to Cold Stress. *J. Integr. Plant Biol.* 2006, 48, 945-951.

## **PART III**

### **Platelet storage temperature and new perspectives through proteomics**

In the last year of my PhD, my activity shifted from plants to samples of clinical interest; in fact, I joined a project concerning platelet quality assessment through proteomic approach. The commonality of such different topics was double. First, proteomic approach was applied almost in the same manner (with proper but minor modifications of the extraction protocols); second, here again, the main attempt was to achieve a greater understanding of a process influenced by temperature through its monitoring over time.

Thus, prior to perform this last work, I tried to delve into this topic, searching in literature for all the available information about the influence of temperature in platelet storage. After that, I made use of proteomic approach to study the modulations occurring in platelet concentrates routinely used in transfusion centers. The experiment (discussed at the end of this section) was conducted at 22°C: the choice of this temperature was mandatory, as will be clearer after reading the first part of this section.

I will first summarize the current knowledge about the influence of temperature on storage of platelet concentrates, describing the main processes occurring at refrigerating/non refrigerating temperatures in a sample with a such fragile homeostasis.

## Background

Platelets represent a key cellular blood component under physiological conditions, due to their implications in the maintenance of vascular integrity and prevention of haemorrhagic phenomena (Josefsson et al., 2007). Dysfunctions associated with thrombocytopenia constitute a significant threat to patients' health. So far, administration of platelet concentrates (PCs) from healthy donors is the only known strategy for medical care of patients with active bleeding, thrombocytopenia caused by bone marrow dysfunctions or due to chemotherapy for treatments of malignancies, or upon preliminary treatments prior to stem cell transplantation. Qualitative and quantitative changes in platelets could also occur following coronary artery bypass surgery and trauma, and may represent a key indicator of likely thrombotic complications (von Ruecker et al., 1989). Platelets are basically collected from donors in two ways: extraction from whole blood throughout centrifugation (buffy-coat) or through apheresis. Both methods are currently employed and have bright sides and disadvantages. Analogously to other blood components, techniques to improve the shelf life of platelets (currently, only five days), while maintaining their safety and effectiveness, are under constant investigation worldwide.

### *Platelet storage temperature*

- 22 °C

Since 1960's, platelets are stored at 22-24 °C as PCs, a methodology that had significantly improved their availability. PCs are stored under continuous gentle agitation in plasticized polyvinylchloride bags with di-(2-ethylhexyl) phthalate (DEHP), which are permeable to oxygen, in order to promote aerobic metabolism instead of glycolysis. This prevents pH drop which would render PCs acidic. However, their shelf life stops at the fifth day of storage because of the risk of bacterial and viral contamination, on the one hand, and the occurrence of structural lesions, on the other. As far as contamination is concerned, a series of studies have been conducted in the USA as to quantify the risk of bacterial contamination associated with platelet transfusion, which resulted to be limited to

one over 1000-3000 platelet/unit (Sullivan and Wallace, 2005). Although rare, this event has elevated probability to cause sepsis in recipients (Bethesda, 2004). In parallel, stored platelets

undergo a series of shape and functional modifications, which are commonly referred to as platelet storage lesions (PSLs). This term indicates the progressive decrease of functionality that accompanies storage of platelet at 22 °C, and in particular represents the final detrimental effect caused by a series of events happening during storage. PSLs include morphological changes with loss of the quiescence-related discoidal shape, release of granule contents, exocytosis of cytosolic proteins, increase of procoagulant properties, modification of glycoprotein patterns (Thon et al., 2008). Notably enough, these features are also typical of platelet activation as well, suggesting for shared molecular pathways between PSLs and activation itself. In conclusion, basic clinical goals to be fulfilled include both the enhancement of platelet shelf life and the development of cheap, fast and reliable pathogen inactivation procedures, which are currently under evaluation.

#### - 4°C

Storage at refrigerating temperatures would prevent many unwanted processes which take place at room temperature, exerting a bacteriostatic effect and thus decreasing the potential for sepsis. Moreover, protocols involving storage of PCs at 4 °C may allow extension of the storage limit beyond 5 days, prolonging platelet shelf life and thus solving current shortages in transfusion services. Finally, refrigeration could also inhibit accumulation of contaminating white cell products, such as cytokines, and contribute alleviating cytokine-associated febrile transfusion reactions (Ferrer et al., 2001). Unfortunately, hypothermic (4°C) storage conditions causes deep modifications in platelet shape and functionality. Platelets stored at temperatures below 15 °C perform very poorly *in vivo*, mainly due to an elevated percentage of cold stored platelet being rapidly cleared from the bloodstream of the recipients (Hoffmeister et al., 2003a). Galactosylation has been proposed to tackle this issue in cold-stored mouse platelets, although it only showed relevant results *in vitro* (Hoffmeister et al., 2003b), while yielding poor survival in *in vivo* studies on human counterparts (Wandall et al., 2008; Hornsey et al., 2008). Removal of refrigerated platelets from the circulation appears to be partly mediated by recognition of clustered beta-N-acetylglucosamine on platelet surface glycoproteins by the alphaMbeta2 hepatic lectin receptor. Capping the exposed beta-N-acetylglucosamine residues by enzymatic galactosylation restored the circulation of short-term chilled murine platelets, introducing a novel method that allows for cold

storage of platelet (Sørensen et al., 2008). Nonetheless, galactosylation is not sufficient to restore circulation of long-term refrigerated platelets. Additional data indicate that differential carbohydrate-mediated mechanisms may exist for clearance of short-term and long-term cold-stored platelets (Wandall et al., 2008; Hornsey et al., 2008). These are relevant issues which compromise viability of cold stored platelets, as they exert their physiological role through their ability to change shape and activate under various conditions.

Low temperature appears to be a triggering factor for activation as well, thus yielding yet activated platelets as unviable blood product at the end of the storage. However, although lowering temperature would prevent occurrence of several PSLs, cold storage seems to trigger different lesions, which end up impairing platelet integrity and functionality.

#### *Cold-induced storage lesions*

The sum of untoward effects occurring upon platelet storage in the cold are generally termed cold-induced storage lesions. One of the first visible effects of platelet impairment is the irreversible loss of the discoid morphology towards a spherical shape, and the appearance of spiny projections on the surface due to calcium dependent gelsolin activation and phosphoinositide-mediated actin polymerization (Shrivastava, 2009). The morphological changes induced in platelets by low temperatures have been observed from 1950's; when platelets are exposed to temperature lower than 20 °C, they undergo fast modifications in shape (White and Krivit, 1967), notably increase intracellular calcium levels (Oliver et al., 1999) and actin polymerization degree. Moreover, stored platelets secrete alpha granule and lysosomal contents (Pribluda and Rotman, 1982), and reorganize the microtubule coil lying under the plasma membrane through depolymerization processes (White and Krivit, 1967).

#### *Cold activation*

Storage of whole blood at 4 °C for 6 h has been demonstrated to induce platelet activation similar to that of patients with cardiovascular diseases (Ayukawa et al., 2009). The molecular basis underlying platelet activation during storage at 4 °C have been extensively studied, but not yet fully characterized. Cold-stored platelets have been demonstrated to be more sensitive to agonist-induced aggregation with respect to platelets stored at room temperature, although low

temperature does not cause an increase of glycoprotein (GpIb, GpIIb/IIIa) and platelet activation markers (CD62p and CD63) upon comparison with storage at 22 °C (Sandgren et al., 2007). This feature has been validated through the analysis of platelet response to signal transduction inhibitors on fibrinogen binding, aggregation, the activation state of GP IIb-IIIa, and cytosolic calcium levels. Moreover, cold-stored platelets show a higher aggregation response (in response to ADP and epinephrine) and a major resistance to disaggregating agents (promethazine, prostaglandin D2, yohimbine, and echistatin) when compared to their counterparts stored at room temperature (Mondoro and Vostal, 2002). Differences between aggregation and disaggregation responses of cold- and room temperature-stored platelets suggest that cold-stored platelets may have different mechanisms to stabilize platelet aggregates during their formation, as it has been extensively documented (Hoffmeister et al., 2003a,b; Wandall et al., 2008; Hornsey et al., 2008).

## References

- Ayukawa O, Nakamura K, Kariyazono H, et al. Enhanced platelet responsiveness due to chilling and its relation to CD40 ligand level and platelet-leukocyte aggregate formation. *Blood Coagul Fibrinolysis* 2009;20(3): 176-84.
- Bethesda MD. American Association of Blood Banks (AABB). Standards for blood banks and transfusion services. AABB, 2004.
- Ferrer F, Rivera J, Lozano ML, et al. Effect of cold-storage on the accumulation of bioreactive substances in platelet concentrates treated with second messenger effectors. *Haematologica* 2001; 86: 530-536.
- Hoffmeister KM, Felbinger TW, Falet H, et al. The clearance mechanism of chilled blood platelets. *Cell* 2003a; 112: 87-97.
- Hoffmeister KM, Josefsson EC, Isaac NA, et al. Glycosylation restores survival of chilled blood platelets. *Science* 2003b; 301: 1531-4.
- Hornsey VS, Drummond O, McMillan L, et al. Cold storage of pooled buffy-coat-derived, leucoreduced platelets in plasma. *Vox Sang* 2008; 95(1): 26-32.
- Josefsson EC, Hartwig JH, Hoffmeister KM. Platelet Storage Temperature - How Low Can We Go? *Transfus Med Hemother* 2007; 34: 253-261.
- Mondoro TH, Vostal JG. Cold temperatures reduce the sensitivity of stored platelets to disaggregating agents. *Platelets* 2002; 13(1): 11-20.
- Oliver AE, Tablin F, Walker NJ, Crowe JH. The internal calcium concentration of human platelets increases during chilling. *Biochim Biophys Acta* 1999; 1416: 349-60.
- Pribluda V, Rotman A. Dynamics of membrane-cytoskeleton interactions in activated blood platelets. *Biochemistry* 1982; 21: 2825-32.

- Sandgren P, Hansson M, Gulliksson H, Shanwell A. Storage of buffy-coat-derived platelets in additive solutions at 4 degrees C and 22 degrees C: flow cytometry analysis of platelet glycoprotein expression. *Vox Sang*. 2007; 93(1): 27-36.
- Shrivastava M. The platelet storage lesion. *Transfus Apher Sci* 2009; 41: 105-113.
- Sørensen AL, Hoffmeister KM, Wandall HH. Glycans and glycosylation of platelets: current concepts and implications for transfusion. *Curr Opin Hematol* 2008;15: 606-611.
- Sullivan MT, Wallace EL. Blood collection and transfusion in the United States in 1999. *Transfusion* 2005; 45: 141-8.
- Thon JN, Schubert P, Devine DV. Platelet Storage Lesion: A New Understanding From a Proteomic Perspective. *Transfusion Medicine Reviews* 2008;22(4): 268-279.
- von Ruecker A, Hufnagel P, Dickerhoff R, et al. Qualitative and quantitative changes in platelets after coronary-artery bypass surgery may help identify thrombotic complications and infections. *Klin Wochenschr* 1989; 67: 1042-1047.
- Wandall HH, Hoffmeister KM, Sorensen AL, et al. Galactosylation does not prevent the rapid clearance of long-term, 4 degrees C-stored platelets. *Blood* 2008;111: 3249-56.
- White JG, Krivit W. An ultra-structural basis for the shape changes induced in platelets by chilling. *Blood* 1967; 30: 625-635.



## **New proteomic applications to study platelet storage**

Due to the great importance of the matter and its direct implication on medical practices, many scientific approaches have tried to delve into platelet modifications occurring during storage. Any improvement in platelet storage able to partly solve problems related to storage of PCs at room temperature (RT) is in fact strongly augurable. So far, experimental approaches to analyze platelet modifications upon storage are based on in vitro assays of platelet functionality and metabolism, animal testing for studies of thrombocytopenia, platelet counts in thrombocytopenic patients and monitoring of radiolabeled autologous platelets in healthy volunteers. However, a gap still persists between in vitro assays and the current knowledge of mechanisms presiding over platelet recovery in vivo (Cardigan and Williamson, 2003). Proteomics allows a comprehensive study of protein modifications, and offers capabilities both for qualitative/quantitative analysis and for high-throughput protein identification, thus potentially enabling a global assessment of processing, inactivation and storage methods of blood-derived therapeutics. This is particularly true in the case of platelets which lack nucleus, thus forbidding most of the genetic approaches refined in classic molecular biology. In this case, proteomics may be used to identify potential storage lesions biomarkers to be used as fingerprints of deterioration processes in platelet concentrates (Thon et al., 2008; Thiele et al., 2007). On this line, Glenister and coworkers recently applied proteomics to the analysis of storage-associated alterations in buffy-coat PCs (Glenister et al., 2008) and 18 proteins resulted to be modified. This protein number cannot clearly represent the totality of protein changes. The reason of this finding relies on the difficulty of proteomics in detecting proteins deeply differing in concentrations in a given sample (Pedersen et al., 2003). This is particularly true in the case of buffy-coat PC supernatants, where the analysis is hampered by the enormous dynamic range of proteins present in the plasma (Thadikkaran et al., 2005). To provide an example, albumin in plasma represents the 90% of the total plasma proteome (Anderson and Anderson, 1977), thus prevailing on and masking most other interesting proteins, such as soluble products which could be taken into account as biomarkers of PC quality. For these reasons, proteomic strategies aimed at increasing the visibility of low-abundance proteins are continuously tweaked, among which equalization technology commercially known as ProteoMiner™ (Righetti et

al., 2006, 2007; Boschetti et al., 2007a,b). The intrinsic originality of this approach with respect to other techniques, such as pre-fractionation or immunodepletion, lies in the preservation of the whole proteome present in a given sample, just giving to all proteins the same chance to be revealed. Thus, while most of these methods are aimed at depleting protein mixtures from highly represented products, ProteoMiner technology “equalizes” protein populations, by sharply reducing the concentration of the most abundant components, while simultaneously enhancing the concentration of the most dilute species. Another benefit in using ProteoMiner™ lies in its ability to retain quantitative information on medium-to-low abundance proteins, while reducing high-abundance ones (Boschetti and Righetti, 2009).

## References

- Anderson L, Anderson NG. High resolution two-dimensional electrophoresis of human plasma proteins. *Proc Natl Acad Sci USA* 1977; 74: 5421-5425.
- Boschetti E, Lomas L, Citterio A, Righetti PG. Romancing the “hidden proteome”, Anno Domini two zero zero seven. *J Chromatogr A* 2007a; 1153: 277-290.
- Boschetti E, Monsarrat B, Righetti PG. The “Invisible Proteome”: How to Capture the Low Abundance Proteins Via Combinatorial Ligand Libraries. *Curr Proteomics* 2007b; 4: 198-208.
- Boschetti E, Righetti PG. The art of observing rare protein species in proteomes with peptide ligand libraries. *Proteomics* 2009; 9: 1492-1510
- Cardigan R, Williamson LM. The quality of stored platelets after storage for 7 days. *Transfus Med* 2003;13: 173-187.
- Glenister KM, Payne KA, Sparrow RL. Proteomic analysis of supernatant from pooled buffy-coat platelet concentrates throughout 7-day storage. *Transfusion* 2008; 48: 99-107.
- Pedersen SK, Harry JL, Sebastian L, Baker J, Traini MD, McCarthy JT, Manoharan A, Wilkins MR, Gooley AA, Righetti PG, Packer NH, Williams KL, Herbert BR. Unseen Proteome: Mining Below the Tip of the Iceberg To Find Low Abundance and Membrane Proteins. *J Proteome Res* 2003; 2: 303-311.
- Righetti PG, Boschetti E, Lomas L, Citterio A. Protein equalizer technology: The quest for a “democratic proteome”. *Proteomics* 2006; 6: 3980-3992.
- Righetti PG, Boschetti E. Sherlock Holmes and the proteome-A detective story. *FEBS J* 2007; 274: 897-905.
- Thadikkaran L, Siegenthaler MA, Crettaz D, Queloz PA, Schneider P, Tissot JD. Recent advances in blood-related proteomics. *Proteomics* 2005; 5: 3019-3034.
- Thiele T, Steil L, Gebhard S, Scharf C, Hammer E, Brigulla M, Lubenow N, Clemetson KJ, Völker U, Greinacher A. Profiling of alterations in platelet proteins during storage of platelet concentrates. *Transfusion* 2007; 47: 1221-1233.

- Thon JN, Schubert P, Duguay M, Serrano K, Lin S, Kast J, Devine DV. Comprehensive proteomic analysis of protein changes during platelet storage requires complementary proteomic approaches. *Transfusion* 2008; 48: 425-435.

## **Proteomic analysis of plasma derived from platelet buffy coats during storage at room temperature. An application of ProteoMiner™ technology.**

### **Aim of the study**

As mentioned in the first part of this section, in the last year of my PhD, I joined a project concerning platelet quality assessment through proteomic approach. The aim of my work was to analyze proteomic changes occurring in platelet concentrates (PCs), which are the current medical product usually provided to patients suffering plateletpenia, in function of time. As will be explained in the section below, the main limit of PCs conservation prior to transfusion is temperature; these blood components are stored at 22°C in continuous agitation to avoid activation and aggregation processes which are demonstrated to occur at refrigerating temperatures (4°C) (this topic will be discussed in the next paragraph).

We used proteomic approach to detect changes in PC supernatants (obtained after brief centrifugation of PCs) after 0, 4 and 7 days of storage at 22°C. To achieve a more complete overview of the protein pool accumulating/disappearing in this sub-proteome, we made use of ProteoMiner™ technology to enrich our final proteome for the low-abundance species, often hidden by high abundant ones (in our case mainly plasma albumin).

Although the bright sides and disadvantages of ProteoMiner technology are still under debate, the introduction of the ProteoMiner enrichment prior to protein separation by 2D E greatly improved the detection of protein species in the supernatants. Several storage-induced protein alterations were identified including changes of major plasma proteins. In particular, a precursor of the secretory form of clusterin was shown to accumulate during storage of PC supernatants, together with platelet-derived tropomyosin, suggesting a progressive loss of platelet integrity. Platelet-released proteins following activation have also been detected (alpha-1-B-glycoprotein, kininogen-1, serpin proteinase inhibitor 8). Moreover, specific protein fragments (vitronectin, plakoglobin, hornerin, apolipoprotein A-IV) were found to be modulated upon storage, likely indicating a time-dependent buffy-coat PC deterioration. Globally, our findings provided the disclosure of unique proteins in PC supernatants with respect to previous studies conducted in similar experimental conditions,

suggesting ProteoMiner<sup>TM</sup> enrichment technology to be a possible complementary tool in the identification of diagnostically relevant proteins as age/quality biomarkers of therapeutic products.

## **Materials and Methods**

### **Sample preparation and storage of platelet concentrates**

All buffy-coat PCs were prepared according to standard procedures (Hardwick, 2008). Briefly, units of whole blood (500 mL) were collected from healthy donors into top-and-bottom bags (Optipac, CPD-SAGM, Baxter Healthcare). The bags were centrifuged within 6 h after collection at  $3100 \times g$  for 12 minutes. After centrifugation, plasma, red cells, and the buffy coat (BC) were separated on an automated extractor system (Optipress, Baxter). BCs (hematocrit,  $54 \pm 3\%$ ; volume,  $55 \pm 5$  mL) were retained in the collection bag and stored for 1-2 hours at room temperature without agitation. For preparation of PCs, five BCs from randomly selected ABO-identical donors were pooled under sterile conditions in a 600-mL transfer pack container (Baxter) and diluted with 270 mL of plasma. Pooled units were centrifuged at  $700 \times g$  for 6 min at room temperature and the platelet-rich plasma supernatant (250 mL) was gently pressed off into a satellite bag (Baxter) until the red cells entered the tube of the transfer bag. A Pall PL-50 filter was used to reduce the leukocytes in the platelet concentrates. Four PCs thus obtained (biological replicates) were stored in 1-L polyolefin bags (Baxter) for 7 days at  $22^\circ\text{C}$  on a horizontal agitator (Helmer, USA) in continuous agitation. Finally, the supernatant was sampled aseptically on days 0, 4, 7 after soft spin centrifugation ( $1000 \times g$ , 10 min) to remove cellular fraction and stored at  $-80^\circ\text{C}$ . At each sampling time, blood cell counts were performed: the mean platelet count was  $2.0 \pm 0.3 \times 10^{11}$  per unit with a leukocyte contamination of less than  $1 \times 10^6$  per unit.

### **ProteoMiner enrichment**

Before proteomic analysis, half of the supernatant sampled after 0, 4, 7 days of storage was pre-fractionated using the ProteoMiner<sup>TM</sup> kit (Bio-Rad Laboratories, Hercules, CA, USA) according to the manufacturer's protocol. The equalized samples (protein concentration of 50 mg/mL) were stored at  $-80^\circ\text{C}$  until use together with corresponding non equalized controls.

## **Two-dimensional gel electrophoresis**

The protein concentration of each sample was determined according to Bradford (1976) using BSA as a standard curve. The protein concentration was estimated on whole supernatant before and after ProteoMiner treatment. A volume of each sample containing 600 µg of proteins was solubilized in 8 M urea, 4% (w/v) CHAPS, 0.5% (w/v) pH 4-7 carrier ampholyte (Bio-lyte; Bio-Rad, Hercules, CA, USA) and 40 mM Tris base with continuous stirring. Proteins were subsequently reduced (10 mM tributylphosphine, 1 h) and alkylated (40 mM IAA, 1 h). To prevent over-alkylation, iodoacetamide (IAA) excess was neutralized by adding 10 mM DTE. IEF was performed using Biorad Multiphore II and Dry Strip Kit (Bio-Rad-Protean-IEF-Cell-System). Eighteen centimeter IPG strips (Bio-Rad, Hercules, CA, USA) pH 4-7 were rehydrated overnight with 345 µL of rehydration solution containing 8 M urea, 4% (w/v) CHAPS, 0.5% (w/v) pH 4-7 carrier ampholyte (Bio-lyte; Bio-Rad, Hercules, CA, USA), 10 mM DTE and 100µl of sample was loaded using the cup-loading method. The total product time x voltage applied was 80 000 V h for each strip at 20 °C. For the second dimension, IPG strips were incubated in the equilibration solution [6 M urea, 50 mM Tris-HCl (pH 6.8), 30% (v/v) glycerol, 3% (w/v) SDS, 0.002% (w/v) bromophenol blue] for 30 min with gentle agitation. Equilibrated strips were then placed on SDS-polyacrylamide gels, 16 cm x 20 cm, 11-18% acrylamide, and sealed with 0.5% (w/v) agarose. SDS-PAGE was performed using the Protean II xi Cell, large gel format (Bio-Rad) at constant current (35 mA per gel) at 7 °C until the bromophenol blue tracking dye was approximately 2–3 mm from the bottom of the gel. Protein spots were stained by sensitive Coomassie Brilliant Blue G-250 stain (Candiano et al., 2004). To ensure protein pattern reproducibility, four technical replicates were done.

## **Image analysis**

Two dimension gel images were digitized using a flatbed scanner (model ImageScanner-II, GE Healthcare, Uppsala, Sweden) with a resolution of 300 dpi and 16-bit greyscale pixel depth. Image analysis was carried out with Progenesis SameSpots software vers. 2.0 (Nonlinear Dynamics), which allows spot detection, background subtraction, and protein spot OD intensity quantification (spot quantity definition). The gel image showing the highest number of spots and the best protein

pattern was chosen as a reference template, and spots in a standard gel were then matched across all gels. Spot quantity values were normalised in each gel dividing the raw quantity of each spot by the total quantity of all the spots included in the standard gel. For each protein spot, the average spot quantity value and its variance coefficient in each group was determined. One-way analysis of variance (ANOVA) was carried out at  $p < 0.05$  in order to assess for absolute protein changes among the different treatments; only 2-fold or higher quantitative variations were taken into consideration.

### **Western Blotting**

10 µg of protein from each sample was resolved on 14% (w/v) SDS-PAGE. Following electrophoresis, proteins were transferred to a PVDF (polyvinylidene difluoride) membrane (Bio-Rad, Hercules, CA, USA) which was then blocked in a solution composed of 5 % (w/v) non-fat dried milk in Tris-buffered saline (TBS) for 2 hours at room temperature to prevent nonspecific binding of antibodies. Incubation with primary antibodies directed against the proteins was performed overnight at 4 °C in TBS with 1% (w/v) BSA and 0.1% Tween 20. Anti-kininogen-1 and anti-angiotensin (serpin proteinase inhibitor 8) antibodies were from Santa Cruz Biotechnology (CA, USA). Membranes were then probed by incubation with the appropriate horseradish peroxidase-conjugated secondary antibodies. The protein bands were detected by enhanced chemiluminescence reagents and the images were captured by scanning using an Image Scanner II flatbed scanner (GE Healthcare, Uppsala, Sweden). Human IgG protein was used as internal control to ensure equal sample loading.

### **In-gel digestion**

Protein spots were carefully excised from Coomassie stained gels and subjected to in-gel trypsin digestion, according to Shevchenko and colleagues (Shevchenko et al., 2007), with minor modifications. Gel spots were first shrunk by dehydration in acetonitrile (20 min incubation), then the solvent was discarded and the gel pieces were dried in a vacuum centrifuge. A volume of 10 mM DTT in 100 mM  $\text{NH}_4\text{HCO}_3$  was added and the proteins were reduced for 45 min at 56 °C. After

cooling to room temperature, the DTT solution was replaced with roughly the same volume of 55 mM iodoacetamide in 100 mM  $\text{NH}_4\text{HCO}_3$  and incubated 30 min at room temperature in the dark. The gel pieces were finally swollen in a digestion buffer containing 50 mM  $\text{NH}_4\text{HCO}_3$  and 12.5 ng/ $\mu\text{L}$  of trypsin (modified porcine trypsin, sequencing grade, Promega, Madison, WI) in an ice bath. After 30 minutes the supernatant was removed and discarded, 20  $\mu\text{L}$  of 50 mM  $\text{NH}_4\text{HCO}_3$  were added to the gel pieces and digestion allowed to proceed at 37 °C overnight. The supernatant containing tryptic peptides was dried by vacuum centrifugation. Prior to mass spectrometric analysis, the peptide mixtures were redissolved in 10  $\mu\text{L}$  of 5% FA (formic acid).

### **Peptide sequencing by nano RP-HPLC-ESI-MS/MS**

Nanoflow LC-MS/MS was performed by coupling an Ultimate 3000 series LC system (Dionex Corporation, Sunnyvale, CA, USA) to a quadrupole time-of-flight (Q-TOF) micro hybrid mass spectrometer (model microTOF-Q, Bruker-Daltonik). A home-built vented column system, consisting of a 20 mm Aqua C18 (Phenomenex, Torrance, CA, USA) trapping column (packed in-house; i.d., 100  $\mu\text{m}$ ; particle size, 5  $\mu\text{m}$ ) and a 200 mm ReproSil-Pur C18-AQ (Dr. Maisch, GmbH, Ammerbuch, Germany) analytical column (packed in-house; i.d., 50  $\mu\text{m}$ ; resin, 3  $\mu\text{m}$ ) was used for online desalting and separation of the peptides as described in (Meiring et al., 2002; Licklider et al., 2002). Trapping was performed at 5  $\mu\text{L}/\text{min}$  for 10 min in solvent A (0.5% acetic acid in water), and elution was achieved with a gradient of 5-50% B (0.6% acetic acid in 98% acetonitrile/2% water) in 60 min in a total analysis time of 80 min. The flow rate was passively split to 120 nL/min when performing the elution analysis. Nanospray was achieved using a distally coated fused-silica emitter (o.d., 360  $\mu\text{m}$ ; i.d., 20  $\mu\text{m}$ ; tip i.d., 10  $\mu\text{m}$ ; New Objective, Cambridge, MA) biased to 1.7 kV. The temperature of the heated sample source was 160 °C. The mass spectrometer was operated in the data-dependent mode to automatically switch between MS and MS/MS. The three most intense precursor ions at a threshold above 2000 were selected in each full scan with a 60 sec dynamic exclusion window. Collision energies were set automatically as a function of the mass and charge state (1+, 2+ and 3+) of the peptides chosen for fragmentation. The collision gas was argon. External mass calibration in quadratic regression mode using an ES Tuning Mix solution



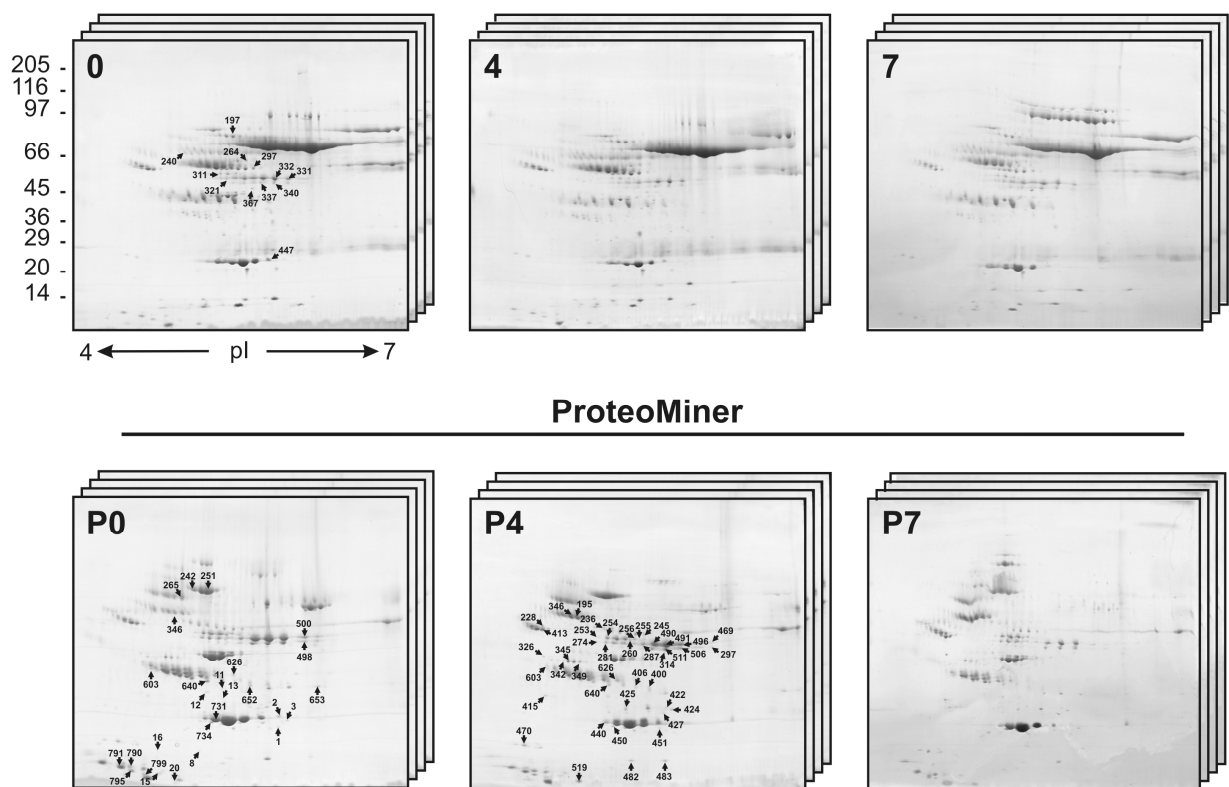
(Agilent Technologies, Santa Clara, CA, USA) resulted in mass errors of typically 1 ppm. Data was searched against the National Center for Biotechnology Information non-redundant database (NCBI nr, version 20100320, 10606545 sequences) using the Mascot software (in-house version 2.2, Matrix Science, London, UK) with the following constraints: taxonomy = human; enzyme = trypsin; missed cleavage = 2; peptide mass tolerance =  $\pm 0.05$  Da; fragment mass tolerance =  $\pm 0.05$  Da; fixed modifications = carbamidomethyl (Cys); variable modifications = oxidation (Met). For positive identification, the score of the result of  $(-10 \times \log(P))$  had to be over the significance threshold level ( $P < 0.05$ ). In auto-MS/MS files, only peptides with Mascot scores  $> 30$  and a delta mass  $< 0.1$  Da were considered. Peptide fragmentation spectra were also manually verified. In this manual verification, the presence of fragment ion series, and the expected prevalence of C-terminus containing (y-type ions) in the high mass range, were all taken into account. All 2-DE spots required a minimum of two verified peptides to be identified. Moreover, replicate measurements ( $n = 3$ ) have confirmed the identity of these protein hits. The stringency of the filtering criteria applied for the identification allowed to consider only the Mascot top hit as true positive.

## References

- Bradford MM. A rapid and sensitive method for the quantitation of microgram quantities of protein utilizing the principle of protein-dye binding. *Anal Biochem* 1976; 72: 248-254.
- Candiano G, Bruschi M, Musante L, Santucci L, Ghiggeri GM, Carnemolla B, Orecchia P, Zardi L, Righetti PG. Blue silver: a very sensitive colloidal Coomassie G-250 staining for proteome analysis. *Electrophoresis* 2004; 25: 1327-1333.
- Hardwick J. Blood processing. *ISBT Sci Ser* 2008; 3: 148-176
- Licklider LJ, Thoreen CC, Peng J, Gygi SP. Automation of nanoscale microcapillary liquid chromatography-tandem mass spectrometry with a vented column. *Anal Chem* 2002;74:3076-83.
- Meiring HD, van der Heeft E, ten Hove GJ, de Jong APJM. Nanoscale LC-MS(n): technical design and applications to peptide and protein analysis. *J Sep Sci* 2002;25:557-568.
- Shevchenko A, Tomas H, Havlis J, Olsen JV, Mann M. In-gel digestion for mass spectrometric characterization of proteins and proteomes. *Nat Protoc* 2007; 1: 2856-2860.

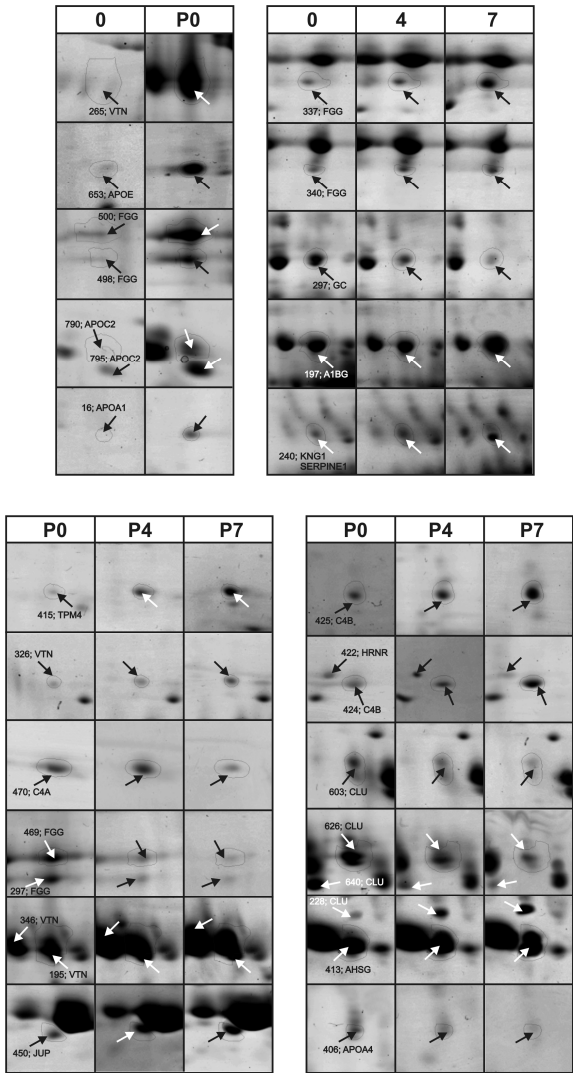
## Results

Figure 1 shows representative 2-DE maps of PC supernatants after 0, 4 and 7 days of storage obtained with (lower panel) and without (upper panel) ProteoMiner enrichment step. We chose a narrow pH interval of 4-7 to perform two-dimensional maps as the best range for plasma protein resolution (Cho et al., 2008). As expected, the analysis of proteomic maps of equalized samples revealed many spots not detectable in the untreated counterpart, increasing the spot count by 20%. The decrease in abundance of over-represented species was evident at first glance looking at the gel region of serum albumin at about 70 kDa before and after the equalization step (Figure 1).



**Figure 1.** Comparison of 2-DE maps of PC supernatants after 0, 4 and 7 days of storage obtained with (lower panel) and without (upper panel) ProteoMiner enrichment step. For each time-point of non-equalized and equalized fraction, a total of 16 maps (4 biological  $\times$  4 technical replicates) was done. Numbered spots indicated by the arrows refer to the results of quantitative analyses reported in Tables I-III.

In this study, three parallel comparisons were conducted by Progenesis SameSpots software (Nonlinear Dynamics): i) analysis of PC supernatants subjected to ProteoMiner equalization compared to their non equalized counterpart harvested at day 0 (P0 vs 0); ii) analysis of non-equalized samples harvested at day 0, 4 and 7 of storage (0, 4, 7); iii) analysis of samples processed with ProteoMiner after 0, 4 and 7 days of storage (P0, P4, P7). Figure 2 displays some zoomed gel areas showing examples of quantitative changes (newly induced or totally repressed, up- or down-regulated spots) in protein expression for each of the analyses performed.



**Figure 2.** Close-up views of some 2D-gel regions showing examples of the observed variations in protein spot intensity for the three analyses performed. Numbers refer to Tables I-III.

### **Ability of ProteoMiner to improve spot resolution in PC supernatant two-dimensional maps**

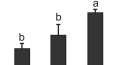
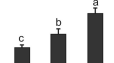
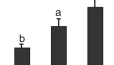
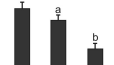
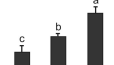
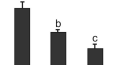
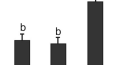
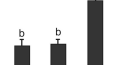
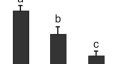
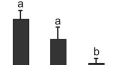
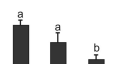
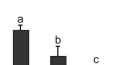
To evaluate the efficacy of ProteoMiner in ameliorating the visibility of low-abundance proteins, a first comparison between 2D gels of equalized (P0) and unprocessed samples (0) was carried out at day 0. Image alignment of equalized vs non-equalized sample was quite difficult due to the great diversity of 2D maps (Figure 1). However, the presence of well defined protein trains which functioned as landmarks (e.g. haptoglobin, apolipoproteins, fibrinogen), along with automatic alignment processing, helped in the overlapping procedure. Only newly-detected spots in 2D maps of equalized sample were cut out of the gels and identified by means of mass spectrometry after tryptic in-gel digestion. Moreover, in the case of charge train patterns typically resulting from the same protein with different post-translational modifications (Anderson and Anderson, 1977), we decided to analyze only the most intense spot as representative of the others. A list of the protein identifications is provided in Table I. Interestingly, several products of specific protein fragmentation were identified (e.g. spot 16, apolipoprotein A1; spot 13, complement component 4A).

### **Time-monitoring of stored buffy-coat PCs not subjected to ProteoMiner equalization**

The second analysis was performed on 2D maps of non equalized platelet supernatants harvested after 0, 4 and 7 days of storage at room temperature. As stated before, the great abundance of plasma proteins such as serum albumin and apolipoproteins partly impaired the observation of some gel areas, however approximately 570 spots were reproducibly matched across all the gels and included in the statistical analysis. Differentially expressed proteins ( $p < 0.05$ , absolute variation of at least 2-fold) identified upon storage are listed in Table II. Among them, it is worthwhile to mention alpha-1-B-glycoprotein (A1BG; spot 197), kininogen-1 (KNG1) and serpin proteinase inhibitor 8 (SERPINA8; spot 240). The proteomic findings for co-migrating KNG1 and SERPINA8 proteins were validated by western blotting analysis which confirmed an increase in expression in either case, especially evident after 7 days of storage (Figure 3).

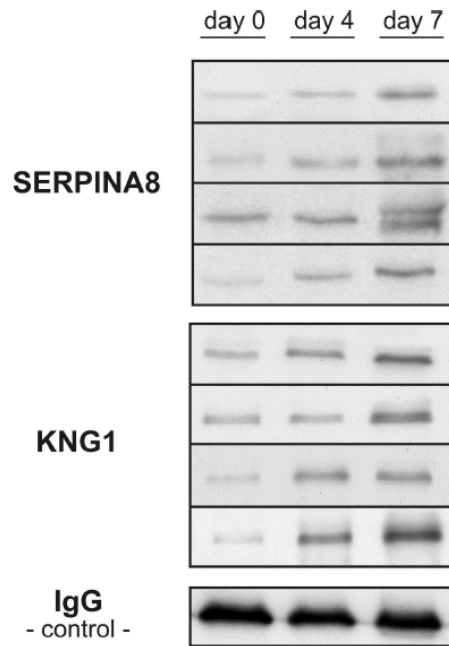
Spot No.	Gene	Protein name	Mr, kDa theor/exp er	pI theor/expe r	NCBI GI No.	No. of peptides	Mascot Score
251	F2	prothrombin preproprotein	71.5/79.5	5.6/5.3	gi 4503635	27	1849
242			71.5/79.5	5.6/5.1		23	1431
498	FGG	fibrinogen gamma chain	50.1/49.8	5.6/6.2	gi 182439	12	632
500			50.1/53.0	5.6/6.2		15	840
640	CLU	apolipoprotein J (fragments)	49.3/37.1	6.3/5.3	gi 178855	10	548
626			49.3/39.6	6.3/5.5		5	299
603			49.3/40.5	6.3/4.8		6	404
20	APOA2	Apolipoprotein A-II	11.3/9.9	6.6/5.0	gi 671882	2	84
652	APOE	apolipoprotein E	36.2/36.0	5.8/5.7	gi 178849	15	956
653			36.2/36.0	5.8/6.3		17	1187
790	APOC2	Apolipoprotein C-II	10.2/11.2	4.6/4.6	gi 178741	3	122
15			10.2/9.1	4.6/4.8		4	212
795			10.2/10.3	4.6/4.6		4	236
734	APOA1	Chain A, Crystal Structure Of Lipid-Free Human Apolipoprotein A-I	28.1/22.4	5.3/5.3	gi 90108664	17	915
731			28.1/22.5	5.3/5.3		24	1496
1		proapolipoprotein	28.9/21.0	5.4/5.9	gi 178775	9	374
16			28.9/16.7	5.4/5.2		3	102
8	APOA4	apolipoprotein A-IV (fragments)	45.3/15.9	5.3/5.2	gi 178757	3	200
12			45.3/32.0	5.3/5.3		6	306
791	APOC3	Chain A, Structure And Dynamics Of Human Apolipoprotein C-II	8.7/13.7	4.7/4.5	gi 186972736	4	286
799			8.7/9.5	4.7/4.7		3	153
346	VTN	Vitronectin	55.1/65.0	5.5/5.0	gi 13477169	12	590
265			55.1/75.5	5.5/5.1		12	572
2	C1QC	complement component 1, q subcomponent, C chain	26.1/27.0	8.6/6.0	gi 33150626	2	108
13	C4A	complement component 4A (fragment)	194.3/28.9	6.6/5.4	gi 179674	2	128
3	GPXP3	plasma glutathione peroxidase	16.8/24.0	8.9/6.1	gi 404108	5	248
11	AMBP	complex-forming glycoprotein HC	20.6/33.0	5.8/5.3	gi 223373	5	234

**Table I.** List of LC-MS/MS identified proteins in ProteoMiner treated (P0) vs untreated (0) samples at 0-day storage

Spot No.	Gene	Protein name	Mr, kDa theor/exper	pI theor/exper	NCBI GI No.	No. of peptides	Mascot Score	Average Normal. Vol. <sup>a</sup> 0-d 4-d 7-d		
337	FGG	fibrinogen gamma	46.8/52.5	5.5/5.7	<u>gi 182439</u>	17	837			
321			46.8/55.0	5.5/5.4		16	888			
340			46.8/52.1	5.5/5.9		15	708			
331			50.1/53.0	5.6/6.0		5	360			
311			50.1/57.3	5.6/5.3		12	571			
332			50.1/54.0	5.7/5.9		14	983			
197	A1BG	alpha-1-B-glycoprotein	52.5/78.3	5.6/5.5	<u>gi 69990</u>	7	401			
240	KNG1	kininogen-1	48.9/69.7	6.3/5.1	<u>gi 4504893</u>	3	104			
	<u>SERPINA8</u>	<u>serpin proteinase inhibitor 8</u>	<u>53.4/69.7</u>	<u>5.9/5.1</u>	<u>gi 15079348</u>	2	<u>77</u>			
297	GC	vitamin D-binding protein/group specific component	54.5/56.0	5.3/5.7	<u>gi 455970</u>	14	651			
367	ALB	albumin-like	53.4/47.5	5.7/5.7	<u>gi 763431</u>	2	122			
264	SERPINC1	Chain I Antithrombin-Iii	49.4/69.0	5.9/5.6	<u>gi 8569385</u>	19	979			
447	APOA1	proapolipoprotein	29.0/25.0	5.4/5.8	<u>gi 178775</u>	4	413			

<sup>a</sup> Histograms represent the variation of the spot normalized volumes (affected by SD). The same letters above the bars indicate no statistically significant difference, whereas different letters indicate a statistically significant difference ( $p < 0.05$ ) according to the LSD (least significant difference) test.

**Table II.** List of differentially expressed proteins identified by LC-MS/MS in non-equalized samples at 0, 4 and 7 days of storage.



**Figure 3.** Western blot identification of kininogen-1 (KNG1) and serpin proteinase inhibitor 8 (SERPINA8) proteins in buffy-coat PCs during storage. Representative gels of four biological replicates are shown. Human IgG was used as internal loading control (one membrane out of the other four with similar results is presented).

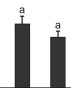
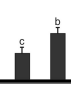
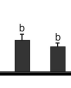
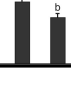
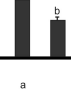
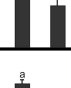
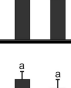
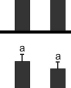
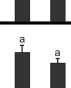
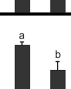
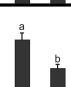
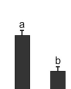

### Analysis of storage-dependent protein changes in samples treated by ProteoMiner

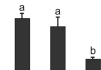
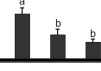
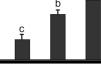
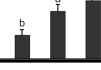
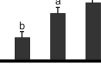
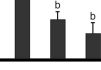
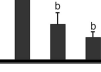
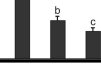
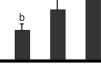
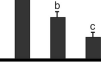
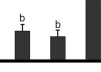
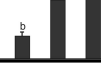
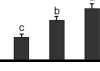
The last step of our analysis was the disclosure of protein modifications in 2D maps of platelet supernatants processed with ProteoMiner after 0, 4 and 7 days of storage at room temperature. The total number of spots counted by Progenesis software was 717. Storage-modulated proteins detected in equalized samples are listed in Table III. PLT-derived proteins identified by this analysis included: beta tropomyosin (TPM4; spot 415), clusterin (CLU; spots 603, 626, 640, 228), vitronectin (VTN; spot 326). A number of proteins were present as train spots with incremental shifts in pI. Several of these protein trains displayed appreciable time-dependent changes, often characterized by one member of the train increasing in intensity, while others decreasing. As an example, fibrinogen gamma (FGG)-containing spots showed conflicting trends (i.e. positive or negative regulation, see Table III). Moreover, distinctive protein fragments (e.g., plakoglobin, hornerin, apolipoprotein A-IV) were subjected to storage modulations and this finding ties in with

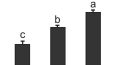
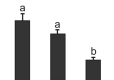
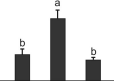
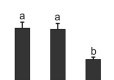
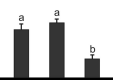


recent beliefs that fragmentation patterns may be predictive of a certain pathological status or represent markers of age/quality of therapeutic products (Geho et al., 2006). Of extreme interest was the case of vitronectin (Figure 4) where MS peptide mapping analysis allowed to exclude its plasma-derived origin (see below). When all combined data from untreated and equalized sample were listed, our analysis revealed some proteins in common to the work of Glenister et al. (2008) (such as proapolipoprotein, clusterin, fibrinogen  $\gamma$ ) and others previously undetected. Table IV summarizes these unique species which were missing from the list of proteins changed during storage of pooled buffy-coat PC supernatants.

Spot No.	Gene	Protein name	Mr, kDa theor/exper	pI theor/exper	NCBI GI No.	No. of peptides	Mascot Score	Average Normal. Vol. <sup>a</sup>		
								0-d	4-d	7-d
422	HRNR	hornerin (fragment)	283.1/27.6	10.0/5.8	<a href="#">gi 57864582</a>	2	67			
415	TPM4	Platelet beta tropomyosin alpha 4 chain	28.6/32.5	4.6/4.6	<a href="#">gi 20178270</a>	19	1005			
228	CLU	apolipoprotein J (clusterin)	49.3/55.2	6.3/4.6	<a href="#">gi 178855</a>	2	84			
603			49.3/42.1	6.3/4.6		5	329			
640			49.3/36.0	6.3/5.3		7	443			
626			49.3/38.2	6.3/5.3		5	347			
236	SERPINA1	alpha-1-antitrypsin	46.8/56.1	5.4/5.1	<a href="#">gi 177827</a>	4	296			
413	AHSG	Alpha-2-HS-glycoprotein	40.1/54.9	5.4/4.7	<a href="#">gi 112910</a>	8	502			
483	TTR	transthyretin precursor	16.0/15.1	5.5/5.9	<a href="#">gi 4507725</a>	10	753			
482		Chain A, Transthyretin-V122I	14.0/14.9	5.3/5.5	<a href="#">gi 1827569</a>	4	220			
245	FGG	fibrinogen gamma chain	50.0/55.0	5.6/5.6	<a href="#">gi 182439</a>	5	211			
253			50.0/53.9	5.6/5.1		11	500			

256			50.0/53.8	5.6/5.3		15	755			
254			50.1/54.6	5.6/5.3		14	738			
274			50.1/50.0	5.6/5.1		10	428			
260			50.1/52.5	5.6/5.0		2	100			
469			50.1/52.0	5.6/6.3		12	653			
506			50.1/50.1	5.7/6.0		20	1127			
496			50.1/53.6	5.7/6.0		22	1100			
511			50.1/48.7	5.7/5.9		24	1495			
490			50.1/53.0	5.7/5.7		24	1408			
491			50.1/53.6	5.7/5.9		23	1673			
281		fibrinogen gamma	46.8/50.1	5.5/5.2	<u>gi 223170</u>	13	697			
255			46.8/54.0	5.5/5.3		15	766			
314			46.8/46.5	5.5/6.0		10	515			

287		fibrinogen gamma-A precursor	50.1/50.0	5.7/5.6	<a href="#">gi 70906437</a>	5	394			
297	FGB	beta-fibrinogen precursor	55.5/49.7	8.3/6.3	<a href="#">gi 182430</a>	2	112			
326	VTN	Vitronectin	55.1/45.0	5.5/4.6	<a href="#">gi 13477169</a>	5	257			
346			55.1/65.0	5.5/5.0		12	590			
195			55.1/64.9	5.5/5.0		11	566			
440	APOA1	Chain A, Apolipoprotein A-I	28.1/23.9	5.3/5.2	<a href="#">gi 90108664</a>	14	862			
451		proapolipoprotein	29.0/23.5	5.4/5.8	<a href="#">gi 178775</a>	5	357			
406	APOA4	apolipoprotein A-IV precursor (probable fragment)	45.3/36.0	5.3/5.5	<a href="#">gi 178757</a>	6	276			
519	APOA2	apolipoprotein A-II, isoform CRA_c	9.1/8.6	6.1/5.1	<a href="#">gi 119573006</a>	7	269			
400	APOE	apolipoprotein E	36.3/36.1	5.6/5.7	<a href="#">gi 178849</a>	15	971			
427	APCS	pre-serum amyloid P component	25.5/25.0	6.1/5.8	<a href="#">gi 337758</a>	9	504			
450	JUP	Plakoglobin (fragment)	82.4/22.1	5.9/5.3	<a href="#">gi 762885</a>	7	317			
424	C4B	complement component 4B (fragments)	48.0/26.5	5.8/5.9	<a href="#">gi 40737343</a>	4	276			

425			48.0/26.4	5.8/5.8		4	221			
470	C4A	complement component 4A	194.3/18.7	6.6/4.5	<a href="#">gi 179674</a>	3	157			
349	C3	Chain C, Human Complement Component C3c	40.2/43.5	4.8/5.1	<a href="#">gi 78101271</a>	22	1248			
342			55.1/44.8	5.5/4.8		16	890			
345			40.2/43.7	4.8/4.8		10	720			

<sup>a</sup> Histograms represent the variation of the spot normalized volumes (affected by SD). The same letters above the bars indicate no statistically significant difference, whereas different letters indicate a statistically significant difference ( $p < 0.05$ ) according to the LSD (least significant difference) test.

**Table III.** List of differentially expressed proteins identified by LC-MS/MS in ProteoMiner treated samples at 0, 4 and 7 days of storage.

Gene	Spot No.	NCBI GI No.	Protein name	Description
F2	242, 251	<a href="#">gi 4503635</a>	prothrombin preproprotein	Functions in blood homeostasis, inflammation and wound healing
APOA2	20	<a href="#">gi 671882</a>	apolipoprotein	stabilization HDL structure, HDL metabolism
	519	<a href="#">gi 119573006</a>	apolipoprotein A-II	
APOE	652, 653, 400	<a href="#">gi 178849</a>	apolipoprotein E	Role in binding, internalization, and catabolism of lipoprotein particles
APOC2	790, 795, 15	<a href="#">gi 178741</a>	Apolipoprotein C-II	Component of VLDL, activator of several triacylglycerol lipases
APOA4	8, 12, 406	<a href="#">gi 178757</a>	apolipoprotein A-IV precursor	Role in chylomicrons and VLDL secretion and catabolism, helps ApoC-I-mediated activation of lipoprotein lipase
APOC3	791, 799	<a href="#">gi 186972736</a>	Chain A, Apolipoprotein C-III	Inhibits lipoprotein lipase and hepatic lipase, decreases the uptake of lymph chylomicrons by hepatic cells
	18, 19	<a href="#">gi 521205</a>	apolipoprotein C-III	
VTN	346, 265, 195, 326	<a href="#">gi 13477169</a>	Vitronectin	Cell adhesion and spreading factor
C1QC	2	<a href="#">gi 33150626</a>	complement component 1, q subcomponent, C chain	component of the serum complement system
C4A	13, 470	<a href="#">gi 179674</a>	complement component 4A	
C3	345, 349	<a href="#">gi 78101271</a>	Chain C, Complement Component C3c	
C4B	424, 425	<a href="#">gi 40737343</a>	complement component 4B	
GPXP3	3	<a href="#">gi 404108</a>	plasma glutathione peroxidase	Protects cells and enzymes from oxidative damage
AMBP	11	<a href="#">gi 223373</a>	complex-forming glycoprotein HC	Inter-alpha-trypsin inhibitor
HRNR	422	<a href="#">gi 57864582</a>	hornerin	Role in cornification
TPM4	415	<a href="#">gi 20178270</a>	Platelet beta tropomyosin alpha 4 chain	Binds to actin filaments in muscle and non-muscle cells
APCS	427	<a href="#">gi 337758</a>	pre-serum amyloid P component	Interacts with DNA and histones, scavenger of nuclear material released from damaged circulating cells
JUP	450	<a href="#">gi 762885</a>	Plakoglobin (fragment)	Junctional plaque protein
SERPINI1	264	<a href="#">gi 8569385</a>	Chain I, Antithrombin-Iii	Serine-type endopeptidase inhibitor activity
A1BG	197	<a href="#">gi 69990</a>	alpha-1-B-glycoprotein	Cell surface proteins
KNG1	240	<a href="#">gi 4504893</a>	Kininogen-1	Inhibitors of thiol proteases, role in blood coagulation, inhibits the aggregation of thrombocytes
SERPINI8		<a href="#">gi 15079348</a>	serpin proteinase inhibitor 8	Role in the regulation of mRNA stability

**Table IV.** Summary of newly identified proteins in PC supernatants upon storage

## References

- Anderson L, Anderson NG. High resolution two-dimensional electrophoresis of human plasma proteins. *Proc Natl Acad Sci USA* 1977; 74: 5421-5425.
- Cho SY, Lee EY, Kim HY, Kang MJ, Lee HJ, Kim H, Paik YK. Protein profiling of human plasma samples by two-dimensional electrophoresis. *Methods Mol Biol* 2008;428:57-75.
- Geho DH, Liotta LA, Petricoin EF, Zhao W, Araujo RP. The amplified peptidome: the new treasure chest of candidate biomarkers. *Curr Opin Chem Biol* 2006; 10:50-55.
- Glenister KM, Payne KA, Sparrow RL. Proteomic analysis of supernatant from pooled buffy-coat platelet concentrates throughout 7-day storage. *Transfusion* 2008; 48: 99-107.

## Discussion

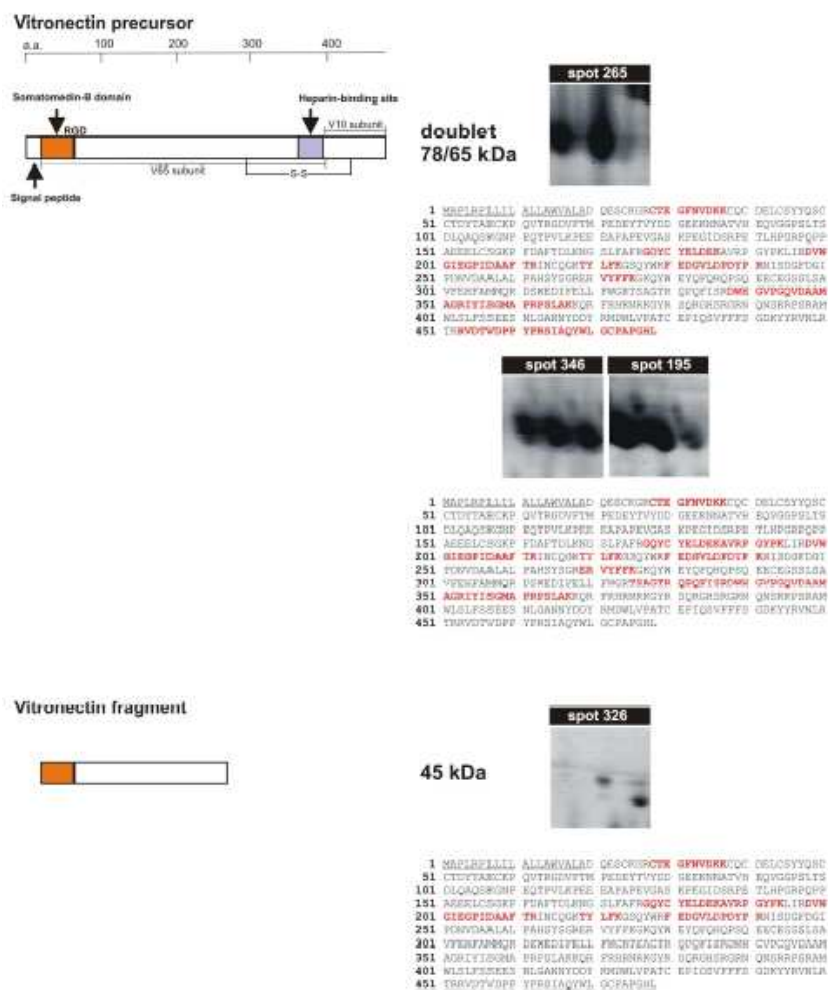
Biomarker discovery currently represents the major tendency in clinical science. In fact, the analysis of modulation of plasmatic proteins under different conditions may lead to the development of new, non-invasive diagnostic tests and become a therapeutic tool with prognostic power (Good et al., 2007). This holds true in the diagnosis and monitoring of pathologies, but also in quality assessment of therapeutic products and their deterioration, such as PCs. Hereby, the use of PC supernatants entirely suspended in plasma did not facilitate the proteomic analysis since the presence of high-abundance proteins hampered the detection of low-abundance protein populations in which potential biomarkers for the so-called "PLT-storage lesions" (Seghatchian and Krailadsiri, 1997) are thought to reside. However, such a recalcitrant system still represents a kind of product which is actually prepared in many hospitals, thus our profiling of stored PC releasates will mainly target to the real modifications occurring therein.

Without using ProteoMiner<sup>TM</sup> protein enrichment technology, we found several interesting protein changes not previously reported. Among these, a spot containing platelet alpha-1-B-glycoprotein (spot 197) has been identified in two-dimensional maps of samples not subjected to equalization step. This is the principal receptor for von Willebrand factor and thrombin, thus playing a major role in platelet signaling during activation, whose presence in platelet releasate after thrombin stimulation has been recently noticed (Piersma et al., 2009). In the present analysis, this protein spot sharply increased in abundance at the 7th sampling day. Moreover, two interesting co-migrating proteins were revealed to increase in expression after 7 days of storage in non-equalized PC supernatants (spot 240). The first one is kininogen-1. High molecular weight kininogen (HMWK) plays a crucial role in blood coagulation, being both the substrate and cofactor of the contact phase (Colman and Schmaier, 1986). This protein has been demonstrated, through immunochemical assays, to be present in and secreted by platelets upon stimulation, participating in the early phase of blood coagulation (Schmaier et al., 1983). The second one is a serpin proteinase inhibitor 8 (PI8 serpin). This protein has been proved to be synthesized by megakaryocytes, subsequently stored in platelets and released upon stimulation to limit the lifespan of serine proteases and thus be involved in anticoagulation systems (Leblond et al., 2006).



By applying the ProteoMiner equalization procedure to the supernatants of stored buffy-coat PCs, we looked at the low-abundance proteins (either plasmatic or derived from platelets) which may represent the potential biomarker-rich population to be considered in the storage-related changes of this therapeutic blood component. One of these proteins is clusterin (also named apolipoprotein J), which has been proven to be a complement lysis inhibitor able to block the terminal complement reaction. The main product of the clusterin gene is a ~60 kDa pre-secretory form (pre-sCLU), which is a heterodimer of two chains ( $\alpha$  and  $\beta$  subunits) linked together by disulphide bonds. This precursor protein is directed to the Golgi apparatus where it is heavily glycosylated (reaching a molecular weight of 70-80 kDa) and cleaved into  $\alpha$  and  $\beta$  subunits. The mature protein (sCLU) is stored in platelet granules and is released into extracellular fluid upon platelet activation (Witte et al., 1993). The mature sCLU appears as a smear at 37-40 kDa on a reducing SDS-PAGE (Rodriguez-Pineiro et al., 2006). In analysis 1 (P0 vs 0), clusterin was detected in three new spots representing either  $\alpha$ - or  $\beta$ -CLU isoforms (spots 603, 640, 626) in equalized samples. Moreover, the same spots were found to be progressively down-regulated up to 7-day storage. Conversely, one clusterin-containing spot (228) showed an up-regulation during platelet storage. Its molecular weight position (about 55 kDa) is higher with respect to the other spots previously mentioned, but not enough to be considered as the full glycosylated uncleaved precursor. On the other hand, this molecular weight well correlates with the precursor of the secretory form (pre-sCLU, 60 kDa). One of the advanced hypotheses to explain this finding is the release of clusterin from platelets following storage-induced cell damage. Another platelet-derived protein appearing in proteomic maps of equalized samples at day 0 with respect to non-equalized counterparts (spots 265 and 346) is vitronectin, a plasmatic glycoprotein currently stored in platelet alpha granules (Preissner et al., 1989). Vitronectin is known to exist in two forms: a single chain 75 kDa form (V75) and a clipped form composed of two chains (65 kDa and 10 kDa) (V65+V10) kept together by a disulfide bond (Dahlback and Podack, 1985). Its position in our two-dimensional maps (doublet at 78 and 65 kDa) coincides with previous studies on electrophoretic mobility of plasma and platelet-derived vitronectin under reducing conditions (Seiffert and Schleef, 1996). Storage-dependent modulation of vitronectin was detected, especially for the V65 subunit (up-regulation of spots 346 and 195).

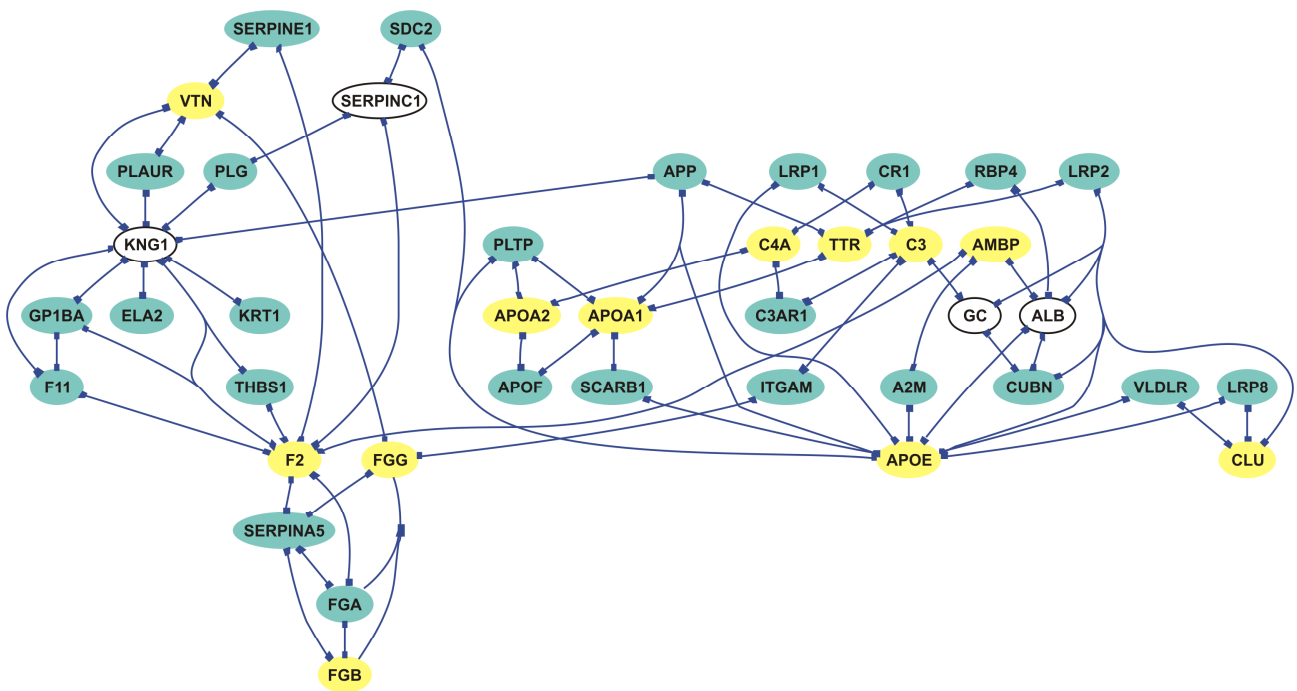
Moreover, a vitronectin truncated form was found to increase over time (spot 326). Vitronectin is known to exist in mono- or multimeric forms, the latter associating in vitro upon particular treatments, or in vivo upon storage in platelet alpha granules (Stockmann et al., 1993). The differential proteolytic fragmentation pattern of vitronectin was extensively studied. In particular, defined fragments for monomeric and multimeric vitronectin were found to be induced by plasmin (Kost et al., 1996). Plasmatic monomeric vitronectin produced a 42/35 kDa truncated form whose N-terminal characterization suggested Gly-108 as the cleavage site. On the contrary, during plasmin proteolysis of multimeric PLT-derived vitronectin a different 40 kDa truncated form was produced showing identical N-terminus of the intact vitronectin. This result was the consequence of the altered conformational state of platelet vitronectin where the Gly-108 cleavage site was not accessible (Kost et al., 1996). The ESI-MS peptide mapping obtained for the spots 265, 346 and 195 is consistent with the presence therein of the intact protein, whereas peptides from the 326 vitronectin-containing spot, along with its molecular weight position, may suggest a platelet derivation of this vitronectin truncated form. In fact, finding of the N-terminal 28CTEGFNVDK37 peptide excludes this fragment to be the plasmin-induced product of the monomeric vitronectin. However, further confirmation is required to establish the exact nature of this truncated form, especially because other mechanisms causing protein fragmentation (e.g., production of reactive oxygen species) (Freedman, 2008) may take part in storage lesions.



**Figure 4.** Mass spectrometric peptide mapping of vitronectin-containing spots. Upper panel: schematic representation of the intact two-chain vitronectin (78/65 kDa doublet) corresponding to spots 265, 346 and 195. Locations of the main protein domains are depicted along the vitronectin amino acid sequence. RGD, cell-attachment site. Lower panel: schematic representation of the 45 kDa fragment (spot 326) generated during plasmatc proteolysis of vitronectin. Peptides identified by MS/MS are shown in red. Underlined amino acids indicate the signal peptide (residues 1-19).

Platelet beta tropomyosin (spot 415) sharply accumulated upon platelet storage; this protein is a structural member of platelet cytoskeleton and together with gelsolin and F-actin capping proteins plays an important role in the remodeling of actin filaments in response to different stimuli (Cohen and Cohen, 1972). Platelet beta tropomyosin has been identified in platelet dense granules (Hernández-Ruiz et al., 2007) and its recruitment to platelet membranes during activation has also been demonstrated (Kaiser et al., 2009). So far, the presence of tropomyosin in the platelet suspension medium after storage at room temperature has never been revealed. The accumulation of tropomyosin during storage in the surrounding medium could be related to platelet loss of integrity during aging. Finally, the equalization step allowed the detection of several protein fragments which have been monitored over time. Spot 450 has been identified as plakoglobin, a protein component of tight junctions, which accumulates after 7 days of PCs storage. On the contrary, a hornerin fragment (spot 422) decreases after 7 days of storage, though temporarily increasing at the fourth day of sampling, and the same holds true for fragmented complement component C4A (spot 470). A truncated form of apolipoprotein A-IV (spot 406) has been found to progressively decrease over time, whereas opposite trend has been found for C4B fragments (spots 424 and 425).

To provide a graphical demonstration of the ability of ProteoMiner at unraveling interesting low-abundant proteins, we used SNAVI to link our results together in a network including almost all proteins found in the present analysis. To make this tool more usable for the readers, we convert codes of our protein results into their corresponding genes. As can be seen from Figure 5, the use of ProteoMiner greatly broadened the scenario of interactions between products differentially expressed upon storage, helping at shedding light to the hidden proteome that often contains key proteins of central signalling networks.



**Figure 5.** Creation of networks using PathwayGenerator Application provided by SNAVI software.

White circles indicate proteins detected without the use of ProteoMiner; yellow circles indicate proteins detected only after the use of ProteoMiner. Blue circles are intermediates nodes automatically introduced by the software to make a link between a source and a target protein.

## References

- Cohen I, Cohen C. A tropomyosin-like protein from human platelets. *J Mol Biol* 1972; 68: 383-387.
- Colman RW, Schmaier AH. The contact activation system: Biochemistry and interactions of these surface-mediated defense reactions. *Crit Rev Oncol Hematol* 1986; 5: 57-85.
- Dahlback B, Podack ER. Characterization of human S protein, an inhibitor of the membrane attack complex of complement. Demonstration of a free reactive thiol group. *Biochemistry* 1985; 24: 2368-2374.
- Freedman JE. Oxidative Stress and Platelets. *Arterioscler Thromb Vasc Biol* 2008;28:s11-s16.
- Good DM, Thongboonkerd V, Novak J, Bascands J-L, Schanstra JP, Coon JJ, Dominiczak A, Mischak H. Body Fluid Proteomics for Biomarker Discovery: Lessons from the Past Hold the Key to Success in the Future. *J Proteome Res* 2007; 6: 4549-4555.
- Hernández-Ruiz L, Valverde F, Jimenez-Nuñez MD, Ocaña E, Sáez-Benito A, Rodríguez-Martorell J, Bohórquez JC, Serrano A, Ruiz FA. Organellar Proteomics of Human Platelet Dense Granules Reveals That 14-3-3[ $\zeta$ ] Is a Granule Protein Related to Atherosclerosis. *J Proteome Res* 2007; 6: 4449-4457.
- Kaiser WJ, Holbrook LM, Tucker KL, Stanley RG, Gibbins JM. A Functional Proteomic Method for the Enrichment of Peripheral Membrane Proteins Reveals the Collagen Binding Protein Hsp47 Is Exposed on the Surface of Activated Human Platelets. *J Proteome Res* 2009; 8: 2903-2914.
- Kost C, Benner K, Stockmann A, Linder D, Preissner KT. Limited plasmin proteolysis of vitronectin. Characterization of the adhesion protein as morpho-regulatory and angiostatin-binding factor. *Eur J Biochem* 1996; 236: 682-688.
- Leblond J, Laprise MH, Gaudreau S, Grondin F, Kisiel W, Dubois CM. The serpin proteinase inhibitor 8: An endogenous furin inhibitor released from human platelets. *Thromb Haemost.* 2006; 95: 243-252.
- Piersma SR, Broxterman HJ, Kapci M. Proteomics of the TRAP-induced platelet releasate. *J Proteomics* 2009; 72: 91-109.
- Preissner KT, Holzhueter S, Justus C, Mueller-Berghaus G. Identification and partial characterization of platelet vitronectin: Evidence for complex formation with platelet-derived plasminogen activator inhibitor- 1. *Blood* 1989; 74:1989-1996.
- Rodriguez-Pineiro AM, de la Cadena MP, Lopez-Saco A, Rodriguez-Berrocal FJ. Differential expression of serum clusterin isoforms in colorectal cancer. *Mol Cell Proteomics* 2006; 5: 1647-1657.
- Schmaier AH, Zuckerberg A, Silverman C, Kuchibhotla J, Tuszynski GP, Colman RW. High-Molecular Weight Kininogen- A Secreted Platelet Protein. *J Clin Invest* 1983; 71: 1477-1489.
- Seghatchian J, Krailadsiri P. The platelet storage lesion. *Transf Med Rev* 1997; 11: 130-144.
- Seiffert D, Schleef RR. Two functionally distinct pools of vitronectin (Vn) in the blood circulation: identification of a heparin-binding competent population of Vn within platelet alpha-granules. *Blood* 1996; 88: 552-560.
- Stockmann A, Hess S, Declerck P, Timpl R, Preissner KT. Multimeric Vitronectin. Identification and characterization of conformation-dependent self-association of the adhesive protein. *J Biol Chem* 1993; 268: 22874-22882.
- Witte DP, Aronow BJ, Stauderman ML, Stuart WD, Clay MA, Gruppo RA, Jenkins SH, Harmony JA. Platelet activation releases megakaryocyte-synthesized apolipoprotein J, a highly abundant protein in atheromatous lesions. *Am J Pathol* 1993; 143: 763-773.

Through the comprehensive analysis of low-abundance protein modulations, either derived from plasma or platelets, we provided new insights into the effects of storage on platelet concentrates. Notwithstanding all the advantages incidental to the introduction of the equalization step, some drawbacks still need to be climbed. Among the limitations of such an enrichment technology, it is worthwhile to mention the residual over-abundance of certain proteins, such as fibrinogen which can account for one third of the total spots obtained from 2D maps of ProteoMiner-treated plasma fractions (Bandow, 2010). Whether fibrinogen bound a variety of peptide hexamers very efficiently or the peptide hexamer(s)-binding fibrinogen was over-represented on the column remains to be clarified. Actually, recent findings seem to demonstrate that ProteoMiner beads interact with protein mixtures according to a general hydrophobic binding mechanism rather than the hexapeptide library coating the equalizer beads (Keidel et al., 2010). Combining the equalization approach with additional fractionation methods may further increase the number of detectable species. This is particularly true in relation to the loss of unique proteins noticed after library treatment with respect to the untreated control (e.g., A1BG, KNG1 and SERPINA8 in our case). For this reason, the use of both data analysis from initial and treated sample has been suggested (Boschetti and Righetti, 2009). Although no generalization can be made from a single instance, our study confirmed proteomics to be a tool offering the potential for new approaches and useful perspectives both to improve quality and safety of blood therapeutics and to set advanced quality requirements at the regulatory level.

## References

- Bando JE. Comparison of protein enrichment strategies for proteome analysis of plasma. *Proteomics* 2010;10:1416-1425.
- Boschetti E, Righetti PG. The art of observing rare protein species in proteomes with peptide ligand libraries. *Proteomics* 2009;9:1492-1510.
- Keidel EM, Ribitsch D, Lottspeich F. Equalizer technology - Equal rights for disparate beads. *Proteomics* 2010;10:2089-2098.



## Supporting Information

Contains tables of peptides identified by means of mass spectrometry

### 1) Cheyenne winter wheat (PART I)

Spot No.	Peptides identified by MS/MS				Mascot Ion Score	NCBI GI Number	Protein ID
	m/z	charge state	start-end <sup>a</sup>	sequence			
90	580.92	2 +	9-19	SGEVVDVTQVK	67	gi 157073742	group3 late embryoogenesis abundant protein (wrab17) [Triticum aestivum]
	734.08	2 +	25-37	KMASETGQSIQDR	49		
	670.27	2 +	26-37	MASETGQSIQDR + Oxid (M)	74		
	790.68	2 +	38-52	AVEAKDQTGSFLGEK	68		
	541.47	2 +	43-52	DQTGSFLGEK	42		
	937.91	2 +	122-138	STEEAAQYVQDTAAQYTK	104		
	860.77	3 +	122-145	STEEAAQYVQDTAAQYTKDPPVAPK	88		
	957.44	2 +	146-164	ENVFQQAGGNMMGAATGAK + 2 Oxid (M)	70		
39	670.88	2 +	165-177	DAVMNTLGMGGDK + 2 Oxid (M)	72	gi 7716956	cold-responsive LEA/RAB-related COR protein (wrab17) [Triticum aestivum]
	782.96	2 +	27-41	AVEAKDQTGAFLGEK	55		
	727.15	3 +	27-47	AVEAKDQTGAFLGEKSEAVTK	65		
	533.50	2 +	32-41	DQTGAFLGEK	51		
	840.94	2 +	32-47	DQTGAFLGEKSEAVTK	90		
	924.93	2 +	111-127	STEEAAQHVQDTAAQYTK	54		
44	878.10	3 +	128-153	DTPVAPKENVFQQAGGNMVGAAATDAK + Oxid (M)	61	gi 13925723	protein disulfide isomerase 1 precursor [Triticum aestivum]
	924.96	2 +	122-138	STEEAAQHVQDTAAEYTK	68		
194	727.55	1 +	139-145	DTPVAPK	30	gi 13925723	protein disulfide isomerase 1 precursor [Triticum aestivum]
	591.76	2 +	111-120	YEVQGFPTLK	48		
	576.13	2 +	137-146	EAEGIVEYLK	40		
	655.15	2 +	158-169	APEDATYLEDGK	76		
	622.93	3 +	196-211	SDYDFGHTVHANHLPR	71		
	395.09	3 +	212-222	GDAVERPLVR	32		
	769.21	2 +	223-235	LFKPFDELVVDK	46		
	1023.63	1 +	236-244	DFDVSALEK	45		
	483.69	2 +	245-253	FIDASSTPK	57		
	704.51	2 +	294-306	SAYYGAVEEFSGK	83		
	1052.63	2 +	310-328	FLIGDIEASQGAQFYFGLK	75		
	827.62	2 +	329-343	EDQAPLILIQSDSK + Glu->pyro-Glu (N-term E)	79		
	558.17	3 +	329-343	EDQAPLILIQSDSK	44		
	736.22	2 +	348-360	EQVEAGQIVAWLK	79		
	776.68	2 +	372-385	KSEPIPEANNEPVK	63		
	728.12	2 +	386-398	VVVADNIHVVFK	94		
	1149.18	2 +	418-439	LAPILDEAAATLQSEEDVVIK	97		
	584.15	2 +	476-485	TADEIVDYIK	61		
	731.26	2 +	487-501	NKETAGQAAAAATEK	84		
46	610.20	2 +	489-501	ETAGQAAAAATEK	62	gi 75246527	Translationally-controlled tumor protein homolog [Triticum aestivum]
	728.32	2 +	502-515	AAEPAATEPLKDEL	47		
	799.97	2 +	8-21	LSGDELLSDSFPYR	74		
68	532.54	2 +	67-75	VVDIVDTFR	52	gi 114145394	glycine-rich RNA-binding protein [Triticum aestivum]
	639.90	2 +	102-112	LEGDDLVDVFKK	49		
	449.14	2 +	29-36	YGDVIDSK	51		
	768.06	2 +	48-61	GFGFVTFASDEAMR	81		
	767.92	2 +	62-75	QAIEAMNGQDLDR + Oxid (M)	49		
66	566.47	2 +	76-85	NITVNEAQR	53	gi 1346964	RuBisCO large chain [Avena sativa]
	778.46	2 +	87-106	SGGGGGGGFSGGGGGYGGQR	73		
	749.59	2 +	320-334	MSGGDHHSHTVVGK + Oxid (M)	48		
	655.82	2 +	340-350	EMTLGFVDLLR + Oxid (M)	57		
	519.56	2 +	351-358	DDFIEKDR	46		
62	826.40	2 +	464-477	AIKFEFEPVDTIDE	61	gi 11990893	RuBisCO small subunit [Triticum aestivum]
	691.09	2 +	83-93	SKWVPCLEFSK	34		
	369.97	2 +	94-99	VGFIIR	37		
	683.84	2 +	100-111	EHNASPGYYDGR	57		
	571.06	2 +	138-146	KEYPDAYVR	34		
	497.82	2 +	139-146	EYPDAYVR + Glu->pyro-Glu (N-term E)	47		
6	491.71	2 +	147-154	IIGFDNMR + Oxid (M)	45	gi 11990893	RuBisCO small subunit [Triticum aestivum]
	961.61	2 +	59-75	FETLSYLPPLSTEALLK	33		
	683.34	2 +	100-111	EHNASPGYYDGR	58		
	571.07	2 +	138-146	KEYPDAYVR	40		
	497.88	2 +	139-146	EYPDAYVR + Glu->pyro-Glu (N-term E)	43		
6	491.35	2 +	147-154	IIGFDNMR + Oxid (M)	47		

167	641.56	3 +	59-75	FETLSYLPPLSTEALLK	45		
	370.03	2 +	94-99	VGIFIR	37		
	683.47	2 +	100-111	EHNASPGYYDGR	70		
	491.53	2 +	147-154	IIGFDNMR + Oxid (M)	34		
	756.83	3 +	155-174	QVQCVSFI AFKPPGCEESGK	39		
45	608.35	2 +	48-57	MQVWPIEGIK + Oxid (M)	36		
	684.21	3 +	58-75	KFETLSYLPPLSTEALLK	47		
	641.57	3 +	59-75	FETLSYLPPLSTEALLK	50		
	690.97	2 +	83-93	SKWVPCLEFSK	32		
	683.40	2 +	100-111	EHNASPGYYDGR	65		
	808.49	3 +	118-138	LPMFGCTDATQVINEVEEVKK + Oxid (M)	77		
	571.06	2 +	138-146	KEYPDAYVR	41		
	497.81	2 +	139-146	EYPDAYVR + Glu->pyro-Glu (N-term E)	45		
	483.37	2 +	147-154	IIGFDNMR	45		
	780.47	3 +	155-175	QVQCVSFI AFKPPGCEESGKA	44		
178	1025.73	2 +	57-74	KFETLSYLPPLSTEALLK	37	gi 3914588	RuBisCO small subunit (chloroplast precursor) [Triticum aestivum]
	454.11	2 +	75-81	QVDYLIR	48		
	370.10	2 +	93-98	VGIFIR	33		
	808.97	3 +	117-137	LPMFGCTDATQVLNEVEEVKK + Oxid (M)	65		
	491.53	2 +	146-153	IIGFDNMR + Oxid (M)	38		
184	533.94	2 +	38-47	ASAYADELVK	46	gi 8272480	fructose 1 6-bisphosphate aldolase precursor [Avena sativa]
	694.42	2 +	73-85	LASIGLENTEANR	86		
	810.97	3 +	140-162	GLVPLVGSNDESWCQGLDGLASR	46		
	579.11	2 +	163-172	EAAYYQQGAR	66		
	756.14	2 +	178-192	TVVSIPNGPSELAVK	35		
	437.45	2 +	193-200	EAAWGLAR	49		
	411.97	2 +	229-235	TFEVAQK	37		
	655.12	2 +	271-282	ATPEEVASYTLK	69		
	1026.55	2 +	338-356	TWGGRPENVAQAQALLLR	79		
	542.66	2 +	368-378	YTSDGEAAAAK	66		
102	351.40	2 +	51-57	TIASPGR	40	gi 195634659	Fructose-1,6- bisphosphate aldolase [Zea mays]
	694.69	2 +	73-85	LASIGLENTEANR	85		
	797.10	2 +	122-136	IVDILVEQGIVPGIK	71		
	578.81	2 +	163-172	EAAYYQQGAR	68		
	437.38	2 +	193-200	EAAWGLAR	41		
	1016.80	3 +	201-228	YAAISQDNLVPIVEPEILLDGEHGIER	69		
	822.42	1 +	229-235	TFEVAQK	45		
	474.33	2 +	330-337	ALQNTCLK	41		
	451.38	2 +	359-367	ANSLAQLGK	44		
	571.50	2 +	368-378	YTSDGEAAAEAK	73		
30	749.57	1 +	18-24	YIATPGK	30	gi 115468886	Os06g0608700 Fructose-1,6- bisphosphate aldolase [Oryza sativa (japonica cultivar-group)]
	666.96	2 +	25-38	GILAADESTGTIGK	86		
	745.05	2 +	25-39	GILAADESTGTIGKR	81		
	382.44	2 +	205-211	VLAAYYK	38		
	738.28	3 +	218-238	VLLEGTLKPNMVTGPSDSPK + Oxid (M)	76		
97	866.19	3 +	114-138	YDSTLGIFDADV KPGVDNAISVDGK	97	gi 115458768	Os04g0459500 glyceraldehyde-3- phosphate dehydrogenase [Oryza sativa (japonica cultivar-group)]
	693.01	2 +	267-281	AAALNIVPTSTGAAK	42		
	519.59	2 +	282-291	AVALVLPNLK	43		
	639.50	2 +	319-329	TLAEENVQAFR	56		
121	477.43	3 +	77-90	RLTSVFGGAAEPPK	55	gi 125580	Phosphoribulokinase chloroplast precursor [Triticum aestivum]
	637.81	2 +	78-90	LTSVFGGAAEPPK	66		
	529.50	2 +	122-131	EKGVTALDPK	42		
	401.04	2 +	124-131	GVTALDPK	38		
	745.11	2 +	132-143	ANDFDLMEYQVK + Oxid (M)	75		
	886.37	3 +	150-173	AIEKPIYNHVTGLLDPAELIQPPK	50		
	860.17	2 +	174-187	IFVIEGLHPMYDER	53		
	435.93	2 +	218-225	GHSLESIK	33		
	711.27	2 +	232-243	KPDFDAFIDPQK	58		
	1206.15	2 +	244-265	QYADAVIEVLPTQLIPDDNEGK	60		
	654.57	3 +	334-350	LDELIYVESHLNLSK	67		
	680.72	2 +	351-361	FYGEVTQQMLK + Oxid (M)	64		
	1087.61	2 +	362-382	HADFPGSNNGTGLFQTIVGLK	34		
	760.31	2 +	383-394	IRDLYEQIIAER	71		
	625.73	2 +	385-394	DLYEQIIAER	60		
	407.66	2 +	395-403	AGVPAAEAK	36		

	613.561 439.988 469.565 593.464 689.313 825.584 618.535 795.173 466.078 427.624 595.078	2 + 2 + 2 + 2 + 3 + 2 + 2 + 2 + 2 + 2 + 2 +	95-104 222-229 259-266 267-276 267-283 290-304 307-318 323-336 352-359 360-367 373-382	LLICMGEAMR TTFVVALK MFSPGNLR ATFDNPDYDK ATFDNPDYDKLVNYYVK YTGGMVPDVNQIIVK GIFTNVTSPYAK LLFEVAPLGFLEIK VISVLDER TQVAYGSK FEETLYGSSR	39 47 36 41 49 68 68 69 56 46 69	gi 1173347	Sedoheptulose-1,7- bisphosphatase, chloroplast precursor [Triticum aestivum]
124	638.61 711.11 787.34	2 + 2 + 2 +	77-89 250-262 421-437	SVGDLTAADLEGK ELDYLDGAVSNPK GVTTIIGGGDSVAAVEK	77 98 70	gi 129915	Phosphoglycerate kinase, chloroplast precursor [Triticum aestivum]
119	688.55 825.75 472.70 797.68	2 + 2 + 2 + 3 +	27-38 98-113 143-151 183-202	MELIDAAFPLK + Oxid (M) VLVVANPANTNALILK LGVQVSDVK ELVQDDEWLNGEFIATVQQR	48 56 68 58	gi 37928995	cytosolic malate dehydrogenase [Triticum aestivum]
113	725.07 483.79 496.54 632.05 717.15 672.68	2 + 3 + 2 + 2 + 2 + 2 +	118-133 118-133 175-183 195-205 243-255 311-322	KAPGGAPANVAVGIAR KAPGGAPANVAVGIAR TALAFVTLR NPSADMLLEEK + Oxid (M) DAGVLISYDPNLR LLLVTEGPEGCR	85 44 64 53 63 36	gi 51535181	putative fructokinase [Oryza sativa Japonica Group]
177	636.82 667.13 765.15 812.22 644.18	2 + 2 + 2 + 2 + 2 +	66-77 81-93 164-177 206-223 319-332	ELMPGGVNSPVR + Oxid (M) SVGGQPIVFDSVK FVNSGTEACMGALR + Oxid (M) AGSGVATLGLPDSGPVVK IIGGLPVGAYGGR	46 57 85 65 55	gi 115477483	Os08g0532200 glutamate-1- semialdehyde aminotransferase [Oryza sativa (japonica cultivar-group)]
34	730.98 757.00	2 + 2 +	252-264 287-300	FVTNEGTYGPYGR ADDTQLIAFGVYTV	57 37	gi 16151819	VER2 [Triticum aestivum]
79	587.04 350.09 636.91 603.37 632.17 719.43	3 + 3 + 2 + 2 + 2 + 2 +	144-159 160-168 169-180 237-247 320-331 358-369	VHQALTEVAISSFDIK TNKPVIFTK SNLAKSPELDAK AEEDPAFASIR VQENALTGTTTK DSPETYEELKLR	61 40 58 66 72 64	gi 122201873	Patatin-13 precursor [Solanum tuberosum]
69	821.02 757.12	2 + 2 +	81-96 82-96	KQLAVPDGTPVTAESK QLAVPDGTPVTAESK	36 62	gi 113165	Acyl carrier protein 1 chloroplast precursor [Hordeum vulgare]
127	701.81 651.19 537.58	2 + 2 + 2 +	67-78 79-91 81-91	SKEEAMSDYITK VKQLLEAAAAAAS QLLEAAAAAAS	46 46 41	gi 115474931	Os08g0162800 Acyl-CoA-binding protein [Oryza sativa (japonica cultivar-group)]
84	905.49 686.51 915.98	2 + 2 + 2 +	198-213 226-237 226-241	AEQYLADSGLPYTIIR ELLVGKDDEILK ELLVGKDDEILKTETK	73 68 77	gi 115461679	Os05g0110300 Similar to putative 3- beta hydroxysteroid dehydrogenase/isomera se protein [Oryza sativa (japonica cultivar-group)]
136	782.06 437.31 731.52 783.99 435.98 862.60 698.87 813.28 736.97 701.24 673.07 658.52 778.40 605.04 691.68 576.91 826.49	2 + 2 + 2 + 2 + 2 + 2 + 2 + 3 + 2 + 3 + 2 + 3 + 2 + 3 + 2 + 2 + 2 +	116-129 160-167 168-180 197-210 219-226 227-242 359-369 477-499 550-563 550-568 551-563 551-568 569-581 569-583 591-602 606-616 683-698	QAVVNPENTFFSVK + Gln->pyro-Glu (N-term Q) LDCAIGK QFAAEEISAQVLR AVVTVPAYFNDSQR IAGLEVLR IINEPTAASLAYGFKEK FEELCSDLIDR SEVFSTAADGQTSVEINVQGER KQDITITGASTLPK KQDITITGASTLPKDEVER QDITITGASTLPK QDITITGASTLPKDEVER MVEEADKFAQEDK MVEEADKFAQEDKEK + Oxid (M) NQADSVVYQTEK ELGDKVPAPVK GPNDGDIVADFTDSN	68 52 81 33 52 106 36 89 78 83 69 53 64 46 84 47 87	gi 115487998	Os12g0244100 molecular chaperone DnaK [Oryza sativa (japonica cultivar-group)]
193	634.56 570.59 690.63	2 + 2 + 2 +	209-219 210-219 223-233	KIVTEILPARK IVTEILPARK AEEYHQYQYLAKE	46 39 59	gi 29469000	peptide methionine sulfoxide reductase [Gossypium]

							barbadense]
128	502.05 356.62 512.41	2 + 2 + 2 +	165-172 173-178 181-189	NLLFKPDR EAFFAK EVYEDIISG	36 35 36	gi 125575528	hypothetical protein OsJ_031021 [Oryza sativa (japonica cultivar-group)]
180	746.69 619.99	3 + 2 +	190-211 242-251	VMIHQPSGGAQQGQATDIAIQAK + Oxid (M) DLFMDPEEAR + Oxid (M)	72 39	gi 115447465	Os02g0634500 [Oryza sativa (japonica cultivar-group)]
112	779.37 715.20 723.23 543.00 479.02 578.66 1104.74 981.62 866.74	2 + 2 + 3 + 2 + 2 + 2 + 2 + 2 + 2 +	51-64 52-64 65-84 92-99 93-99 103-112 178-196 197-214 221-235	KLPSILVDETSVQK LPSILVDETSVQK IQSLTPNIGVVYSGMGPDFR KQAQQYYR QAQQYYR ETIPVTQLVR YTEDMELDDAIHTAILTK + Oxid (M) EGYEGQISANNIEIGVIR VLTPAEIKDFLEEVE	79 82 74 44 33 53 82 62 46	gi 115447473	Os02g0634900 Proteasome alpha type 2 [Oryza sativa (japonica cultivar-group)]
88	908.72 881.60 770.62 991.84 630.88 776.74 475.12 490.57 791.45 721.24 469.64	2 + 2 + 2 + 3 + 2 + 3 + 2 + 2 + 2 + 3 + 2 +	66-80 81-96 101-114 115-141 170-180 181-199 232-239 321-329 339-352 354-373 387-394	MQQLLDMDTTPFTDK +2 Oxid (M) IIAEYIWVGSGIDLR TISKPVEDPSELPK WNYDGSSTGQAPGEDSEVILYPQAIFK HMAAQIFSDPK + Oxid (M) VTSQVPWFGEIEQYTLMQR + Oxid (M) DISDAHVK EDGGFDDVIK HDLHIAAYGEGNER LTGLHETASISDFSWGVANR GKGYLEDR	69 74 56 51 56 62 35 51 78 73 44	gi 121340	Glutamine synthetase chloroplast precursor [Hordeum vulgare]
80	908.45 881.52 770.96 991.82 777.08 490.61 791.40 721.21 469.34	2 + 2 + 2 + 3 + 3 + 2 + 2 + 3 + 2 +	66-80 81-96 101-114 115-141 181-199 321-329 339-352 354-373 387-394	MQQLLDMDTTPFTDK + 2 Oxid (M) IIAEYIWVGSGIDLR TISKPVEDPSELPK WNYDGSSTGQAPGEDSEVILYPQAIFK VTSQVPWFGEIEQYTLMQR + Oxid (M) EDGGFDDVIK HDLHIAAYGEGNER LTGLHETASISDFSWGVANR GKGYLEDR	80 79 69 70 65 50 80 66 44		
153	900.41 881.42 770.51 991.81 490.59 527.75 721.20 469.58	2 + 2 + 2 + 3 + 2 + 3 + 3 + 2 +	59-73 74-89 94-107 108-134 314-322 332-345 347-366 380-387	MQQLLDMDTTPFTDK + Oxid (M) IIAEYIWVGSGIDLR TISKPVEDPSELPK WNYDGSSTGQAPGEDSEVILYPQAIFK EDGGFDDVIK HDLHIAAYGEGNER LTGLHETASISDFSWGVANR GKGYLEDR	78 65 64 60 50 72 60 44	gi 71362640	plastid glutamine synthetase GS2c [Triticum aestivum]
156	631.08 721.04	2 + 3 +	163-173 347-366	HMAAQIFSDPK + Oxid (M) LTGLHETASISDFSWGVANR	42 65	gi 71362638	plastid glutamine synthetase GS2b [Triticum aestivum]
165	751.34 803.95 727.46 444.47 478.57 490.46	2 + 2 + 2 + 2 + 2 + 2 +	50-62 77-91 240-254 294-302 330-337 366-374	TNMVMVFGEITTK + 2 Oxid (M) NIGFISDDVGLDADR FVIGGPHGDAGLTGR SIASGLAR IPDKEILK TAAYGHFGR	75 107 84 48 59 45	gi 115589744	S-adenosylmethionine synthetase 1 [Triticum monococcum]
148	813.41 824.54 821.85 425.91 412.77 803.50 522.84 768.86 380.76	2 + 2 + 3 + 2 + 2 + 2 + 2 + 3 + 3 +	107-120 147-161 147-168 162-168 194-200 201-214 241-250 251-271 272-281	VYVGNLPYDVSER GFGFVTMSTIEEADK GFGFVTMSTIEEADKAIEETFNR AIETFNR QFASSFR + Gln->pyro-Glu (N-term Q) AYVGNLPWQAEDSR GFGFVTMASK EDLDSAISALDQGEMDGRPLR + Oxid (M) VNVAAPERQQR	70 89 73 53 32 71 60 71 33	gi 3550483	cp31BHv [Hordeum vulgare subsp. vulgare]
36	544.72 515.42	2 + 2 +	154-163 199-207	GVIPLAYSIR LNADDDVIR	40 70	gi 115456525	Os03g0843400 30S ribosomal protein S6, chloroplast precursor [Oryza sativa (japonica cultivar-group)]

195	705.74 394.40	2 + 2 +	93-105 134-140	DADIFAVVMIGSR + Oxid (M) VLLVSTR	61 37	gi 115445399	Os02g0259600 50S ribosomal protein L21, chloroplast precursor [Oryza sativa (japonica cultivar-group)]
3	433.89 844.20	2 + 3 +	81-88 89-112	AGETITFK NNAGYPHNVFDEDAVPSGVDVSK	77 44	gi 22705	plastocyanin precursor [Hordeum vulgare]
59	661.92 502.48	2 + 2 +	129-140 215-222	GDPTYLVVESDK TGDNPWWK	62 46	gi 68566191	Cyt b6-f complex iron- sulfur subunit chloroplastic [Triticum aestivum]
197	816.18 654.54	2 + 2 +	143-158 167-178	LYSIASSALGDFGDSK LVYTNDAGEVVK	108 62	gi 20302473	ferredoxin-NADP(H) oxidoreductase [Triticum aestivum]
57	708.94 523.68 695.55	2 + 2 + 2 +	379-390 487-495 487-498	IVGNEHYETAQR AITLEENK AITLEENKSQK	71 33 58	gi 11583	ATPase beta subunit [Hordeum vulgare]
33	815.68 905.12 627.91 1057.00 596.69 504.54 523.63 665.12 706.75 438.54 809.78 736.59	2 + 2 + 2 + 2 + 2 + 2 + 2 + 2 + 3 + 2 + 2 + 2 +	3-18 23-39 76-87 88-109 135-145 146-154 155-163 192-205 208-225 218-225 232-246 249-261	TNPTTSPPGASTIEEK IDQIIGPVLDTFPPGK AVAMSATDGLMR + 2 Oxid (M) GMEVIDTGAPLSVPVGGATLGR + Oxid (M) SAPAFIELDTK LSIFETGIK VVDLLAPYR AHGGVSVFGGVGER EGNDLYMEMKESGVINEK ESGVINEK VALVYQGMNEPPGAR + Oxid (M) VGLTALTMAEYFR	65 70 90 85 63 45 48 73 35 60 83 88	gi 14017579	ATP synthase CF1 beta subunit [Triticum aestivum]
109	595.98 488.36 809.43 736.66 717.61 1038.95 709.01 523.83 695.52	2 + 2 + 2 + 2 + 2 + 2 + 2 + 2 + 2 +	135-145 168-178 232-246 249-261 278-291 360-378 379-390 487-495 487-498	SAPAFIELDTK IGLFGGAGVGK VALVYQGMNEPPGAR + Oxid (M) VGLTALTMAEYFR FVQAGSEVSALLGR GIYPAVDPLDSTSTMLQPR + Oxid (M) IVGNEHYETAQR AITLEENK AITLEENKSQK	57 47 73 81 78 56 59 36 54		
196	668.54 595.35 531.02 610.23 1048.62 937.52 579.51 674.53 755.22 620.63	2 + 2 + 2 + 2 + 3 + 3 + 2 + 1 + 2 + 2 +	1-11 2-11 3-11 12-20 21-50 70-95 96-106 112-117 125-137 127-137	MKLNLYVLTPK + Oxid (M) KLNLYVLTPK LNLYVLTPK RIIWDCEVK EILSTNSGQIGVLPNHAPINTAVDMGPLR + Oxid (M) IVNNEIILGNDAELGSDIDPEEAQK ALEIAEANLSK DLVEAK IRIEAVNWIPPSN IEAVNWIPPSN	67 61 52 40 84 39 79 44 43 45	gi 14017578	ATP synthase CF1 epsilon subunit [Triticum aestivum]
115	337.542 730.599 805.587 451.097	2 + 2 + 1 + 2 +	114-120 114-127 121-127 142-150	AELGGVK AELGGVKDASEEVR DASEEVR AEIAAALNK	36 89 45 42	gi 115452259	Os03g0278900 ATP synthase B/B' CF(0) [Oryza sativa (japonica cultivar-group)]
190	608.20 553.55 703.01 626.21 731.61 365.72 660.11 466.60 625.02 703.08	2 + 2 + 3 + 2 + 3 + 2 + 2 + 2 + 2 + 2 +	35-46 55-64 68-86 117-126 129-147 182-187 188-198 199-206 207-217 207-218	EAAPVSGDDLLK KFETALGVLK ITIDPDDPTAVANYAQVMR + Oxid (M) TYLDTLQQLR SGLIDDMGIEDMMMEALEK + 4 Oxid (M) KEDLPK IEENLEMELAK AELTELKK EVVEAMEGQLK +Oxid (M) EVVEAMEGQLKR +Oxid (M)	36 59 97 58 72 45 86 39 57 55	gi 47607439	mitochondrial ATP synthase precursor [Triticum aestivum]
118	468.96 730.55 554.04	2 + 2 + 2 +	28-35 44-55 128-136	MLVSDEAR + Oxid (M) TFEDVNHQLQTK ELAEIQEMK + Oxid (M)	52 66 32	gi 115476908	Os08g0478200 ATP synthase D chain, mitochondrial [Oryza sativa (japonica cultivar-group)]

103	786.48 849.01 733.63 889.59 686.50 335.03	2 + 2 + 2 + 1 + 2 + 3 +	102-115 118-132 133-143 168-175 176-188 189-197	FYLQPLPPAEAAVR ESAQDILNLKPLIDK KQWPYVMNDLR + Oxid (M) DLKDLTGK LFATLDGLDHAAC IKSPTEAEK	54 34 43 42 58 53	gi 134290407	putative oxygen-evolving complex precursor [Triticum aestivum]
35	782.17 717.89 606.91 748.08 918.10 613.98 1042.48 627.44 663.90 599.84	2 + 2 + 2 + 3 + 3 + 2 + 2 + 2 + 2 + 2 +	87-100 88-100 112-121 122-141 170-197 198-207 208-228 217-228 246-258 247-258	KNTDFVAYSSEGFK NTDFVAYSSEGFK EREFPQQVLR + Glu->pyro-Glu (N-term E) YEDNFDATSNLSVIINPTTK TDSEGGFESDAVATANVLESSAPVVDGK QYYISITVLR + Gln->pyro-Glu (N-term Q) TADGDEGGKHQLITATVADGK HQLITATVADGK KFVENAAGSFSVA FVENAAGSFSVA	94 94 55 57 84 61 77 82 82 66	gi 131394	Oxygen-evolving enhancer protein 2 [Triticum aestivum]
4	781.92 717.89 1121.49	2 + 2 + 2 +	87-100 88-100 122-141	KNTDFVAYSSEGFK NTDFVAYSSEGFK YEDNFDATSNLSVIINPTTK	80 83 70		
160	685.34 547.49 538.07 742.75 678.56	2 + 2 + 3 + 2 + 2 +	59-68 61-68 141-155 142-155 143-155	FKESIYHCR EESIYHCR KKYPGGAFFDPLGFSK KYPGGAFFDPLGFSK YPGGAFFDPLGFSK	64 64 52 65 38	gi 544700	LHC I [Hordeum vulgare]
104	393.93 779.35 756.80 881.03 760.82	2 + 2 + 3 + 2 + 3 +	95-100 141-154 161-181 186-202 211-231	TYMEVK AEGIQKNEPPAFQK LTYTLDEMEGPLEVGADGTLK + Oxid (M) DGIDYAAVTQPLGGER QLVATGKPESFSGPFLVPSYR	36 54 79 86 42	gi 147945622	oxygen-evolving enhancer protein 1 [Leymus chinensis]
58	541.19 778.97 880.93 475.94	2 + 2 + 2 + 2 +	86-94 141-154 186-202 203-210	LTFDEIQSK AEGIQKNEPPAFQK DGIDYAAVTQPLGGER VPFLFTVK	55 46 51 46		
169	467.36 799.03 395.56 652.19 587.99 831.09 729.96	2 + 2 + 2 + 2 + 2 + 3 + 2 +	98-105 109-122 128-134 270-279 271-279 280-304 338-350	YALPIDNK EVQKPLEDITSLK + Glu->pyro-Glu (N-term E) ALDSVER KFYDGMIEQR + Oxid (M) FYDGMIEQR + Oxid (M) ADGFVVQTDGPEGAEGFIDPSTGK LPFNAFGTMAMAR +2 Oxid (M)	37 63 54 38 61 72 44	gi 115476198	Os08g0382400 Cyclophilin TLP40 like [Oryza sativa Japonica Group]
143	599.92 727.13 829.04 762.76	2 + 2 + 3 + 3 +	101-109 140-152 218-240 220-240	FLEYLDKDR VQLPGLSQELLQK AKFQMEPNTGVTFDDVAGVDEAK + Oxid (M) FQMEPNTGVTFDDVAGVDEAK + Oxid (M)	47 45 55 68	gi 4325041	FtsH-like protein Ptf precursor [Nicotiana tabacum]
100	610.67 695.42 617.58	2 + 2 + 2 +	169-179 233-245 234-245	LFGVTTLDVVR RTQDGGTEVVEAK TQDGGTEVVEAK	64 58 72	gi 115438875	Os01g0649100 Malate dehydrogenase [Oryza sativa (japonica cultivar-group)]
114	575.59 781.12 849.68 495.02 590.05	2 + 2 + 3 + 2 + 2 +	58-67 144-157 144-165 158-165 233-243	YTSKPLGDR EDDIIGVLETDVVK EDDIIGVLETDVVKDMKPLNDR + Oxid (M) DMKPLNDR GADGTNYIVLR	50 47 41 37 71	gi 51090748	putative chaperonin 21 precursor [Oryza sativa Japonica Group]
158	680.93 671.29 398.71 626.27 374.27 874.99 511.68 743.46 854.98	2 + 3 + 2 + 3 + 2 + 2 + 2 + 2 + 2 +	11-23 24-41 42-48 105-122 106-113 106-122 114-122 127-140 148-163	AAAEYDLPLVGNK APDFAAEAVFDQEFINVK LSDYIGK KSGGLGDLKYPLVSDVTK SGGLGDLK SGGLGDLKYPLVSDVTK YPLVSDVTK SFGVLIPDQGIALR EGVIQHSTINNLGIGR	63 69 35 49 42 60 47 71 44	gi 2829687	2-Cys peroxiredoxin BAS1 [Triticum aestivum]
179	681.02 671.16 743.70	2 + 3 + 2 +	11-23 24-41 127-140	AAAEYDLPLVGNK APDFAAEAVFDQEFINVK SFGVLIPDQGIALR	53 52 62		

96	539.44	2 +	23-32	QYTLEGQGAK + Gln->pyro-Glu (N-term Q)	57	gi 26017213	cold regulated protein (wcor18) [Triticum aestivum]
	644.12	3 +	33-49	KDISPPLEWYGVPDGTR	39		
	901.52	2 +	34-49	DISPPLEWYGVPDGTR	62		
	711.02	2 +	129-141	LYALDDVLSLGNK	80		
32	539.46	2 +	23-32	QYTLEGQGAK + Gln->pyro-Glu (N-term Q)	49		
	901.53	2 +	34-49	DISPPLEWYGVPDGTR	67		
	758.58	2 +	50-63	SLAVVQDVVDADER	98		
	530.16	2 +	115-124	GPVPDSHGHR	61		
146	855.78	2 +	63-77	GLAYDISDDQQDITR	86	gi 12643756	RuBisCO activase A [Hordeum vulgare]
	398.53	2 +	131-137	LVVHLSK	38		
	615.07	2 +	162-171	SFQCELVFAK	55		
	779.43	3 +	172-194	MGINPIMMSAGELESGNAGEPAK +2 Oxid (M)	76		
	548.86	2 +	200-208	YREAADMIK	50		
	1038.06	2 +	268-286	VPIVVTGNDFSTLYAPLIR	75		
	819.53	2 +	308-322	GIFQTDNVSDSVVK	85		
	942.10	2 +	323-339	IVDTFPGQSIDFFGALR	68		
	895.47	1 +	342-348	VYDDEV	46		
	559.56	2 +	368-377	DGPVTFEQPK	49		
	644.77	3 +	383-398	LLEYGHMLVQEQDNVK + Oxid (M)	82		
	844.05	3 +	399-421	RVQLADTYMSQAALGDANQDAMK +2 Oxid (M)	102		
	786.66	3 +	400-421	VQLADTYMSQAALGDANQDAMK + Oxid (M)	78		
	380.43	2 +	422-428	TGSFYGK	45		
73	855.42	2 +	64-78	GLAYDISDDQQDITR	92		
	398.70	2 +	132-138	LVVHLSK	38		
	583.90	2 +	148-158	IPLILGIWGGK	51		
	614.98	2 +	163-172	SFQCELVFAK	54		
	785.08	3 +	173-195	MGINPIMMSAGELESGNAGEPAK +3 Oxid (M)	73		
	470.85	2 +	294-300	FYWAPTR	33		
	819.46	2 +	309-323	GIFQTDNVSDSVVK	92		
	628.48	3 +	324-340	IVDTFPGQSIDFFGALR	86		
	895.36	1 +	343-349	VYDDEV	46		
	559.39	2 +	369-378	DGPVTFEQPK	48		
	958.38	2 +	384-399	LLEYGHMLVQEQDNVK	71		
	843.71	3 +	400-422	RVQLADTYMSQAALGDANKDAMK	82		
	786.49	3 +	401-422	VQLADTYMSQAALGDANKDAMK + Oxid (M)	92		
159	855.43	2 +	64-78	GLAYDISDDQQDITR	85	gi 32481061	RuBisCO activase alpha form precursor [Deschampsia antarctica]
	788.46	3 +	112-131	KYDFDNTMGGFYIAPAFMDK +2 Oxid (M)	38		
	398.64	2 +	132-138	LVVHLSK	42		
	583.80	2 +	148-158	IPLILGIWGGK	44		
	614.97	2 +	163-172	SFQCELVFAK	44		
	785.06	3 +	173-195	MGINPIMMSAGELESGNAGEPAK +3 Oxid (M)	69		
	819.39	2 +	309-323	GIFQTDNVSDSVVK	81		
	628.29	3 +	324-340	IVDTFPGQSIDFFGALR	80		
	448.66	2 +	343-349	VYDDEV	37		
	559.42	2 +	369-378	DGPVTFEQPK	47		
	696.78	3 +	384-400	LLEYGHMLVQEQDNVKR + Oxid (M)	64		
	843.72	3 +	400-422	RVQLADTYMSQAALGDANKDAMK +2 Oxid (M)	79		
182	855.47	2 +	64-78	GLAYDISDDQQDITR	92		
	777.93	3 +	112-131	KYDFDNTMGGFYIAPAFMDK	33		
	1102.05	2 +	113-131	YDFDNTMGGFYIAPAFMDK	75		
	398.62	2 +	132-138	LVVHLSK	39		
	539.68	2 +	139-147	NFMTLPNIK	38		
	584.22	2 +	148-158	IPLILGIWGGK	50		
	615.03	2 +	163-172	SFQCELVFAK	57		
	1153.07	2 +	173-195	MGINPIMMSAGELESGNAGEPAK	118		
	366.47	3 +	201-209	YREAADMIK	47		
	380.46	2 +	203-209	EAADMIK + Glu->pyro-Glu (N-term E)	44		
	864.61	2 +	213-227	MCCLFINDLDAGAGR + Oxidation (M)	45		
	940.51	1 +	294-300	FYWAPTR	34		
	819.85	2 +	309-323	GIFQTDNVSDSVVK	83		
	942.29	2 +	324-340	IVDTFPGQSIDFFGALR	78		
	448.48	2 +	343-349	VYDDEV	41		
	559.56	2 +	369-378	DGPVTFEQPK	46		
	644.97	3 +	384-399	LLEYGHMLVQEQDNVK + Oxid (M)	78		
	843.85	3 +	400-422	RVQLADTYMSQAALGDANKDAMK + 2 Oxid (M)	64		
48	650.37	3 +	6-22	IKVANPIVEMDGDDEMTR +2 Oxid (M)	39	gi 75267781	cytosolic NADP+- isocitrate dehydrogenase [Populus tremula x Populus alba]
	854.86	2 +	8-22	VANPIVEMDGDDEMTR +2 Oxid (M)	60		
	497.51	2 +	135-142	HAFGDQYR	34		
	805.46	2 +	239-251	SKYEAGIWEYHR	67		
	697.39	2 +	241-251	YEAAGIWEYHR	58		
	626.42	2 +	252-262	LIDDMVAYALK	58		
	678.39	2 +	304-316	TIEAEAAHGTVTR	73		

131	596.96 463.41 631.49	2 + 2 + 2 +	94-103 96-103 329-338	QRSEFQSSIK + Gln->pyro-Glu (N-term Q) SEFQSSIK INYEAYTYPK	66 40 66	gi 38344143	OSJNBa0041A02.10 Plant peroxidase [Oryza sativa (japonica cultivar-group)]
18	430.89 573.31	2 + 2 +	64-71 140-150	AAQDAWAK STYNEITGSSS	57 39	gi 115472001	Os07g0469100 Thylakoid membrane phosphoprotein 14 kDa, [Oryza sativa (japonica cultivar-group)]
9	431.03 573.50	2 + 2 +	64-71 140-150	AAQDAWAK STYNEITGSSS	56 50		
38	457.57 604.51	2 + 2 +	154-162 163-173	AYAVGASFK GTDFTNAVIDR	39 98	gi 115482792	Os10g0502000 Thylakoid lumenal 17.4 kDa protein, [Oryza sativa (japonica cultivar-group)]
67	840.67 559.55	2 + 2 +	163-177 185-194	VKDEEGYPAMALVNK + Oxid (M) HSIGQSHPVVR	32 52	gi 115434012	Os01g0104400 Ricin B-related lectin domain containing protein [Oryza sativa (japonica cultivar-group)]

## 2) Kohdasht spring wheat (PART II)

Spot No.	Peptides identified by MS/MS				Mascot Ion Score	NCBI Accession Number	Protein ID
	m/z	charge state	start-end <sup>a</sup>	sequence			
22	670.03	2 +	26-37	MASETGQSIQDR + Oxid (M)	92	gi 157073742	group3 late embryogenesis abundant protein (Wrab17) [Triticum aestivum]
	541.72	2 +	43-52	DQTGSFLGEK	44		
	783.58	2 +	89-103	AVEGKDQTGGFLSEK	37		
	671.02	2 +	165-177	DAVMNTLGMGGDK + 2 Oxid (M)	68		
48	448.94	2 +	29-36	YGDVIDSK	41	gi 114145394	glycine-rich RNA-binding protein [Triticum aestivum]
	767.39	2 +	62-75	QAIEAMNGQDLDR + Oxid (M)	43		
	566.43	2 +	76-85	NITVNEAQRS	50		
116	704.80	2 +	22-32	LTYYPPEYETK	46	gi 14017580	ribulose-1,5-bisphosphate carboxylase/oxygenase large subunit [Triticum aestivum]
	511.81	2 +	33-41	DTDILAAFR	64		
	1281.30	3 +	42-79	VSPQPGVPPEEAGAAVAASSTGTWTTVWTDGLTSLDR	40		
	733.52	2 +	147-159	TFQGPPHGNQVER	86		
27	704.57	2 +	22-32	LTYYPPEYETK	40		
	511.62	2 +	33-41	DTDILAAFR	64		
	733.86	2 +	147-159	TFQGPPHGNQVER	79		
114	780.36	1 +	15-21	AGVKDYK	30		
	704.77	2 +	22-32	LTYYPPEYETK	46		
	511.86	2 +	33-41	DTDILAAFR	64		
	329.35	3 +	132-139	ALRLEDLR	55		
	729.49	3 +	195-213	GGLDFTKDDENVNSQPFMR + Oxid (M)	47		
	726.57	2 +	202-213	DDENVNSQPFMR	57		
	482.02	2 +	228-236	SQAETGEIK	47		
	457.21	2 +	296-303	AMHAVIDR	39		
	741.56	2 +	320-334	MSGGDHIHSGTVVGK	56		
	655.80	2 +	340-350	EMTLGFVDLLR + Oxid (M)	50		
	519.48	2 +	351-358	DDFIEKDR	32		
	774.12	2 +	451-463	WSPELAAACEVWK	76		
	826.68	2 +	464-477	AIKFEPVDTIDK	63		
	670.71	2 +	467-477	FEFEPVDTIDK	44		
30	704.44	2 +	22-32	LTYYPPEYETK	40		
	511.34	2 +	33-41	DTDILAAFR	59		
	369.36	2 +	195-201	GGLDFTK	44		
	726.49	2 +	202-213	DDENVNSQPFMR	68		
	624.43	2 +	218-227	FVFCAEAIYK	34		
	481.80	2 +	228-236	SQAETGEIK	40		
	464.74	2 +	296-303	AMHAVIDR + Oxid (M)	44		
	494.93	3 +	320-334	MSGGDHIHSGTVVGK	67		
	655.51	2 +	340-350	EMTLGFVDLLR	56		



	519.43 773.90 826.47 670.02	2 + 2 + 2 + 2 +	351-358 451-463 464-477 467-477	DDFIEKDR WSPELAAACEVWK AIKFEFEPVDTIDK FEFEPVDTIDK	49 76 53 59		
35	773.85 826.57 670.70	2 + 2 + 2 +	451-463 464-477 467-477	WSPELAAACEVWK AIKFEFEPVDTIDK FEFEPVDTIDK	72 43 43		
64	961.74 691.05 369.99 674.57 765.65 808.50 571.11 497.90 491.57	2 + 2 + 2 + 2 + 3 + 3 + 2 + 2 + 2 +	59-75 83-93 94-99 100-111 118-137 118-138 138-146 139-146 147-154	FETLSYLPPLSTEALLK SKWVPCLEFSK VGFIFR EHNASPGYYDGR + pyro-Glu (N-term E) LPMFGCTDATQVINEVEEVK + Oxid (M) LPMFGCTDATQVINEVEEVKK + Oxid (M) KEYPDAYVR EYPDAYVR + pyro-Glu (N-term E) IIGFDNMR + Oxid (M)	33 38 33 50 37 54 40 42 42		
19	684.27 691.08 370.01 674.49 808.65 570.99 497.90 491.66	3 + 2 + 2 + 2 + 3 + 2 + 2 + 2 +	58-75 83-93 94-99 100-111 118-138 138-146 139-146 147-154	KFETLSYLPPLSTEALLK SKWVPCLEFSK VGFIFR EHNASPGYYDGR + pyro-Glu (N-term E) LPMFGCTDATQVINEVEEVKK + Oxid (M) KEYPDAYVR EYPDAYVR + pyro-Glu (N-term E) IIGFDNMR + Oxid (M)	51 45 33 53 70 39 39 39	gil170771	ribulose-1,5-bisphosphate carboxylase/oxygenase [Triticum aestivum]
72	608.23 369.99 683.42 571.14 497.78 483.84	2 + 2 + 2 + 2 + 2 + 2 +	48-57 94-99 100-111 138-146 139-146 147-154	MQVWPIEGIK + Oxid (M) VGFIFR EHNASPGYYDGR KEYPDAYVR EYPDAYVR + pyro-Glu (N-term E) IIGFDNMR	45 36 56 34 41 38		
55	889.47 808.58 570.92 484.28	1 + 3 + 2 + 2 +	76-82 118-138 138-146 147-154	QVDYLIR LPMFGCTDATQVLNEVEEVKK + Oxid (M) KEYPDAYVR VIGFDNMR + Oxid (M)	32 60 42 55		
23	684.42 691.07 370.05 674.56 765.68 808.73 571.09 497.94 483.66	3 + 2 + 2 + 2 + 3 + 3 + 2 + 2 + 2 +	57-74 82-92 93-98 99-110 117-136 117-137 137-145 138-145 146-153	KFETLSYLPPLSTEALLK SKWVPCLEFSK VGFIFR EHNASPGYYDGR + pyro-Glu (N-term E) LPMFGCTDATQVLNEVEEVK + Oxid (M) LPMFGCTDATQVLNEVEEVKK + Oxid (M) KEYPDAYVR EYPDAYVR + pyro-Glu (N-term E) IIGFDNMR + Oxid (M)	35 46 33 52 52 65 43 48 46		
24	507.15 491.56	2 + 2 +	102-109 110-117	EYPDAYVR IIGFDNMR + Oxid (M)	30 42	gil170771	ribulose-1,5-bisphosphate carboxylase/oxygenase [Triticum aestivum]
40	641.42 362.80 690.85 765.84 808.66 570.97 497.78 484.29	3 + 2 + 2 + 3 + 3 + 2 + 2 + 2 +	59-75 94-99 100-111 118-137 118-138 138-146 139-146 147-154	FETLSYLPPLSTEALLK VGFVFR EHNSSPGYYDGR LPMFGCTDATQVLNEVEEVK + Oxid (M) LPMFGCTDATQVLNEVEEVKK + Oxid (M) KEYPDAYVR EYPDAYVR + pyro-Glu (N-term E) VIGFDNMR + Oxid (M)	49 37 70 44 67 38 40 45		
171	684.29 962.01 363.01 690.86 766.16 570.94 497.91 467.59	3 + 2 + 2 + 2 + 3 + 2 + 2 + 2 +	58-75 59-75 94-99 100-111 118-137 138-146 139-146 147-154	KFETLSYLPPLSTEALLK FETLSYLPPLSTEALLK VGFVFR EHNSSPGYYDGR LPMFGCTDATQVLNEVEEVK + Oxid (M) KEYPDAYVR EYPDAYVR + pyro-Glu (N-term E) VIGFDNLR	44 45 37 75 50 32 43 39		
122	392.11 531.58 645.60 471.38 406.99 786.73 406.73 693.23 898.08 676.22 740.15 887.07	2 + 2 + 2 + 2 + 2 + 2 + 2 + 2 + 2 + 2 + 2 + 2 +	117-123 124-132 137-148 194-202 195-202 252-265 266-272 279-293 313-329 330-342 330-343 389-402	NASHLLK YDSMLGTFK IVDDQTISVDGK KVIITAPAK VIITAPAK GTMTTTHSYTGDQR + Oxid (M) LLDASHR AAALNIVPTSTGAAK VPTPNVSVVDLVINTVK TGITADDVNAAFR TGITADDVNAAFRK VVAWYDNEWGYSQR	36 45 66 46 38 68 48 75 85 70 59 80	gil115450493	Os03g0129300 [Oryza sativa (japonica cultivar- group)] glyceraldehyde-3- phosphate dehydrogenase

75	375.65 666.89 745.09 745.65 382.46 732.87	2 + 2 + 2 + 3 + 2 + 3 +	18-24 25-38 25-39 107-129 205-211 218-238	YIATPGK GILAADESTGTIGK GILAADESTGTIGKR GTVDIAGTNGETTTQGLDSLGR VLAAVYK VLLEGTLKPNMVTGPSDSPK	35 82 86 67 41 62	gi 115468886	Os06g0608700 [Oryza sativa (japonica cultivar-group)] Fructose-bisphosphate aldolase
136	839.00 789.09 889.40 566.53 354.39 497.53 529.24 626.68 578.98 678.69 899.73	2 + 2 + 2 + 2 + 2 + 2 + 2 + 2 + 2 + 2 + 2 +	8-22 30-42 52-68 58-68 69-74 135-142 143-153 250-260 261-270 302-314 322-338	VANPIVEMDGDEMTR + Oxid (M) DKLIFPFLDLIK DATDDKVTVVEAAEATLK VTVEAAEATLK YNVAIK HAFGDQYR ATDAVLKGP GK LIDDMVAYALK SEGgyvwack TIEAAAHGTVTR GGETSTNSIASIFAWTR	85 46 89 69 50 46 48 66 60 112 90	gi 115438939	Os01g0654500 NADP-isocitrate dehydrogenase [Oryza sativa (japonica cultivar-group)]
189	462.89 570.53 704.45 946.45 750.71 694.21 610.64 487.76 728.15	2 + 2 + 2 + 2 + 2 + 2 + 3 + 2 + 3 +	163-170 214-222 224-236 253-269 296-307 315-326 315-330 374-381 382-400	LHILTDGR YENDWSVVK GWDAQVLGEAPHK ANDQYLPPFVIVDESGK ALEFPDFDKFDR YAGMLQYDGELK YAGMLQYDGELKLP SK + Oxid (M) SGYFDETR EEYVEIPSDSGITFNEQPK	34 36 59 40 46 67 60 49 45	gi 115464537	Os05g0482700 [Oryza sativa (japonica cultivar-group)] phosphoglycerate mutase
145	908.03 704.53 702.56 449.11 521.97	3 + 2 + 2 + 2 + 2 +	65-92 224-236 315-326 341-348 353-361	AHGTA VGLPSDDDMGNSEVGHNALGAGR + Oxid (M) GWDAQVLGEAPHK YAGMLQYDGELK + Oxid (M) TSGEYLVK TFACSETVK	100 73 62 44 39		
95	533.96 734.00 694.69 810.93 579.29 437.46 655.16 685.09 551.04 451.54 542.57	2 + 2 + 2 + 3 + 2 + 2 + 2 + 3 + 2 + 2 + 2 +	38-47 58-71 73-85 140-162 163-172 193-200 271-282 338-356 357-367 359-367 368-378	ASAYADELVK GILAMDES NATCGK LASIGLENTEANR GLVPLVGSNDES WCQGLDGLASR EAAYYQGAR EAAWGLAR ATPEEVASYTLK TWGGRPENVAAAQEALLR AKANSLAQLGK ANSLAQLGK YTS DGEAAA K	49 91 83 52 55 38 65 67 37 41 64	gi 8272480	fructose 1,6-bisphosphate aldolase precursor [Avena sativa]
94	769.07 733.18 621.12 631.91 578.65 830.69 908.62 1028.16 762.58 649.14 755.67 606.99 495.65 702.16	2 + 2 + 2 + 3 + 2 + 2 + 2 + 2 + 2 + 2 + 2 + 2 + 2 + 2 +	52-65 66-78 157-167 169-185 190-201 202-217 202-218 311-328 329-340 331-340 358-371 381-390 539-546 569-579	NGHVEI IANDQGNR ITPSWVGFTDGER MKETA EAYLGK INDAVVTVPAYFNDAQR DAGVIAGLNVAR IINEPTAAAIAYGLDK IINEPTAAAIAYGLDKR VEIESLFDGTD FSEPLTR ARFEELNNDLFR FEELNNDLFR TQIHEIVLVGGSTR DYFDGKEPNK LSQEEIDR NQLETYVYNMK + Oxid (M)	63 77 52 52 79 87 88 59 52 72 88 40 58 70	gi 476003	HSP70 [Hordeum vulgare subsp. vulgare]
108	364.91 790.70 504.60 731.67 523.22 436.02 862.71 798.93 699.07 907.39	2 + 2 + 2 + 2 + 3 + 2 + 2 + 2 + 2 + 3 +	108-114 116-129 136-144 168-180 197-210 219-226 227-242 357-369 359-369 414-441	LVGQIAK QAVVNPENTFFSVK MAEVDDEAK QFAAEEISAQVLR AVVTVPAYFNDSQR IAGLEVLR IINEPTAASLAYGF EK AKFEELCSDLIDR FEELCSDLIDR DPNVTVPNPDEVVSLGAAVQGGVLAGDVK	40 72 47 89 55 58 101 107 53 36	gi 115487998	Os12g0244100 [Oryza sativa (japonica cultivar-group)] Heat shock 70 protein
	813.27 737.14 701.34 673.13 978.67 770.54 899.04	3 + 2 + 3 + 2 + 2 + 2 + 2 +	477-499 550-563 550-568 551-563 551-568 569-581 569-583	SEVFSTAADGQTSVEINV LQGER KQDITITGASTLPK KQDITITGASTLPKDEVER K.QDITITGASTLPK QDITITGASTLPKDEVER + pyro-Glu (N-term Q) MV E EADKFAQEDK MVEEADKFAQEDK	42 82 78 76 54 75 46		

	826.53	2 +	683-698	GPNDGDVIDADFTDSN	90		
103	365.00 782.15 731.66 784.06 862.76 701.26 672.60 691.52	2 + 2 + 2 + 2 + 2 + 3 + 2 + 2 +	108-114 116-129 168-180 197-210 227-242 550-568 551-563 591-602	LVGQIAK QAVVNPENTFFSVK + pyro-Glu (N-term Q) QFAAEEISAQVLR AVVTVPAYFNDSQR IINEPTAASLAYGFEK KQDITITGASTLPKDEVER QDITITGASTLPK NQADSVVYQTEK	41 58 93 52 102 52 51 77		
99	731.09 770.17 637.28 783.46 436.81 889.28 705.79 717.64 625.04 970.16 911.65	2 + 2 + 2 + 2 + 2 + 2 + 1 + 2 + 2 + 2 + 2 +	146-159 160-173 174-184 189-202 211-218 219-235 371-377 378-390 394-404 409-428 468-484	APNGDAWVETTDGK QYSPSQIGAFVLTK MKETAESYL GK + Oxid (M) AVITVPAYFNDAQR IAGLDVQR IINEPTAAALSYGTNNK DAGITTK EVDEVLLVGGMTR + Oxid (M) VQEIVSEIFGK GVNPDEAVAMGAAIQGGILR SQVFSTAADNQTQVGIR	81 75 60 54 51 74 31 83 33 99 90	gj 115448989	Os02g0774300 [Oryza sativa (japonica cultivar-group)] molecular chaperone DnaK
4	771.84 1215.71 655.82 457.62 544.57 480.72 959.60 753.55 415.31 643.42 367.60 531.03 891.14 712.12 840.90 731.66 679.65 615.67 468.92 725.71	2 + 2 + 2 + 2 + 2 + 2 + 2 + 2 + 2 + 2 + 2 + 2 + 2 + 2 + 2 + 3 + 2 + 2 + 2 + 2 + 2 +	13-26 35-59 60-72 80-87 125-134 126-134 135-150 151-163 173-179 185-195 231 - 237 265-275 281-297 304-315 304-317 304-321 346-357 347-357 424-431 469-481	EVELEDPVENIGAK TNDLAGDGTTSVLAQGLIAEGVK VIAAGANPVQITR ALVLELKK KGVVTLLEGR GVVTLLEGR SSENNLYVVEGMQFER + Oxid (M) GYISPYFVTDSEK LLLVDKK DLINVLEEAIR APGFGER ADNTVLGTAAK ESTTIVGDGSTQEEVTK NLIEAAEQDYEK NLIEAAEQDYEKEK NLIEAAEQDYEKEKLNER KLRVEDALNATK LRVEDALNATK VLSNDNFK TFLTSDVVVVEIK	73 98 74 46 69 54 77 70 40 86 30 70 82 70 71 69 43 57 50 52	gj 2493650	RuBisCO large subunit-binding protein subunit beta, chloroplastic [Secale cereale] (CPN60, GroEI like)
56	771.72 655.77 544.40 480.38 959.44 753.71 642.97 925.50 495.45 531.10 882.02 969.01 840.83 850.96 809.69 372.28 468.91 816.02 939.98	2 + 2 + 2 + 2 + 2 + 2 + 2 + 2 + 2 + 2 + 2 + 2 + 2 + 2 + 2 + 2 + 2 + 2 + 3 + 2 +	13-26 60-72 125-134 126-134 135-150 151-163 185-195 239-255 256-264 265-275 281-297 281-298 304-317 358-374 379-392 393-399 424-431 432-454 482-499	EVELEDPVENIGAK VIAAGANPVQITR KGVVTLLEGR GVVTLLEGR SSENNLYVVEGMQFER + Oxid (M) GYISPYFVTDSEK DLINVLEEAIR TQYLDIDIALTG GTVIR DEVGLTLDK ADNTVLGTAAK ESTTIVGDGSTQEEVTK + pyro-Glu (N-term E) ESTTIVGDGSTQEEVTKR NLIEAAEQDYEKEK AAVEEGIVVGGGCTLLR VDAIKDTLENDEQK VGAEIVR VLSNDNFK FGYNAATGQYEDLMAAGIIDPTK EPEAAPLANPMDNSGFGY	74 82 84 47 108 71 68 88 45 74 91 70 64 52 71 58 45 63 58	gj 2493650	RuBisCO large subunit-binding protein subunit beta, chloroplastic [Secale cereale] (CPN60, GroEI like)
57	444.04 584.44 624.53 522.33 877.72 855.73 778.82 562.21 644.03 749.43	2 + 2 + 2 + 2 + 2 + 2 + 2 + 3 + 2 + 3 +	15-23 24-35 38-48 49-58 59-75 81-97 102-117 102-118 123-133 146-168	AALQAGVEK LANAVGVTLGPR NVVLDEYGNPK VVNDGVTIAR AIELANPMENAGAALIR TNSAGDGT TACVLAR LGILSVTSGANPVSLK LGILSVTSGANPVSLKK TVQGLIEELER AVASISAGNDELIGAMIADAIDK	63 72 66 71 82 123 72 60 56 82	gj 134102	RuBisCO large subunit-binding protein subunit alpha, chloroplastic (60 kDa chaperonin subunit alpha) [Triticum aestivum]

	748.78 533.15 777.92 450.12 382.43 952.05 888.49 943.01 876.15 548.69 758.57 422.52 660.48 572.49 429.46 765.41 845.89 774.67 550.51	2 + 2 + 2 + 2 + 2 + 2 + 2 + 2 + 3 + 3 + 2 + 2 + 2 + 2 + 2 + 3 + 2 + 2 + 2 +	198-210 211-219 232-244 269-277 278-284 286-303 287-303 304-321 322-345 351-364 352-364 372-380 381-392 431-439 440-447 448-470 473-486 487-500 533-543	GYIS PQFVTNLEK SIVEFENAR EIIPLEQTTQLR GIINVAAIK APSFGER KAVLQDIAIVTGAEYLAK AVLQDIAIVTGAEYLAK DLGLLVENATVDQLGTAR KITIHQTTTTLIADAASKDEIQAR KELSETDSIYDSEK ELSETDSIYDSEK LSGGVAVIK VGATTETELED ETIEDHDER LGADIIQK ALQAPASLIANNAGVEGEVVEIK ESEWEMGYNAMTDK YENLIESGVIDPAK VAEPAEGQLSV	75 44 72 60 37 100 68 109 79 42 67 53 81 47 60 104 37 76 59		
54	575.59 765.84 781.12	2 + 3 + 2 +	52-61 118-137 138-151	YTSIKPLGDR LPMFGCTDATQVLNEVEEVK + Oxid (M) EDDIIGILDTDDVK	50 44 79	gj 115479353	Os09g0438700 [Oryza sativa (japonica cultivar-group)] Chaperonin 10 Kd subunit
81	537.05 779.20 715.10 723.30 578.56 981.99	2 + 2 + 2 + 3 + 2 + 2 +	40-50 51-64 52-64 65-84 103-112 197-214	AANGVVIATEK KLPSILVDETSVQK LPSILVDETSVQK IQSLTPNIGVVYSGMGPDR + Oxid (M) ETIPVTQLVR EGYEGQISANNIEGVIR	54 66 81 67 44 64	gj 115447473	Os02g0634900 [Oryza sativa (japonica cultivar-group)] proteasome alpha type 2
53	908.78 881.59 770.46 623.04 771.54 490.38 554.40 791.41 773.45 721.40 469.33	2 + 2 + 2 + 2 + 3 + 2 + 2 + 2 + 3 + 3 + 2 +	59-73 74-89 94-107 163-173 174-192 314-322 314-323 332-345 346-366 347-366 380-387	MQQLLMDTTPFTDK + 2 Oxid (M) IIAEYIWVGGSGIDL TISKPVEDPSELK HMAAQIFSDPK VTAQVPWFGEIEYTLMQR + Oxid (M) EDGGFDVIK EDGGFDVIK HDLHIAAYGEGNER RLTGLHETASISDFSWGVANR LTGLHETASISDFSWGVANR GKGYLEDR	90 65 56 51 46 64 35 94 104 54 44	gj 11362640	plastid glutamine synthetase isoform GS2c [Triticum aestivum]
184	689.48 531.45 591.51 657.03 587.52 557.52	2 + 2 + 2 + 2 + 2 + 3 +	69-80 211-218 296-306 323-334 366-375 441-455	LQAGYLFPEIAR YGNIEYMR + Oxid (M) EVAIETASFSK ELLFSDGHPVAK AMQDVGIFYK + Oxid (M) VSAFGHRENIIEAAR	53 60 51 52 54 56	gj 195634861	unknown [Zea mays] Aspartate aminotransferase family
32	530.31 466.26 509.77	2 + 2 + 2 +	71-79 72-79 193-202	KLYVGNIPR LYVGNIPR GEVLSATVSR	29 43 53	gj 115478330	Os09g0279500 [Oryza sativa (japonica cultivar-group)] Plastid-specific 30S ribosomal protein 2
67	586.94 536.49 526.28	2 + 2 + 2 +	38-48 68-78 136-145	QVFAGPIVTLK VLVVDGGGSLR HVPVTIAGTR	35 79 45	gj 18461241	S-adenosylmethionine:2-demethylmenaquinone methyltransferase-like [Oryza sativa Japonica Group]
78	751.86 803.91 660.35 369.19 444.25 478.28	2 + 2 + 3 + 2 + 2 + 2 +	50-62 77-91 172-189 283-289 294-302 330-337	TNMVMVFGEITTK + 2 Oxid (M) NIGFISDDVGLDADR TQVTVEYLNEDGAMVPVR + Oxid (M) SGAYIAR SIASGLAR IPDKEILK	88 98 74 52 47 44		
111	735.13 413.71 804.35 1019.15 883.93 888.63 727.61 655.22 802.43 369.59 444.51 490.65 832.08 685.17	2 + 2 + 2 + 2 + 3 + 2 + 2 + 3 + 3 + 2 + 2 + 2 + 2 + 3 +	50-62 63-69 77-91 172-189 190-213 225-239 240-254 256-275 256-279 283-289 294-302 366-374 375-388 375-391	TNMVMVLGEITTK + 2 Oxid (M) ATVDYEK NIGFISDDVGLDADR TQVTVEYLNEDGAMVPVR + Oxid (M) VHTVLISTQHDETVTNDIEAADLK YLDENTIFHLNPSGR FVIGGPHGDAGLTGR IIIDTYGGWGAHGGGAFSGK IIIDTYGGWGAHGGGAFSGKDPTK SGAYIAR SIASGLAR TAAYGHFGR DDADFTWEVVKPLK DDADFTWEVVKPLKFDK	109 36 107 113 88 73 79 46 82 49 52 44 55 63	gj 115589744	S-adenosylmethionine synthetase 1 [Triticum monococcum]

85	505.05 636.54 667.08 757.07 812.24 644.08	2 + 2 + 2 + 2 + 2 + 2 +	48-56 57-68 72-84 155-168 197-214 310-323	SEEIFNAAK ELMPGGVNSPVR + Oxid (M) SVGGQPIVFDSVK FVNSGTEACMGALR AGSGVATLGLPDSPGVPK IIGGGLPVGAYGGR	45 52 59 89 61 49	gi 1170029	Glutamate-1-semialdehyde 2,1-aminomutase, chloroplast precursor [Hordeum vulgare]
21	823.56 831.73	2 + 2 +	157-171 211-224	GFGFVTMSTIEEAEK IYVGNLPWQVDDSR	60 76	gi 2443390	Ps16 protein [Triticum aestivum]
2	813.64 831.57 580.06	2 + 2 + 2 +	117-130 211-224 225-234	VYVGNLPYDVSER IYVGNLPWQVDDSR LVELFSEHGK	75 31 35		
28	824.75 804.37	2 + 3 +	147-161 194-214	GFGFVTMSTIEEADK + Oxid (M) QFASSFRAYVGNLPWQAEDSR + pyro-Glu (N-term Q)	69 45		
154	812.97 824.48 803.69 531.19 768.91 570.45	2 + 2 + 2 + 2 + 3 + 2 +	107-120 147-161 201-214 241-250 251-271 272-281	VYVGNLPYDVSER GFGFVTMSTIEEADK + Oxid (M) AYVGNLPWQAEDSR GFGFVTMASK + Oxid (M) EDLDSAISALDQGEMDGRPLR + Oxid (M) VNVAERPQR	61 89 71 48 79 41	gi 3550483	Cp31BHv [Hordeum vulgare subsp. vulgare] nucleic acid-binding protein
110	610.57 695.67 617.52	2 + 2 + 2 +	176-186 239-251 240-251	LFGVTTLDVVVR RTQDGGTEVVEAK TQDGGTEVVEAK	79 42 70	gi 126896	Malate dehydrogenase, mitochondrial precursor [Triticum aestivum]
150	626.45 605.62 721.69	2 + 2 + 2 +	111-121 116-125 122-133	GMTAKNFDVPR + Oxid (M) NFDVPRYSGR YSGRWFEVASLK	42 37 48	gi 77744909	chloroplast lipocalin [Hordeum vulgare] cytosolic fatty-acid binding protein
156	638.32 716.36 500.29 710.84 567.97 787.41 801.40	2 + 2 + 2 + 2 + 3 + 2 + 2 +	77-89 77-90 146-154 250-262 420-437 421-437 462-476	SVGDLTAADLEGK SVGDLTAADLEGKR FSLAPLVPR ELDYLDGAVSNPK KGVTTIIGGGDSVAAVEK GVTTIIGGGDSVAAVEK ELPGVVALDEGVMTR + Oxid (M)	63 41 43 68 87 52 38	gi 129915	Phosphoglycerate kinase chloroplastic [Triticum aestivum]
93	708.21 662.02	2 + 2 +	103-114 129-140	LGNDILVEDWLK GDPTYLVVESDK	35 65	gi 68566191	Cytochrome b6-f complex iron-sulfur subunit, chloroplast precursor [Triticum aestivum]
80	808.19 732.73 654.82 988.21 412.41 585.22 842.62 644.18 641.83 577.72	2 + 2 + 2 + 2 + 2 + 3 + 2 + 2 + 2 + 2 +	133-148 156-168 157-168 199-217 268-274 268-283 290-302 319-330 344-353 345-353	LYSIASSALGDFGDAK RLVYTNDAGEVVK LVYTNDAGEVVK DPNATIIMLATGTGIAPFR + Oxid (M) VDYAIRS VDYAIRSEETNAAGEK MAEYKDELWELLK + Oxid (M) GIDEIMIPLASK KSEQWNVEVY SEQWNVEVY	103 53 77 67 48 43 56 76 35 52	gi 20302471	ferredoxin-NADP(H) oxidoreductase [Triticum aestivum]
38	730.92 805.78 451.07	2 + 1 + 2 +	114-127 121-127 142-150	AELGGVKDASEEVR DASEEVR AEIAAALNK	85 42 46	gi 115452259	Os03g0278900 [Oryza sativa (japonica cultivar- group)] ATP synthase B/B' CF(0)
120	893.65 815.58 905.20 768.74 820.99 620.16 1057.15 596.72 523.43 401.40 488.49 736.73 664.57 623.07 801.80 736.63 747.50 717.69 1031.48 709.25 1086.10 523.94 695.57	2 + 2 + 2 + 2 + 3 + 2 + 2 + 2 + 2 + 3 + 2 + 2 + 2 + 2 + 2 + 2 + 2 + 2 + 2 + 2 + 2 + 2 + 2 +	2-18 3-18 23-39 40-52 53-73 76-87 88-109 135-145 155-163 155-164 168-178 179-191 192-205 208-217 232-246 249-261 266-277 278-291 360-378 379-390 400-418 487-495 487-498	RTNPTTSPPGASTIEEK TNPTTSPPGASTIEEK IDQIIGPVLDVTFPPGK LPYIYNALVVQSR DTDDKQINVTCEVQQLGNRR AVAMSATDGLMR + Oxid (M) GMEVIDTGAPLSVPVGGATLGR + Oxid (M) SAPAFIELDTK VVDLLAPYR VVDLLAPYRR IGLFGGAGVGK TVLIMELINNIK AHGGVSFVGGVGER EGNDLYMEMK VALVYQGMNEPPGAR VGLTALTMAEYFR QDVLLFIDNIFR FVQAGSEVSALLGR GIYPAVDPLDSTSTMLQPR IVGNEHYETAQR ELQDIIAILGLDELSEEDR AITLEEENK AITLEEENKSQK	77 61 71 54 43 83 69 63 47 41 39 68 54 36 79 72 69 92 70 71 75 38 57	gi 14017579	ATP synthase CF1 beta subunit [Triticum aestivum]

112	809.76	2 +	232-246	VALVYQGMNEPPGAR + Oxid (M)	76		
	744.68	2 +	249-261	VGLTALTMAEYFR + Oxid (M)	74		
	717.87	2 +	278-291	FVQAGSEVSALLGR	96		
	1149.57	2 +	292-312	MPSAVGYQPTLSTEMGSLQER + Oxid (M)	59		
	1031.56	2 +	360-378	GIYPAVDPLDSTSTMLQPR	85		
	709.17	2 +	379-390	IVGNEHYETAQR	71		
	437.74	2 +	391-397	VKETLQR	39		
	524.26	2 +	487-495	AITLEENK	35		
115	695.66	2 +	487-498	AITLEENKSQK	57		
	1039.16	2 +	360-378	GIYPAVDPLDSTSTMLQPR + Oxid (M)	55		
	709.27	2 +	379-390	IVGNEHYETAQR	71		
130	695.76	2 +	487-498	AITLEENKSQK	60	gi 14017578	ATP synthase CF1 epsilon subunit [Triticum aestivum]
	668.62	2 +	1-11	MKLNLYVLTPK + Oxid (M)	65		
	595.15	2 +	2-11	KLNLVYLTPK	60		
	531.08	2 +	3-11	LNLYVLTPK	61		
	610.01	2 +	12-20	RIIWDCVK	40		
	936.91	3 +	70-95	IVNNEIILGNDALGSDIDPEEAQK	36		
	580.07	2 +	96-106	ALEIAEANLSK	79		
	581.07	2 +	107-117	AEGTKDLVEAK	52		
	674.55	1 +	112-117	DLVEAK	44		
	755.30	2 +	125-137	IRIEAVNWIPPSN	46		
	620.55	2 +	127-137	IEAVNWIPPSN	61		
25	782.44	2 +	87-100	KNTDFVAYSSEGFK	75	gi 131394	Oxygen-evolving enhancer protein 2, chloroplast precursor (OEE2) [Triticum aestivum]
	718.17	2 +	88-100	NTDFVAYSSEGFK	94		
	337.11	2 +	101-106	LMIPAK	32		
	473.51	2 +	114-121	EFPGQVLR	39		
	1121.64	2 +	122-141	YEDNFDATSNLSVIINPTTK	110		
	918.29	3 +	170-197	TDSEGGFESDAVATANVLESSAPVVDGK	55		
	613.99	2 +	198-207	QYYSITVLTR + pyro-Glu (N-term Q)	55		
	1042.63	2 +	208-228	TADGDEGGKHQLITATVADGK	56		
	627.63	2 +	217-228	HQLITATVADGK	53		
	664.24	2 +	246-258	KFVENAAGSFSVA	82		
	599.74	2 +	247-258	FVENAAGSFSVA	61		
26	782.37	2 +	87-100	KNTDFVAYSSEGFK	75	gi 131394	Oxygen-evolving enhancer protein 2, chloroplast precursor (OEE2) [Triticum aestivum]
	1121.70	2 +	122-141	YEDNFDATSNLSVIINPTTK	92		
	918.36	3 +	170-197	TDSEGGFESDAVATANVLESSAPVVDGK	34		
	614.21	2 +	198-207	QYYSITVLTR + pyro-Glu (N-term Q)	55		
	1042.73	2 +	208-228	TADGDEGGKHQLITATVADGK	83		
33	781.96	2 +	87-100	KNTDFVAYSSEGFK	68		
	717.91	2 +	88-100	NTDFVAYSSEGFK	91		
	337.19	2 +	101-106	LMIPAK	32		
	606.91	2 +	112-121	EREFPGQVLR + pyro-Glu (N-term E)	55		
173	412.95	3 +	85-94	RLTFDEIQSK	48		
	386.21	2 +	95-100	TYMEVK	32		
	779.01	2 +	141-154	AEGIQKNEPPAFQK	56		
	880.97	2 +	186-202	DGIDYAAVTVQLPGGER	74		
	475.93	2 +	203-210	VPFLFTVK	38		
	760.91	3 +	211-231	QLVATGKPESFSGPFLVPSYR	43		
31	393.92	2 +	95-100	TYMEVK	36	gi 147945622	chloroplast oxygen-evolving enhancer protein 1 (OEE1) [Leymus chinensis]
	779.30	2 +	141-154	AEGIQKNEPPAFQK	54		
	756.84	3 +	161-181	LYTYLDEMEGPLEVGADGTLK + Oxid (M)	79		
	881.01	2 +	186-202	DGIDYAAVTVQLPGGER	86		
	760.80	3 +	211-231	QLVATGKPESFSGPFLVPSYR	42		
63	412.97	3 +	85-94	RLTFDEIQSK	44		
	541.20	2 +	86-94	LTDFEIQSK	52		
	779.24	2 +	141-154	AEGIQKNEPPAFQK	50		
	765.69	3 +	182-202	FEEKDGIDYAAVTVQLPGGER	56		
	881.42	2 +	186-202	DGIDYAAVTVQLPGGER	72		
	1132.22	2 +	211-231	QLVATGKPESFSGPFLVPSYR + pyro-Glu (N-term Q)	42		
	425.90	2 +	232-239	GSSFDPK	34		
168	808.21	2 +	109-122	EVQKPLEDITDSLK	53	gi 195650293	unknown [Zea mays], peptidyl-prolyl cis-trans isomerase (cyclophilin)
	587.87	2 +	271-279	FYDGMEIQR + Oxid (M)	56		
	831.06	3 +	280-304	ADGFVVQTDGPEGPAEGFIDPSTGK	74		
	713.92	2 +	338-350	LPFNAFGTMAMAR	65		
	1008.03	2 +	351-367	EEFDDNSASSQVFWLLK	80		
	815.77	3 +	401-423	VGDVIESIQVVSGLDNLVNPSYK	77		
142	882.84	2 +	235-250	VVTIDGYEDVPVNSEK	48	gi 111073715	triticain alpha [Triticum aestivum], cysteine proteinase
	777.04	2 +	255-270	AVANQPISVAIEAGGR	93		
	820.92	2 +	310-323	NSWGTVWGEDGYIR	64		
128	855.62	2 +	63-77	GLAYDISDDQQDITR	92	gi 109940135	Ribulose biphosphate carboxylase/oxygenase activase, chloroplastic [Oryza sativa Japonica Group]
	788.60	3 +	111-130	KYDFDNTMGGFYIAPAFMDK + 2 Oxid (M)	41		
	1102.07	2 +	112-130	YDFDNTMGGFYIAPAFMDK	66		
	398.44	2 +	131-137	LVVHLSK	35		
	539.61	2 +	138-146	NFMTLPNIK	43		
	584.05	2 +	147-157	IPLILGIWGGK	51		
	615.21	2 +	162-171	SFQCELVFAK	48		

	1153.07 548.98 1038.21 940.56 819.83 942.45 895.58 512.43 559.62 639.53 691.65 843.85 1171.11 380.44	2 + 2 + 2 + 1 + 2 + 2 + 1 + 2 + 2 + 3 + 3 + 3 + 2 + 2 +	172-194 200-208 268-286 293-299 308-322 323-339 342-348 342-349 368-377 383-398 383-399 399-421 400-421 422-428	MGINPIMMSAGELESGNAGEPAK YREAADMIK VPIVVTGNDFSTLYAPLIR FYWAPTR GIFQTDNVSDSESVVK IVDTFPGQSIDFFGALR VYDDEV VYDDEV VYDDEV DGPVTFEQPK LLEYGHMLVQEEDNVK LLEYGHMLVQEEDNVK RVQLADTYMSQAALGDANQDAMK + 2 Oxid (M) VQLADTYMSQAALGDANQDAMK TGSFYGK	119 43 76 34 82 75 46 40 49 79 67 69 83 46		
121	855.80 788.60 1118.08 398.62 539.51 583.88 615.15 768.95 549.07 864.58 470.90 819.85 628.55 895.61 512.82 559.56 958.54 843.80	2 + 3 + 2 + 2 + 2 + 2 + 2 + 3 + 2 + 2 + 1 + 2 + 3 + 1 + 2 + 2 + 2 + 3 +	64-78 112-131 113-131 132-138 139-147 148-158 163-172 173-195 201-209 213-227 294-300 309-323 324-340 343-349 343-350 369-378 384-399 400-422	GLAYDISDDQQDITR KYDFDNTMGGFYIAPAFMDK + 2 Oxid (M) YDFDNTMGGFYIAPAFMDK + 2 Oxid (M) LVVHLSK NFMTLPNIK IPLILGIWGGK SFQCELVFAK MGINPIMMSAGELESGNAGEPAK YREAADMIK MCCLFINDLDAGAGR + Oxid (M) FYWAPTR GIFQTDNVSDSESVVK IVDTFPGQSIDFFGALR VYDDEV VYDDEV DGPVTFEQPK LLEYGHMLVQEEDNVK RVQLADTYMSQAALGDANKDAMK + 2 Oxid (M)	86 37 69 35 45 55 42 79 50 93 29 79 78 46 37 46 65 59	gi 32481061	Rubisco activase alpha form precursor [Deschampsia antarctica]
147	855.39 547.28 583.86 614.80 470.73 819.40 559.27 644.65 791.68	2 + 2 + 2 + 2 + 2 + 2 + 2 + 3 + 3 +	63-77 138-146 147-157 162-171 293-299 308-322 368-377 383-398 400-421	GLAYDISDDQQDITR NFMTLPNIK + Oxid (M) IPLILGIWGGK SFQCELVFAK FYWAPTR GIFQTDNVSDSESVVK DGPVTFEQPK LLEYGHMLVQEEDNVK + Oxid (M) VQLADTYMSQAALGDANQDAMK + 2 Oxid (M)	104 28 63 25 26 74 38 69 65		
165	398.49 584.20 859.93 819.36 942.03 895.37 559.37 644.77 843.85 792.10	2 + 2 + 3 + 2 + 2 + 1 + 2 + 3 + 3 + 3 +	132-138 148-158 301-323 309-323 324-340 343-349 369-378 384-399 400-422 401-422	LVVHLSK IPLILGIWGGK EDRIGVCKGIFQTDNVSDSESVVK + pyro-Glu (N-term E) GIFQTDNVSDSESVVK IVDTFPGQSIDFFGALR VYDDEV DGPVTFEQPK LLEYGHMLVQEEDNVK + Oxid (M) RVQLADTYMSQAALGDANKDAMK + 2 Oxid (M) VQLADTYMSQAALGDANKDAMK	36 51 40 85 82 46 48 66 104 82	gi 32481061	Rubisco activase alpha form precursor [Deschampsia antarctica]
175	855.40 547.29 583.86 614.80 784.68 470.73 819.41 559.28 644.65 843.72 791.69	2 + 2 + 2 + 2 + 3 + 2 + 2 + 2 + 3 + 3 + 3 +	63-77 138-146 147-157 162-171 172-194 293-299 308-322 368-377 383-398 399-421 400-421	GLAYDISDDQQDITR NFMTLPNIK + Oxid (M) IPLILGIWGGK SFQCELVFAK MGINPIMMSAGELESGNAGEPAK + 3 Oxid (M) FYWAPTR GIFQTDNVSDSESVVK DGPVTFEQPK LLEYGHMLVQEEDNVK + Oxid (M) RVQLADTYMSQAALGDANQDAMK + 2 Oxid (M) VQLADTYMSQAALGDANQDAMK + 2 Oxid (M)	108 38 50 34 57 30 74 35 81 44 77		
162	869.46 805.73 475.48	2 + 2 + 2 +	87-103 88-103 104-112	KIIGATNPLASEPGTIR IIGATNPLASEPGTIR GDFAVDIGR	99 87 53	gi 9652119	Nucleoside diphosphate kinase [Lolium perenne]
52	591.40 575.93 630.88 654.87 622.76 769.07 1023.38 483.61 634.19 478.31 704.39	2 + 2 + 2 + 2 + 3 + 2 + 1 + 2 + 3 + 2 + 2 +	111-120 137-146 137-147 158-169 196-211 223-235 236-244 245-253 254-269 270-277 294-306	YEYQGFPTLK EAEGIVEYLK EAEGIVEYLK + pyro-Glu (N-term E) APEDATYLEDGK SDYDFGHTVHANHLPR LFPFDELVDVSK DFDVSALEK FIDASSTPK VVTFDKNPDNHPYLLK YFQSNAPK SAYYGAVEEFGSK	39 46 38 83 79 56 46 54 50 45 72	gi 1709620	Protein disulfide-isomerase [Triticum aestivum]

	827.35 891.38 735.97 776.55 727.94 808.91 1148.51 1001.42 583.92 647.93 730.48 601.35 549.20 727.45	2 + 2 + 2 + 2 + 2 + 3 + 2 + 3 + 2 + 2 + 2 + 2 + 2 + 2 +	329-343 329-344 348-360 372-385 386-398 417-439 418-439 440-467 476-485 476-486 487-501 489-501 502-512 502-515	EDQAPLILIQSDSK + pyro-Glu (N-term E) EDQAPLILIQSDSKK + pyro-Glu (N-term E) EQVEAGQIVAWLK KSEPIPEANNEPVK VVVADNIHVVFK KLAPILDEAAATLQSEEDVVIK LAPILDEAAATLQSEEDVVIK IDATANDVPGEFDVQGYPTLYFVTPSGK TADEIVDYIK TADEIVDYIKK NKETAGQAAAAATEK ETAGQAAAAATEK + pyro-Glu (N-term E) AAEPAATEPLK AAEPAATEPLKDEL	82 48 65 48 58 51 77 41 64 52 90 80 46 58		
183	751.88 448.41 612.53 616.99 655.38 557.39	2 + 2 + 3 + 2 + 2 + 2 +	40-53 54-62 63-80 121-131 132-143 201-210	LAWHSAGTFDVATK TGGPFGTMK CPAELAHGANAGLDIAVR QDKPEPPPEGR + pyro-Glu (N-term Q) LPDATQGSDDLH EGLQLPTDK	30 56 72 50 69 50	gi 15808779	ascorbate peroxidase [Hordeum vulgare]
51	609.94 472.76 788.44 873.96 933.96 601.80 803.94 703.27 674.33 549.78	3 + 2 + 2 + 2 + 2 + 2 + 2 + 3 + 3 + 2 +	8-24 25-32 40-52 69-83 84-101 102-111 122-135 136-156 172-189 200-209	AAVGHPTDLGDCPFSQR VLLTLEEK LIDVSNKPDWFLK WIADSDVITQVIEEK YPTPSLVTPAEYASVGSK IFSTFVTFLK ALVDELQALEEHLK AHGPYINGANISAVDLSLAPK VPETLTSVHAYTEALFSR ENLIAGWAPK	64 42 41 94 79 62 54 39 62 62	gi 28192421	dehydroascorbate reductase [Triticum aestivum]
187	498.84 611.65	2 + 2 +	21-27 215-226	NPYWFNR VTTTIGFGSPNK	39 65	gi 55296168	putative transketolase 1 [Oryza sativa Japonica Group]
178	634.62 504.22 680.34 1022.09 586.31	3 + 2 + 2 + 2 + 2 +	284-299 291-299 328-339 340-360 569-579	FAEYEEKYPEDAATLK YPEDAATLK NLSQQCLNALAK VVPGLLGGSADLASSNMTLLK ESVLPEAVTAR	45 49 66 78 53		
1	539.56 603.53 901.98 758.87 640.99 925.55 711.15	2 + 2 + 2 + 2 + 3 + 3 + 2 +	23-32 23-33 34-49 50-63 64-79 80-109 129-141	QYTLEGQGAK + pyro-Glu (N-term Q) QYTLEGQGAKK + pyro-Glu (N-term Q) DISPPLEWYGVPDGTR SLAVVVQDQDADER VPWTHWVVVNISPEEK GLPEGFSGAGGNANAGGGDGGVQEGVNDWK LYALDDVLSLGNK	45 41 56 109 41 113 85	gi 26017213	cold regulated protein (Wcor18) [Triticum aestivum]